

BACHELOR THESIS

ARTIFICIAL INTELLIGENCE

Radboud University



Predicting hand motor performance from
pre-trial slow cortical potentials

Author:

Mats Robben
s1054883

First supervisor:

dr. M.W. Tangermann
Artificiële intelligentie
michael.tangermann@donders.ru.nl

Second reader:

dr. S. Ahmadi
Artificial Intelligence
sara.ahmadi.1@ru.nl



June 28, 2023

Abstract

Rehabilitation of pinch control is a significant area of focus in rehabilitation research. This study aims to contribute to this field by analysing the pre-trial neural markers present in EEG recordings of a pinch control task, with the goal of predicting trial performances before the trial onset. Specifically, the study investigates slow cortical potentials as the neural markers of interest. The research addresses an underreported aspect of the pinch control paradigm, which is the predictive power of slow cortical potentials in this specific setting. By developing an analysis pipeline tailored to identify and assess the predictive potential of these slow cortical potentials, the study aims to fill the existing gap in knowledge. The analysis successfully extracts signals resembling slow cortical potentials, which exhibit predictive power for the majority of participants. However, it is important to note that the components of activation carrying the most predictive power are evoked by the trial onset. Consequently, these significant components fall outside the pre-trial area of interest and cannot be effectively used to predict trial performance prior to trial onset. Despite this limitation, the study provides valuable insights into the potential role of slow cortical potentials within the pinch control paradigm.

Contents

1	Introduction	2
1.1	Hand motor rehabilitation	2
1.2	Slow cortical potentials	3
1.3	Research questions	4
1.4	Analysis	4
2	Methods	5
2.1	Explanation of SVIPT	5
2.2	Data	6
2.2.1	Performance metric	6
2.3	Analysis pipeline	7
2.3.1	Loading data	7
2.4	Parameter selection	9
2.4.1	Detection of bad channels	10
2.4.2	Independent Component Analysis	10
2.4.3	Epoch outlier detection	13
2.5	Feature selection	14
2.6	Prediction models	16
2.7	Holdout set	17
2.8	Performance evaluation	17
2.8.1	Statistical tests	18
3	Results	19
3.1	Reaction times	19
3.2	Pre-trial analysis	21
3.3	Pre-movement analysis	23
4	Discussion	27
4.1	Pre-trial	27
4.2	Pre-movement	27
4.3	Limitations	28
4.4	Further work	28
5	Acknowledgments	30
6	Source code	31
	References	32
A	Appendix	34

Chapter 1

Introduction

1.1 Hand motor rehabilitation

Accurate hand motor control is important for everyday life. Unfortunately, hand motor control is often negatively affected for post-stroke patients. The possibility of regaining some or all of the lost functionality will increase with proper hand motor rehabilitation. Hand motor rehabilitation approaches can vary widely. However, common to most is the use of a repetitive hand motor task. In theory, this would create new or strengthen existing neural pathways, in a process called neuroplasticity (Hallett, 2005). Neuroplasticity allows the brain to adapt to new circumstances. In the case of rehabilitation it would allow the neighbouring brain regions to take over the functionality of the damaged area, restoring the lost functionality.

In this work, emphasis is placed on force or pinch rehabilitation. Precise control of hand force is crucial for tasks such as grasping objects, manipulating tools, and performing fine motor actions. One common paradigm employed in rehabilitating hand force control is the sequential visual isometric pinch task (SVIPT), where participants navigate a cursor on a screen by pinching a force sensor. SVIPT aims to restore a patient's hand force control with repetitive trials. These trials are set up in a way where participants first receive a "get-ready" cue, indicating that they should begin preparing and anticipating the upcoming trial. After a short period, a "go" cue is provided, signalling the start of the trial and allowing participants to pinch the force sensor accordingly.

A previous study conducted by Meinel, Castaño-Candamil, Reis, and Tangermann (2016) utilised the SVIPT paradigm in an effort to find pre-trial oscillatory neural markers indicative of a participant's upcoming trial performance. Thus, their analysis only considered neural markers that occurred before the "go" cue. The research hypothesised that trial-to-trial fluctuations in performance could be explained by neural oscillations before the task onset. The paper was successful in identifying subject-specific oscillatory neural markers that were predictive of the SVIPT performance. The analysis was carried out offline on pre-recorded EEG data. However, in the future these findings could be used to create a closed-loop system, where the pre-trial brain state could inform the difficulty or start time of the upcoming trial. In theory, this closed-loop system has the potential to enhance the learning speed and, consequently, accelerate the recovery process.

1.2 Slow cortical potentials

For this reason it would be beneficial to find additional predictive neural markers that could possibly improve the accuracy of the predictions. One type of neural marker that might contain additional neural information is the slow cortical potential, also known as event related potential. These potentials are time-locked to the movement onset and have a relatively long buildup time. The underlying mechanism is often referred to as the pre-movement buildup, and corresponds with a slow buildup of neuronal firing peaking around the movement onset. Many slow cortical potentials have been described over the years (Schurger, Pak, Roskies, & et al., 2021) (Shakeel et al., 2015), differing mostly in experimental paradigms used to elicit them.

One of the more famous potentials is the Bereitschafts potential or readiness potential (RP). The RP, originally described by (Kornhuber & Deecke, 1965), is linked to voluntary motor activity. This is not very applicable to the experimental setup with the SVIPT, as it is not based on voluntary motor activity. The participants receive explicit "get-ready" and "go" cues. A more appropriate cortical potential for the SVIPT paradigm would be the contingent negative variation (CNV) (Walter, Cooper, Aldridge, McCallum, & Winter, 1964). The CNV response consists of an early component (O-wave) and a late component (E-wave), see figure 1.1. The early component is evoked by a warning stimulus (s1), which corresponds with the "get-ready" cue from the SVIPT. The late component is evoked by a stimulus requiring a motor response (s2), which corresponds to the "go" cue from the SVIPT.

As shown, the CNV response lines up well with the SVIPT procedure; therefore, it is hypothesised that a CNV-like response can be observable in brain signals recorded during SVIPT trials. It is important to note that the trials start at the time point at which the "go" or s2 stimulus is given. Therefore, the late component will not be taken into consideration for the pre-trial analysis. However, it can still be interesting to see how much additional information is present in the late component. This additional time window, containing the late component, will be referred to as the pre-movement window, as it falls between the start of the trial and the first movement onset, and will be investigated separately.

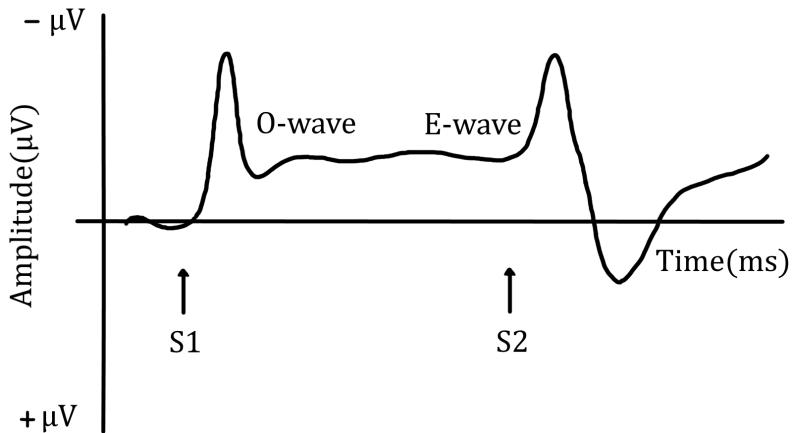


Figure 1.1: Graphical depiction of Contingent Negative Variation (Masi, 2021). Showing the O-wave and E-wave, in addition to the stimuli that evoke them. The vertical axis is reversed, where the negative values start at the top and positive values are below.

1.3 Research questions

This leads to the main research question, that reads as follows: *Can single-trial time-locked slow potentials extracted from pre-trial EEG data predict the upcoming performance of a hand force task?*

In order to properly answer this question, two sub-questions have been established:

1. Is the predictive power of the pre-trial analysis pipeline above chance level?
2. Is there significant cortical information in the pre-movement activity?

1.4 Analysis

To address these questions, it is necessary to create an analysis pipeline. One potential approach for extracting the slow potentials and predicting performance for the SVIPT trials, would be the employment of an event-related potential (ERP) pipeline. Such a pipeline would involve processing the EEG data to isolate the relevant slow potential features, and subsequently, utilising those features for performance prediction of the SVIPT task.

The process of isolating the relevant slow potentials within the ERP pipeline encompasses various techniques. These techniques include channel-wise and trial-wise outlier selection, in addition to artefact removal. By employing these methods, the analysis pipeline aims to enhance the accuracy, reliability and signal to noise ratio of the extracted slow potentials, enabling more precise predictions.

From the obtained slow potential a set of features has to be carefully selected. This selection procedure aims to select the most predictive features, without allowing overfitting to occur. The selected features are subsequently used to train predictive models. Reaction time was selected as the measure of performance of the SVIPT trials, and is the variable the models aim to predict. The fully trained models are applied on previously unseen data, in combination with the parameters selected during the training models. This step should show how well the model generalises to unseen data.

The analysis is conducted on both the pre-trial and pre-movement recordings for each individual subject. This approach recognizes the significance of individual variability in cortical layout and brain responses. As a result, a unique set of parameters is selected for each subject to account for these variations. By considering subject-specific parameters, the analysis pipeline can provide more personalised and precise predictions of performance in the SVIPT paradigm.

Chapter 2

Methods

The following chapter provides a detailed explanation on the methods used during this research. First, it will go over the experimental setup used to acquire the brain data. Second, the properties of the data itself will be discussed. Third, the analysis pipeline will be treated in great detail, discussing the different parts from pre-possessing, to feature selection and model training. Fourth, the methods for evaluating the results are considered, this section also includes the descriptions on the statistical tests.

2.1 Explanation of SVIPT

The sequential visual isometric pinch task (SVIPT), was used in Meinel et al. (2016). This research builds on the data collected in that work. The specific implementation of this particular SVIPT setup was first discussed in an earlier paper (Meinel, Castaño-Candamil, Dähne, Reis, & Tangermann, 2015), see figure 2.1. In this specific setup the patient has a force sensor in their non-dominant hand, which is used to move a cursor over a screen. The goal of each trial is to move the cursor between three fields T0, T1 and T2, in a specific order. Where each target field corresponds to a specific force value. In addition, each trial has three phases. During the first phase, a light blue cursor appears on the leftmost edge of the T0 field, indicating the start of the "get-ready" phase. This phase requires the user to slightly touch the force sensor while waiting for a period that varies randomly between 2 and 3 seconds. During this phase, the conversion of force into the cursor is deactivated, and the user's attention level is enhanced. The cursor then changes colour from light to dark blue, giving the "go" cue and indicating the start of the running phase. In this phase, the user can control the position of the cursor by applying force to the sensor. The cursor moves horizontally, and increasing force moves it towards the rightmost position, which represents 30% of the user's maximum force. The user must navigate the cursor quickly and accurately to visit a sequence of target fields, indicated visually by a green shading. A successful hit of a target field requires a dwell time of 200 ms, and skipping a target field is not allowed. Each trial is randomly chosen from two conditions, each with a specific required target field sequence (T1-T0-T2-T0 or T2-T0-T1-T0). Trial duration is presented visually as immediate performance feedback during the pause phase between trials.

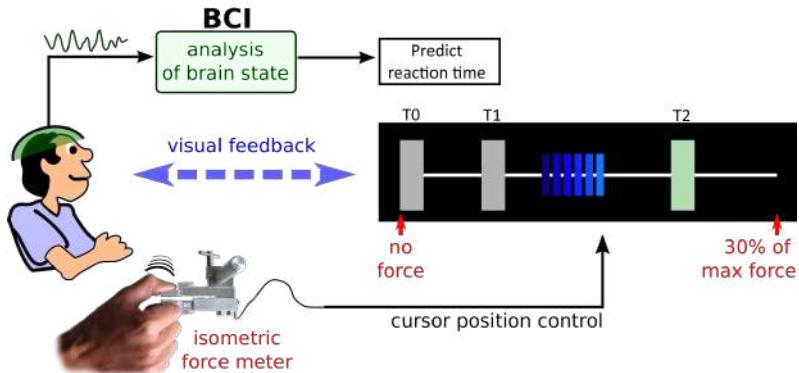


Figure 2.1: The setup of the SVIPT experiment (Meinel et al., 2016).

2.2 Data

The data utilised in the subsequent analysis was collected in the study conducted by (Meinel et al., 2016). Electroencephalography (EEG) was employed as the method for capturing the participants' brain signals throughout the SVIPT trials. EEG allows for the non-invasive measurement of electrical activity in the brain. The EEG signals were recorded with a sampling frequency of 1000 Hz and a 63 electrode setup. The experiment was conducted with 18 subjects, from which 8 were female and all were right handed. The average age was 53 years with a standard deviation of 6 years. The subjects were selected to be "normally aged", which translates to the participant group representing the target group of first-time stroke patients. The subjects were selected to not have any known neurological or psychological history and were to all knowledge healthy. Each participant completed 20 blocks of 20 SVIPT trials in a single session.

2.2.1 Performance metric

The analysis in this paper aims to predict the performance for each SVIPT trial. The reaction time was selected as the performance metric and is defined as the time between the start of the trial and the time the participant first applies pressure to the force sensor. The specific times at which these events occur are taken from the marker file provided for every block of trials. The markers for the go cue are s210 and s211. There are two types of go cue markers, because there are two different orders in which the participant has to visit the target fields. The marker that shows the first force sensor activation has a value of s150.

A number of assumptions is made on the order in which the markers appear. First, the first go cue event (s210, s211) will not be preceded by an activation event (s150). Second, after the last activation event no more go cue events will take place. Third, between two go cue events there will always be an activation event. As well as the other way around, between two activation events there always is a go cue event. If these assumptions are not met, the trials are not computable and are not considered for further analysis.

2.3 Analysis pipeline

The analysis pipeline is divided into three distinct sections. The first section is responsible for loading the data and doing the first basic pre-processing. The second section selects the appropriate parameters, for example bad channels, bad trials, and selecting the appropriate spatial filtering. The third section of the pipeline does the feature selection, which are used to train the prediction models. Subsequently, the selected parameters and trained models are applied to unseen data, the so-called holdout set, to test how generalizable the results are. This analysis pipeline is employed for both the pre-trial and pre-movement analysis. The primary distinction between these two analyses lies in the event to which the epochs are time-locked. In the pre-trial analysis, the epochs are time-locked to the "go" cue event, which indicates the start of the trial. Conversely, in the pre-movement analysis, the epochs are time-locked to the event of the first movement onset.

2.3.1 Loading data

The full data set consisting of 18 participants, with each 20 sessions, containing 20 trials, takes up about 63 GB of disk-space. However, only part of the data is interesting for the following analysis. Therefore, only the parts of interest are cut out and saved to local disk for later use in the analysis. This will increase efficiency, as the raw data only has to be loaded once. This procedure is depicted in figure 2.2.

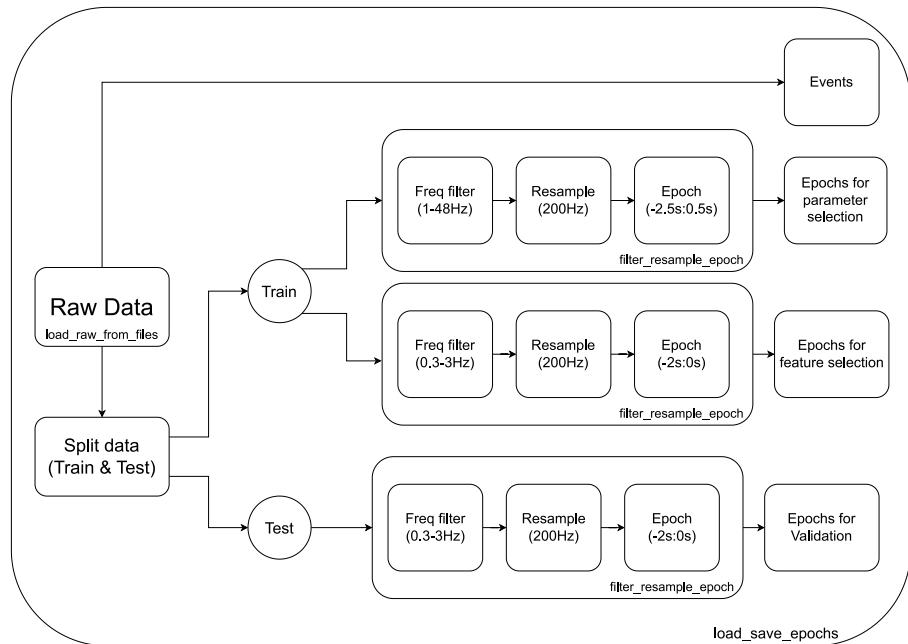


Figure 2.2: Illustrates the process of loading and pre-processing the raw data. It depicts how four data sets are extracted, which are subsequently saved to disk for later use.

From figure 2.2 it becomes apparent that the raw data is used to extract four different data sets, that will all be saved to the local disk. Of the four, the *events* data is the most straightforward. It is gathered from the marker file (.vmrk) and contains a time ordered list of markers and the time points at which they occur. Apart from the events, three collections of epochs are created with both different functions. The raw data is first split up

into a train set and a test/ holdout set, as can be seen in figure 2.2. For the final analysis low-frequency signals are of interest. The epochs that solely contain these low-frequent signals are called 'Epochs for feature selection' and 'Epochs for validation', where the former are used during the training stage and the latter during the validation procedure. The pre-processing steps are equivalent between the two types of low-frequency epochs.

The difficulty with the low frequent signals is that a large part of the information in the signal is discarded. Information that is needed for making decisions on cleaning the data. For instance deciding which channels or epochs are considered outliers, or finding spatial filters with independent component analysis (ICA). For this purpose a different collection of epochs are created called 'Epochs for parameter selection', see figure 2.2. They are used to find a set of appropriate parameters that can later be applied to the low-frequency epochs.

Creating epochs

In order to create the epochs as mentioned above, from raw data, three steps are required. First, the continuous data is band pass filtered to the desired frequency interval. This is done with a zero-phase filter (Kormylo & Jain, 1974) to ensure that the signal is not shifted in time. Zero-phase filtering will create distortion at the start and end of the signal. Therefore, the filtering step is done on the continuous data, as the distortion happens only twice and in parts of the data that are not significant to the later analysis. Second, the signal is re-sampled to a lower sampling frequency. This step is done after the frequency filtering and with a wide enough margin to ensure no aliasing will occur. The motive behind this step is to reduce the size of the data, which will simplify later computations. Third, the continuous data is cut up into epochs based on one or more events in the data. A period time before and after the event(s) can be specified to be included in the epochs. From figure 2.2 follow two types of epochs that will be used in the analysis.

First, the two sets low-frequency epochs that are created from the train and holdout data. These epochs are first band passed filtered to a range of 0.3-3 Hz, as the low frequencies are the point of interest. The actual range was selected based on similar studies (Ofner et al., 2019; Ofner, Schwarz, Pereira, & Müller-Putz, 2017; Abou Zeid, Sereshkeh, & Chau, 2016). Then the signals are re-sampled to 200 Hz, which is a signal reduction of five times. The signals could be re-sampled to a much lower sampling frequency given the upper-bound of the band pass filter. However, it is beneficial to keep the same sampling frequency between the two sets of epochs. Lastly, the signal is cut up into the individual epochs based on the area of interest. The pre-trial analysis defines the area of interest as a window of 2000ms before the "go" cue. While the per-movement analysis is interested in a window of 2000ms before the first movement onset.

Second, the epochs that are used for parameter selection. They are band-pass filtered to a range of 1-48 Hz. Where the high-pass part of the filter is set to 1 Hz and is used to remove low frequent artefacts, such as breathing (Suleiman, Fatehi, & et al., 2007). In combination with removing any drifts that might occur over time. Furthermore, using a high-pass filter of 1-2 Hz can create a better signal-to-noise ratio (SNR) when paired with ICA (Winkler, Debener, Müller, & Tangermann, 2015). The low-pass part of the filter is set to 48 Hz, which gives enough frequency information to properly perform the parameter selection. In addition, 48 Hz was selected to stay right under the 50 Hz power-

line noise, while retaining most of the important neural information. Subsequently, the signal is re-sampled to 200 Hz, similarly to the low-frequency epochs. Lastly, the epochs are created in a comparable way as the low-frequency epochs. However, both at the start and the end of the epoch a window of .5 seconds is added. This is done to accommodate certain pre-processing steps in the parameter selection.

2.4 Parameter selection

The following section presents a description of the parameter selection procedure. It begins by loading the epochs mentioned in the previous section as "epochs for parameter selection", and subsequently applies multiple pre-processing steps. Each pre-processing step generates a set of parameters that will later be applied to the low-frequency signals.

First, a channel-wise outlier detection method is employed to identify and remove channels exhibiting abnormal behaviour. This step ensures the removal of channels that may introduce noise or distortions to the analysis. Next, Independent Component Analysis (ICA) is utilised for artefact removal. This step involves transforming the data to a set of independent components, from which the artefact components are identified. Following artefact removal, epoch-wise outlier detection is performed. This step helps identify outlier epochs, which may be influenced by noise or other irregularities. These three pre-processing steps yield a list of bad channels, a set of spatial ICA filters, and a list of outlier epochs. These results are saved for later use. This procedure can be viewed in figure 2.3.

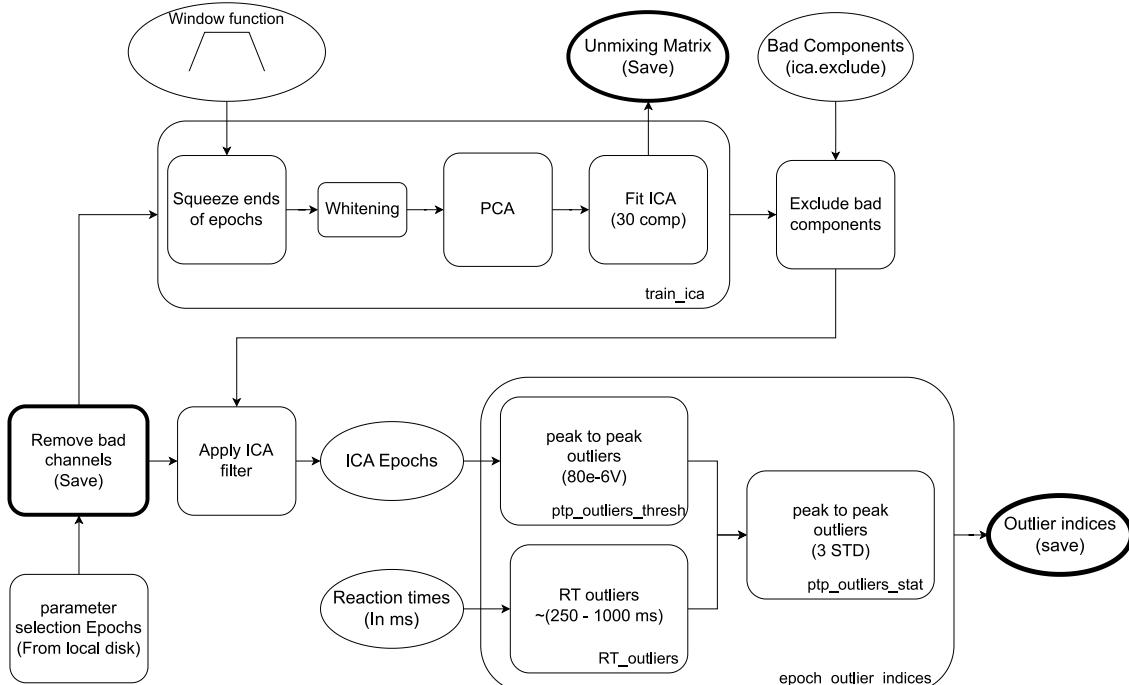


Figure 2.3: Depicts the parameter selection procedure. Where variables are depicted as circles and functions as boxes. The names of the most important functions are given in the lower right corners; these names correspond to those used in the actual code. The sections highlighted with thicker lines indicate the parameters of interest.

2.4.1 Detection of bad channels

The first step of the parameter selection involves the detection of 'bad' channels. Bad channels are most often caused by problems during the recording of the EEG signals. These problems can range from electrodes that slowly lose their connection to ones that are broken or are short circuiting. These inconsistencies can be manually detected, by inspecting the raw data. However, to save on time an automatic channel detection strategy was implemented to save on time. The results of this detection were still checked for any missing bad channels or inconsistencies. The detection strategy in question is a modified version of the one described by Komosar, Fiedler, and Haueisen (2022). First, the standard deviation is calculated for every individual electrode channel. Where the standard deviation for one of the channels is denoted by SD_j for the j -th channel and where N denotes the length of the recorded signal.

$$SD_j = \sqrt{\frac{1}{N-1} \sum_{i=1}^N |V_{(i,j)} - \bar{V}_j|^2}$$

The identification of channel-wise outliers involves three criteria. The first criteria inspects whether the median-corrected standard deviation is larger than the 75th percentile of standard deviations, where the median over the channel standard deviations is denoted by M . This criterion helps identify channels with higher variability compared to the majority of channels. The second and third criteria make use of the absolute thresholds. Where the second criterion checks if the standard deviation exceeds a threshold of $100\mu V$, ensuring that excessively large deviations are flagged as outliers. For the second and third criteria an absolute threshold is used that checks if the standard deviation does not exceed $100\mu V$ and does not go below $10^{-4}\mu V$.

$$\begin{aligned} |SD_j - M| &> 75th \text{ percentile} \\ SD_j &< 10^{-4}\mu V \\ SD_j &> 100\mu V \end{aligned}$$

This procedure of automatic outlier detection and manual inspection is done separately for every participant. Subsequently, the names of the outlier channels are saved and removed from all the channels of the participant in question.

2.4.2 Independent Component Analysis

ICA is used to separate a set of mixed signals into their underlying independent components or sources. It is an unsupervised method, meaning it can extract original source signals from a mixture without any prior knowledge about the sources or the mixing process. Moreover, ICA makes the following assumptions about the data. First, the sources are a linear mixture of the recorded signals. Second, at least $n - 1$ of the sources follow a non-Gaussian distribution. Third, the independent components or sources are independent from each other at each point in time. Thus, ICA tries to find an unmixing matrix W that unmixes the signals x into the independent components or sources s , giving:

$$x = Ws$$

The entire left hand side of the function is unknown, this makes ICA nondeterministic. This means ICA uses an iterative method that in each iteration tries to find a set of

independent components that is more and more non-Gaussian.

As can be seen in the procedure `train_ica` depicted in figure 2.3, training the ICA model requires a number of additional steps apart from the actual fitting of the model. First, each epoch is multiplied with a so-called squeeze function. This function ensures that each epoch starts and ends at 0 μ V. In order to gradually transition from 0 μ V to the real EEG signal and back to 0 μ V, an area of .5 seconds was added on both sides of each epoch in Creating epochs 2.3.1. The squeeze function is applied before ICA, because the continuous data were previously divided into epochs. When the ICA function reserves epochs they will be concatenated, which leads to jumps in amplitude between the successive epochs. This could in turn lead to the ICA using one or more independent components to model these jumps in amplitude. Figure 2.4 depicts the application of the squeeze function on one channel of one epoch.

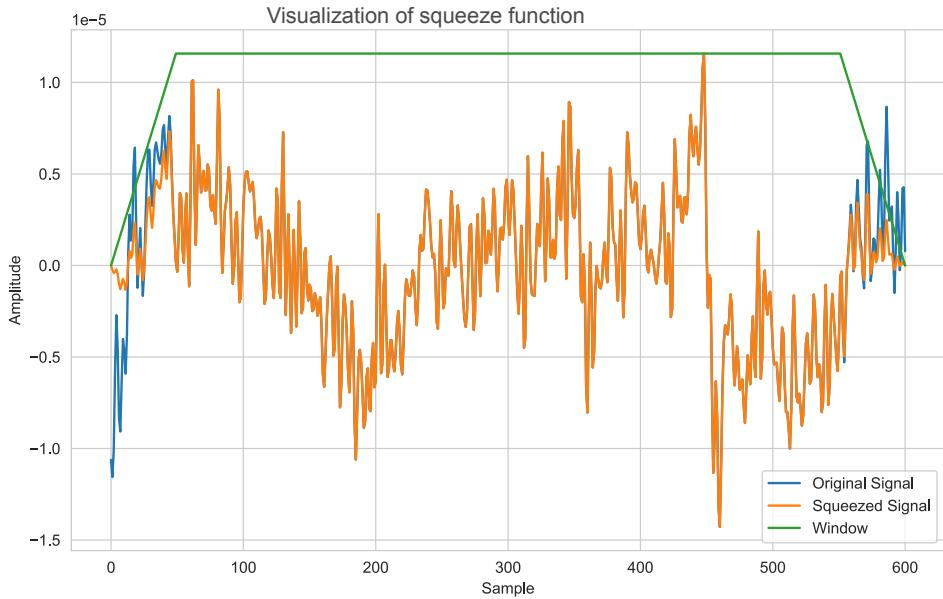


Figure 2.4: Showcases the squeeze function on a single epoch, channel instance. The green line corresponds to the window that is applied on the signal, in order to make it start and stop at zero amplitude. Therefore, the difference between the original signal (blue) and squeezed signal (orange) is only present at the start and end of the epoch.

Second, the squeezed epochs are transformed with a pre-whitening step. This is done by taking the standard deviation for each channel and calculating the dot product between it and the data. This should help to standardise the variance of each channel, ensuring that each channel contributes equally to the ICA decomposition and stops certain sources from dominating the independent components (Makeig, Bell, Jung, & Sejnowski, 1995). Third, this is followed with a Principal Component Analysis (PCA). PCA maps the whitened data to a new space of principal components. These components are based on variance and are orthogonal to each other. This will increase the computational efficiency of fitting the ICA model, by creating a initial decomposition between the sources of interest and the noisy sources (Delorme, Palmer, Onton, Oostenveld, & Makeig, 2012). After these steps the ICA model can be fitted, resulting in the unmixing matrix W , which is saved to

local disk for later reuse. Additionally, the mixing matrix A is also computed, this is done with a pseudo inverse of the unmixing matrix, $A = W^+$. The specific implementation of ICA that is used is FastICA (Hyvärinen & Oja, 2000).

After finding and excluding the independent components that contain artefacts, see section below, the ICA is applied to the origin epochs. This means that the epoch data is first unmixed into its independent components. After, the ‘bad components’ are removed from the set of independent components. Finally, the mixing matrix is applied to get back to the sensor space. This is the explanation offered by the documentation of the mne library (Gramfort et al., 2013). However, after having a closer look at the source code, the procedure is slightly different. First, the eigenvector matrix V obtained during PCA is used to reverse both the mixing matrix A and unmixing matrix W out of PCA space, which will be called \bar{A} and \bar{W} respectively.

$$\bar{A} = V^T \cdot A$$

$$\bar{W} = W \cdot V$$

Second, a selection is made from both of these matrices based on the independent components that were not excluded, denoted as \bar{A}_{sel} and \bar{W}_{sel} . From these two matrices the dot product is taken in order to create a projection P that can be applied on the epoch data.

$$P = \bar{A}_{sel} \cdot \bar{W}_{sel}$$

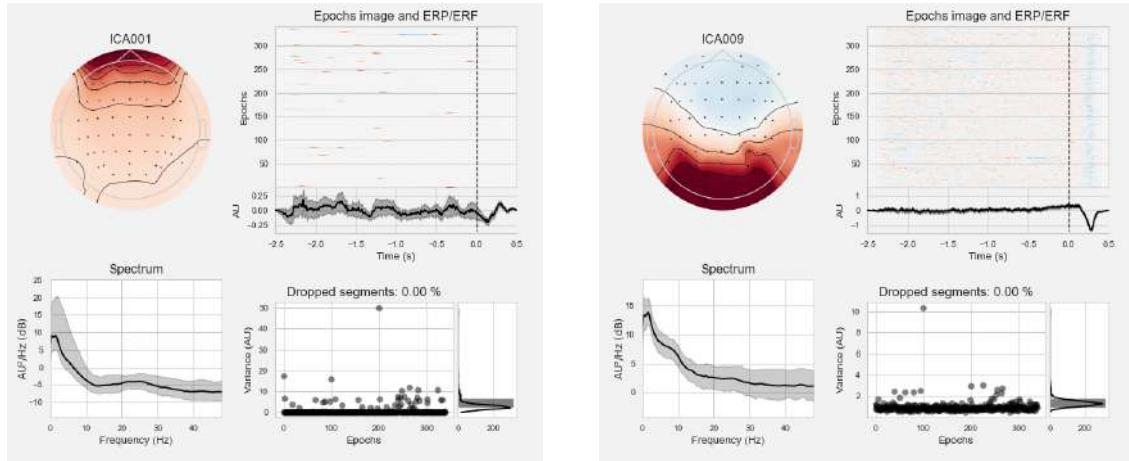
Third, this projection cannot be directly applied to the data, as it assumes the data is whitened, which is not the case. This could be resolved directly in the projection, but it was not. Instead, the epoch data was first whitened in the same way as in the ICA train procedure, and after applying the projection on the whitened data, the whitening is reverted. Giving the epoch data in the original sensor space, with a number artefact sources removed. It is important to keep in mind that removing independent components reduces the rank of the data by one for every removed component. However, none of the further methods require the full rank data, so this will not be of concern.

Selecting artifact ICA components

The correct independent components have to be selected in order to properly remove artefacts and retain as much brain data as possible. There are a number of automatic techniques developed for this purpose (Dharmaprani et al., 2016; Hanna, Kim, & Müller-Voggel, 2020; Viola et al., 2009). Nevertheless, the gold standard still requires visual inspection of the independent components (Chaumon, Bishop, & Busch, 2015). In figure 2.5 three example ICA components are shown. For each component the spatial pattern, a heat map of the epochs over time together with the average signal, the frequency spectrum, and the variance in each epoch with its corresponding distribution are plotted.

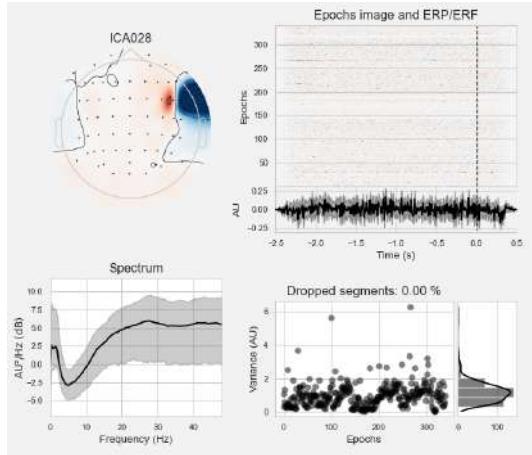
In figure 2.5, three examples are given of commonly seen ICA components. For each a short explanation will be given on what class of components it belongs to. First, in figure 2.5a it can be observed that almost all of the activity is at the front electrodes. In combination with many short bursts in the epoch heat map and high variances for those epochs. These characteristics are in line with what is expected from an eye-blink artefact. Therefore, it might be beneficial to exclude this specific component. Second,

the spatial pattern evident in Figure 2.5c shows promising characteristics, notably with a distinct activation in the occipital lobe. Coupled with a frequency spectrum displaying a downward slope and a consistent activation over epochs, it is highly probable that this component encapsulates brain data. Third, the spatial pattern in Figure 2.5c, being concentrated in a single location, along with a consistent noisy time course and significant high-frequency activity in the frequency spectrum, strongly suggests that it represents muscle muscle artefact.



(a) Component likely to be related to eye blinks.

(b) Component likely to be contain brain signals.



(c) Component likely to be contain muscle artefacts.

Figure 2.5: Contains three examples of Independent components. Where for each component the spatial pattern, heat map of the epochs over time together with the average signal, frequency spectrum, and variance in each epoch with its corresponding distribution are displayed.

2.4.3 Epoch outlier detection

After cleaning the data by removing the independent components that contain artefacts, it could still be the case that some of the epochs should not be included in the training of the prediction models. Therefore, an epoch wise outlier detection is done. Three different types of detection are applied to the epochs, as can be viewed in the

`epoch_outlier_indices` selection in figure 2.3. The first of which is a simple peak to peak filter, which is often referred to as a min-max filter. It calculates the distance between the smallest and largest point for each epoch-channel combination. If one of the channels crosses the set peak to peak threshold for any given epoch, then the corresponding epoch will be marked as an outlier. Next, the reaction times are scanned for any outliers. A reaction time is considered an outlier if it is either too fast or too slow, or if it is not computable. What are considered fast and slow reaction times may vary between participants, where the thresholds are adjusted based on the individual. A reaction time might be uncomputable due to problems in the marker files from which they are calculated. The procedure for finding the uncomputable reaction times is described in section 2.2.1. These two types of outliers are aggregated and the resulting indices are stored. A copy is made of the epoch data from which the aggregated outliers are removed. On the remaining epochs a third outlier detection step, based on a statistical threshold is executed. Again, the peak to peak distances for each epoch-channel combination are used. Then, the mean and standard deviation of the peak to peak distances are computed for each channel. If an epoch is more than three standard deviations away from the mean, it is considered an outlier and added to the list of outliers from before. The indices from the resulting outliers are saved for later use.

2.5 Feature selection

In the following section, the parameters obtained through the parameter selection process are applied to the low-frequency epochs created for feature selection. If present, the slow cortical potentials of interest should be observable within these cleaned low-frequency signals. From these signals the most prominent features are selected. These features can then be used to train the prediction models. The full procedure is depicted in figure 2.6. Where the steps at the top of the figure apply the obtained parameters to the epochs, and the steps at the bottom of the figure extract the features.

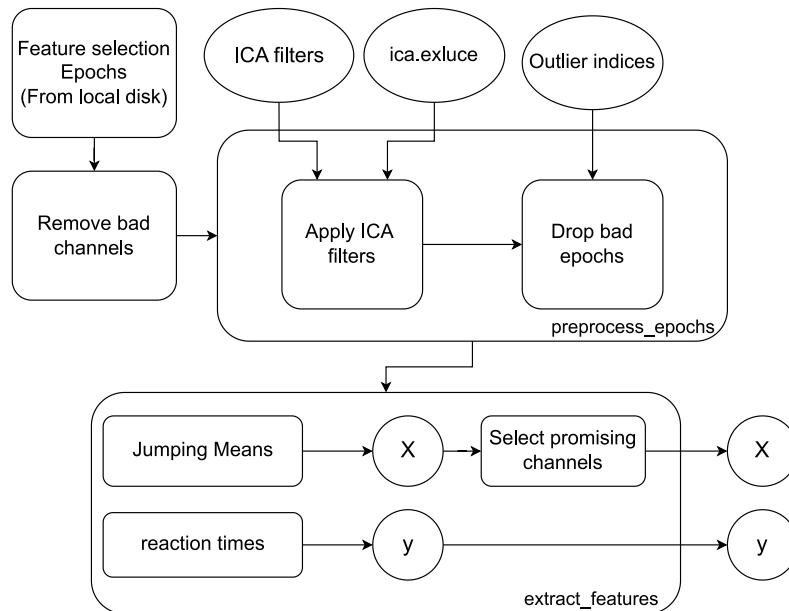


Figure 2.6: Depicts the feature selection procedure. Where the round elements represent variables and the rectangular ones represent functions.

The steps at the top of the figure 2.6 involve the exclusion of the previously selected outlier channels. Subsequently, the channels are transformed into the independent components by applying the ICA unmixing matrix. After removing the independent components which were found to contain artefacts, the remaining independent components are transformed to the original channel space by applying the ICA mixing matrix. Finally, the epochs identified as outliers during the parameter selection step are removed.

These cleaned epochs are subsequently used to create the y (dependent variable) and X (independent variables). For the value of y , the reaction times corresponding to each epoch are used. The number of features in the epochs, without performing any feature selection, is extremely high. With an epoch length of 2 seconds, a sample rate of 200 Hz, and 63 channels, there would be a total of 25,200 features. Technically, the signal could be resampled to around 10 Hz; however, even with this lower sample rate, the number of features would still be 1,134.

To address this issue, the feature selection process aims to select a limited number of features from both the temporal and spatial domains, separately for each of the participants. In the time domain, participant-specific selection involves choosing 3 windows, represented by the grey intervals in figure 2.7. For each time window, the mean value per channel is calculated, this step corresponds to the Jumping Means in figure 2.6. Identifying the time windows is based on finding the most prominent peaks and valleys in the averaged signal, as these sections are expected to contain the most informative data. Furthermore, in the spatial domain, 5-6 channels are selected based on the distinctiveness in the selected windows, along with an examination of their topographic activation. The topographic maps used for feature selection are specifically chosen from the centre of each of the three windows, see figure 2.7. Given the 3 averaged windows and 5-6 selected channels, the resulting number of features that will be employed to train the prediction models ranges from 15 to 18 features.

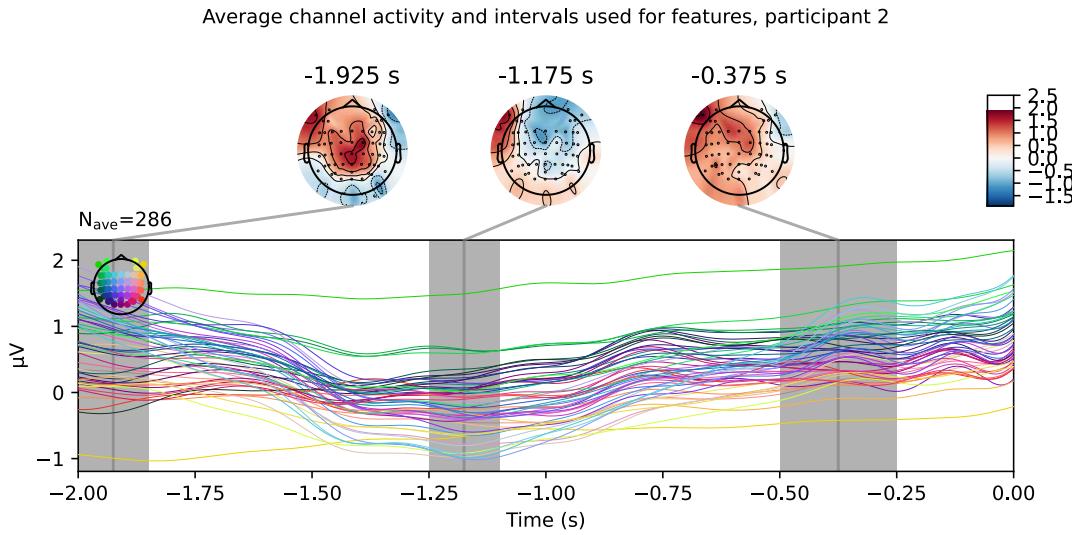


Figure 2.7: Contains the average channel activation of the pre-trial activations for participant 2. The colours of the plotted lines correspond with a specific channel, which are indicated at the top left corner of the plot. Additionally, three grey windows are present, which mark interesting sections in the signal. For the centre of each of the grey windows a topographic map is shown.

2.6 Prediction models

The following section covers the models employed to predict the reaction times of the SVIPT trials. Two models were utilised for this purpose: a regression and a classification model. The regression model directly attempts to predict the reaction time, while the classification model splits the reaction times into slower and faster classes at the median. The inclusion of the classification model in addition to the regression model is motivated by the possibility that predicting individual reaction times may not be feasible. By using the classification model, it provides an alternative approach that might simplify the prediction task, possibly leading to an improved performance. Both models are trained on the same selection of features and subsequently evaluated with the same methods, although using different test statistics.

The regression model utilises a simple linear regression approach, assuming linear relationships between the variables. Additionally, the classification model employs Linear Decomposition Analysis (LDA) to achieve optimal linear separation between distinct groups (Shinmura, 2011). Regularisation is applied to the coefficients of both models to enhance generalizability and combat overfitting. In this case, L1 or Lasso regularisation is used, which adds a penalty for large coefficient values and effectively shrinks them (Santosa & Symes, 1986). Lasso regularisation was selected over other regularisation techniques, such as Ridge, due to its comparatively milder penalty on larger coefficients. Unlike Ridge regularisation, which squares the values of the coefficients, Lasso regularisation only takes the absolute values. This property was found to be quite important for the performance of the models.

2.7 Holdout set

After training the prediction models it was important to apply them to unseen data. If the models were working correctly, they should retain the same level of predominance between the train and holdout data. If this would not be the case, it would be a sign that the models were overfitting on the train data. To combat this, a portion of the data was reserved at the start of the analysis, and is only used towards the very end. For this process, the parameters were copied from the training analysis, as no new parameters should be learned by the holdout data. The only exception being, the epoch-wise outliers, as they are not transferable. The only epochs that were discarded from the holdout set, were those for which the reaction times were not computable. Additionally, the exact same features selection was applied on the holdout set. Finally, the selected features would be applied to the pre-trained models.

2.8 Performance evaluation

Creating the analysis as laid out in the previous sections, was partially an iterative procedure. As aspects of the analysis were changing it was important to have a strong grasp on whether the performance of the models were improving or worsening. For this, both performance metrics and visual inspection by plotting the results were used. This iterative procedure was carried out on the portion of trials selected for training the data. In addition, it is important to test if the performance that was achieved on the train data generalises to unseen data. For this reason part of the data was withheld from train data called the holdout set, see previous section. Then, the results of the prediction models on the holdout set were tested for significance, to see if the possible improvements in performance could be due to random chance.

For the evaluation of the classification model a 5-fold cross-validation was selected. The 5 folds were chosen because it offers the right ratio between train and test data, as the number of data points is not extremely large. The performance measure AUC (Area Under The Curve) of the ROC (Receiver Operating Characteristics) curve was used. In addition, two plots were saved for visual inspection; the ROC curve was plotted in combination with the confusion matrix. For a binary classifier, the confusion matrix is a 2x2 matrix that contains the number of correctly predicted values for both classes, in addition to the false-positives and false-negatives. Instead of plotting these two plots for every one of the five folds, the average over the folds was taken.

The evaluation of the regression model did not use cross-validation. Instead, the data was simply split into a train and validation set. This is much less data efficient than cross validation, but does increase the readability of the plots. As a score metric the R^2 score was selected, which is very interpretable due to it being a probability range. In order to visually inspect the results, the predicted reaction times were plotted in the same plot as the real reaction times. In addition, to make this relationship more clear, a scatter plot with the real against the predicted reaction times was plotted.

2.8.1 Statistical tests

In order to properly validate the results of the analysis, a statistical test called permutation testing is used. Permutation testing belongs to a group of non-parametric tests, which means that the method does not assume any underlying distribution, such as the normal distribution. This flexibility makes it suitable for a wide range of use cases. The permutation test requires a statistic that quantifies the performance of the prediction model. In the case of the classification model, the chosen statistic is the accuracy or Jaccard similarity, which measures the agreement between predicted and actual class labels. On the other hand, for the regression model, the selected statistic is the R^2 score, which indicates the proportion of variance explained by the model. Both of these statistics are subjected to a one-sided test in order to determine whether there is a significantly higher statistical value than expected by random chance.

The validation procedure involves applying the pre-trained models to the holdout data, from which the resulting statistics are noted down. After this, the order of the dependent variable (reaction time or reaction time split into two classes) is randomly permuted/shuffled. This means that any set of features can be paired with any dependent variables. By computing the test statistic on the permuted data, an estimate is obtained of what the score would be if there were no relationship between the features and the dependent variable. Repeating the steps of permuting and computing the test statistic many times, creates a distribution of possible test statistics. If the number of permutations is high enough, it is likely that the discovered distribution matches the underlying one. From this distribution, the p-value can be computed. proportion, or the normalised number, of permutations that yield test statistics greater than or equal to the value observed in the original unpermuted data. A p-value below 0.05 indicates statistical significance, suggesting that the results are unlikely to be due to random chance.

Chapter 3

Results

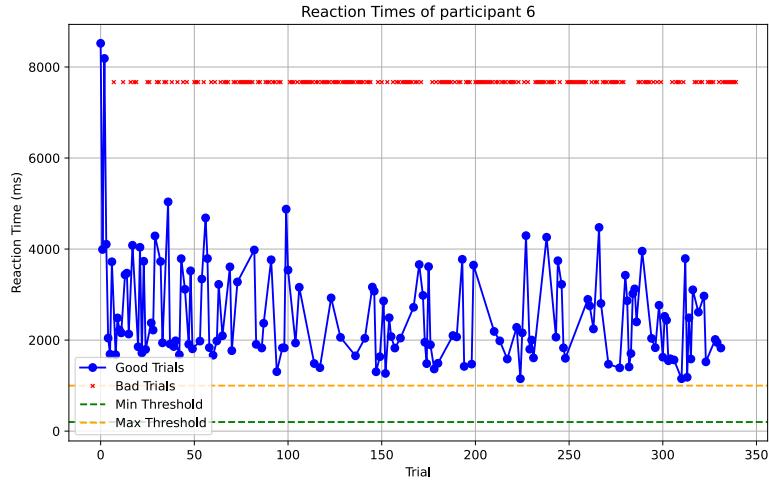
The following chapter presents the outcomes of the proposed slow potential analysis applied to the SVIPT data recorded by (Meinel et al., 2016). First, noteworthy results regarding the acquisition of the reaction times are discussed. Moreover, a distinction is made between the pre-trial and pre-movement analysis. For each of these analysis a further distinction is made between the results of the training and holdout sets.

To address the proposed research questions, the analysis was conducted on both the pre-trial and the pre-movement slice of the EEG signals. (Refer back to the section explaining the difference between pre-trial and pre-movement). Both approaches are individually discussed for the model training and holdout validation. By examining the various stages of analysis, a comprehensive overview of the results is presented.

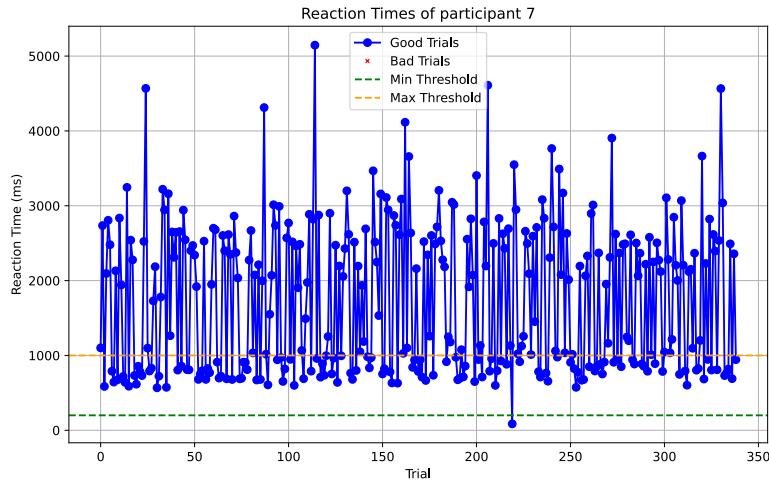
3.1 Reaction times

In the section on creating the reaction times 2.2.1, the procedure for finding trials with uncomputable reaction times was outlined. The computable reaction times were subjected to an outlier detection, where extremely slow or extremely fast reaction times were removed. Grouping both the uncomputable and outlier reaction times together, it was found that participants 6, 7 and 8 had substantially more rejected reaction times than the others, ranging from 70-100% of reaction times. For this reason the three participants in question were excluded from further investigation.

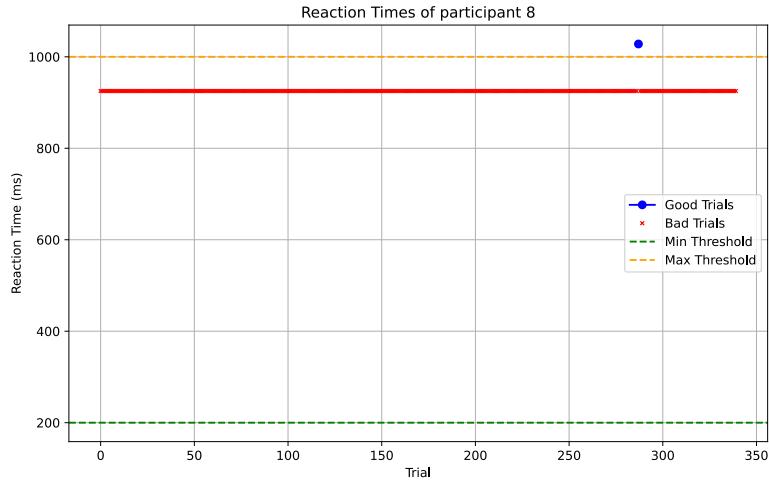
When inspecting the reaction time plots 3.1, it becomes apparent that the three participants have quite large differences between their reaction time plots. The reaction times of participant 8 (fig.3.1c) are composed of only uncomputable reaction times, except one. After closer inspection it was found that the marker representing the first force detection only occurred once. Therefore it was not possible to compute the reaction times. In contrast, the reaction times for participant 7 (fig.3.1b) only contain computable entries. However, many of the reaction times are over 2000 ms long, which is not normal behaviour. Observing the plot it is noticeable that the large reaction times form a group centred around 2200 ms, besides an expected group of reaction times centred around 800 ms. The reaction times of participant 6 (fig.3.1a) seem to fall somewhere in between the reaction times of participants 7 and 8. Where a large number of the reaction times were not computable and those that were computable are considered too slow.



(a) Reaction times of participant 6



(b) Reaction times of participant 7



(c) Reaction times of participant 8

Figure 3.1: The sub-figures display the reaction time plots for each of the three problematic participants. Where the trials marked with a red 'x' were not commutable, and those with a blue 'o' were. The orange and green dashed lines represent the minimum and maximum thresholds. Reaction times that fall outside of the given thresholds are considered outliers.

3.2 Pre-trial analysis

The pre-trial analysis plays an important role in addressing the main research question. It involves examining the EEG signals recorded prior to the trial onset or go-cue, with the objective of predicting the subsequent trial's performance, specifically in terms of reaction time. The initial phase of this analysis involves data cleaning to extract the slow potentials of interest. This pre-processing step hopefully ensures that the subsequent analysis focuses on the desired signals.

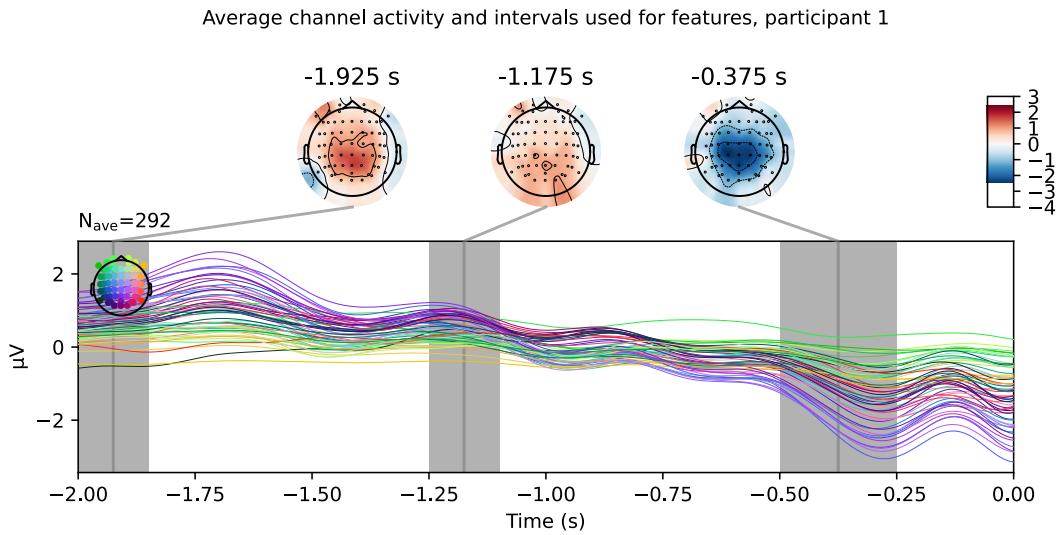


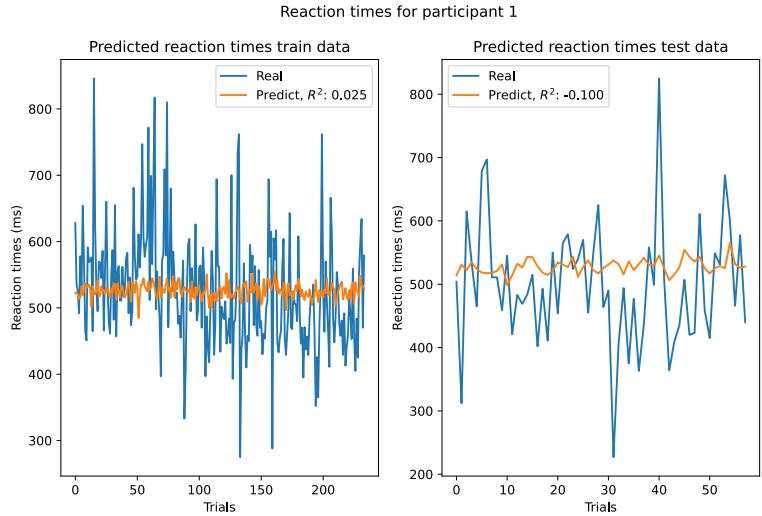
Figure 3.2: Contains the average channel activation of the pre-trial activations for participant 1. The colours of the plotted lines correspond with a specific channel, which are indicated at the top left corner of the plot. Additionally, three grey windows are present, which mark interesting sections in the signal. For the centre of each of the grey windows a topographic map is shown.

Figure 3.2 shows the pre-trial cleaned signals for participant 1. The cleaned signals do not show any pronounced activity, for example in the form of strong peaks or valleys. There is, however, an observable difference between the signals towards the front and the center/back of the brain, where the former does not show any activity and the latter shows a downward trend combined with a slow oscillation. Unfortunately, this observation does not seem to be very consistent over the participants. Furthermore, no other patterns could be recognised for the pre-trial activations.

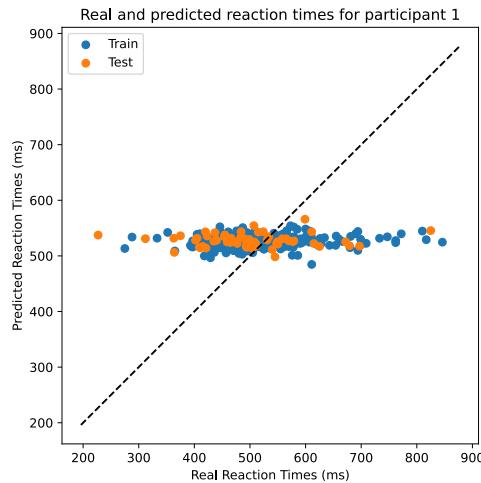
This caused issues during the feature selection, as it is based on selecting the interesting parts of the signals. Some experimentation was done by moving the time windows around, however, this did not yield any significant results. These issues were also problematic for the channel selection, as it was non-trivial to find the channels with promising activation. For this reason, the channels were selected based on prior knowledge of the slow cortical potentials, as they occur most prominently in the central and lateral part of the brain.

The features are subsequently used to train both the regression and classification

models. The results of the regression model on the pre-trial signals of participant 1 can be viewed in figure 3.3. From the figure it is apparent that the regression model does capture the mean of the data, but not much else. This is especially apparent when observing the scatter plot in 3.3b, where the predictions for all of the reaction times are roughly the same. This trend holds for all of the participants.



(a) Predicted and real reaction times for the train and test data.



(b) Scatter plot of the real against the predicted reaction times.

Figure 3.3: Shows the results of the regression model on the train data for participant 1.

Similar behaviour can be observed for the classification model. Where the performance is not above chance level for any of the participants. To illustrate this point the averaged ROC curve and confusion matrix for participant 1 are plotted in figure 3.4.

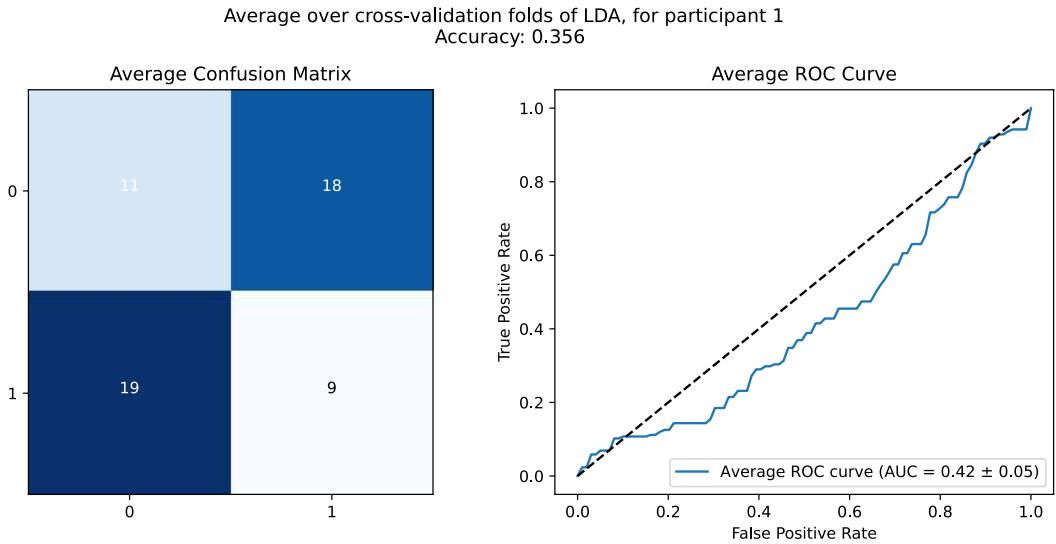


Figure 3.4: Shows the results of the classification model trained on the pre-trial signals for participant 1. The left hand side shows the confusion matrix, with the light cells being predicted correctly and the darker ones incorrectly. On the right side the ROC curve is plotted.

As is to be expected, applying the trained models to the holdout data yields similar results as have already been shown. Where there were no significant results above random chance for any of the participants.

3.3 Pre-movement analysis

The pre-movement analysis, is interested in the signals after the trial onset but before the first movement. It was hypothesised that these signals may include additional information to that found in the pre-trial signals. As described earlier, the analysis on the pre-movement signals was identical to the one performed on the pre-trial signals. Therefore, the same type of plots are displayed as in the previous section on pre-trial analysis 3.2.

After the data cleaning and visually inspecting the averaged signals, it becomes apparent that most participants can be divided into two groups, based on the shape of the activation. The activations of the first group start with a downward motion followed by an upward sweep. An example of this type of activation can be found for participant 1, see figure 3.5a. The second group of activations only has one large peak, without ever going down. An example of this activation can be found for participant 5, see figure 3.5b.

Most of the participants belong to the first group, while not all of them have as distinct activation as participant 1. These participants are: 1, 2, 3, 9, 11, 12, 13, 14, 17 and 18. The other group only contains three participants: 5, 15, 16. This leaves participants 4 and 10, where participant 4 has quite unclear activation and participant 10 can best be described as a mix between the first and second groups. See appendix for all corresponding plots.

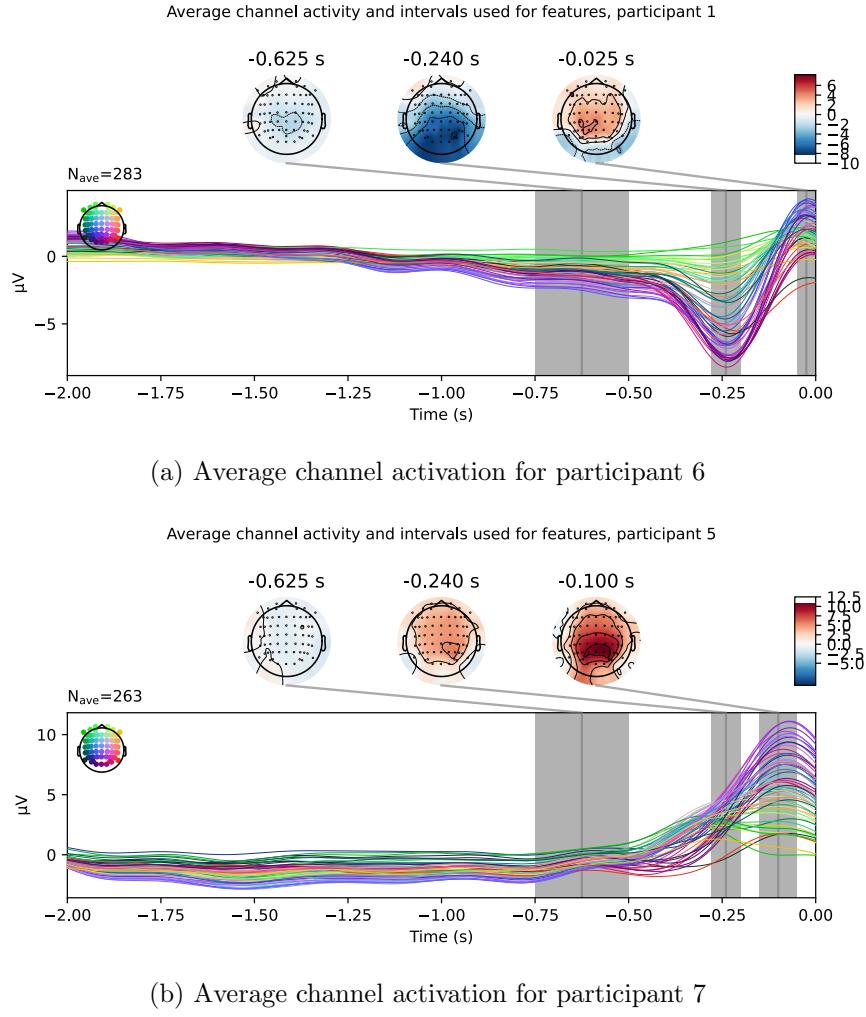
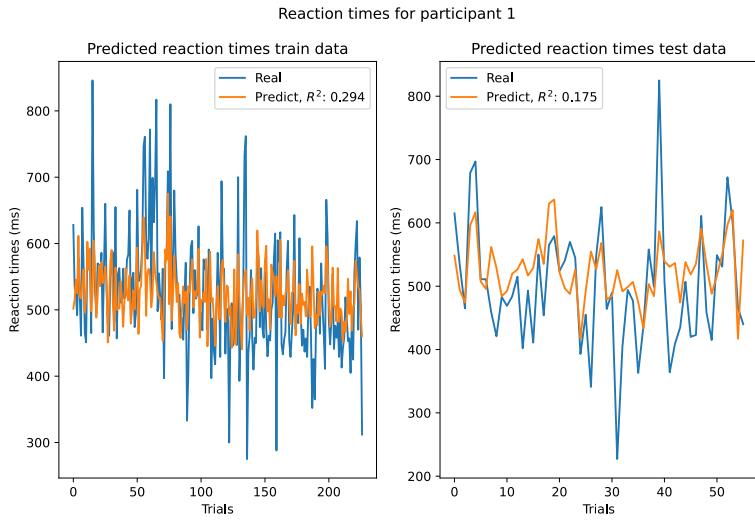
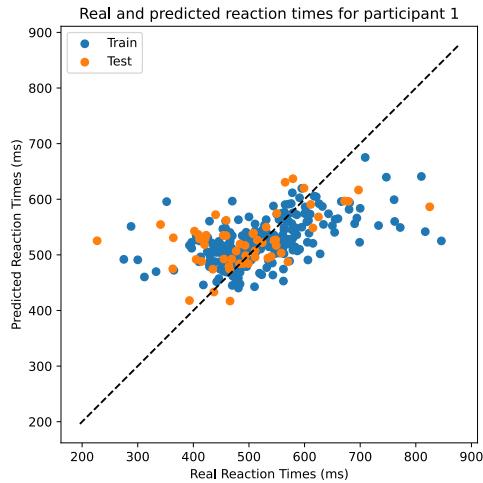


Figure 3.5: Contains the average channel activation of the pre-trial activations for participant 1. The colours of the plotted lines correspond with a specific channel, which are indicated at the top left corner of the plot. Additionally, three grey windows are present, which mark interesting sections in the signal. For the centre of each of the grey windows a topographic map is shown.

Inspecting the results of the pre-movement analysis for participant 1 on the training data in figure 3.6, it is apparent that the regression model performs better than the one trained on the pre-trial data. The model struggles with properly predicting really fast or slow reaction times, which harms the correlation score (R^2). However, the model does seem to follow the general trend in the reaction times.



(a) Predicted and real reaction times for the train and test data.



(b) Scatter plot of the real against the predicted reaction times.

Figure 3.6: Shows the results of the regression model on the train data for participant 1.

For the classification model on the pre-movement analysis, it can be observed that the predictions are quite a bit better than those of the model trained on the pre-trial data.

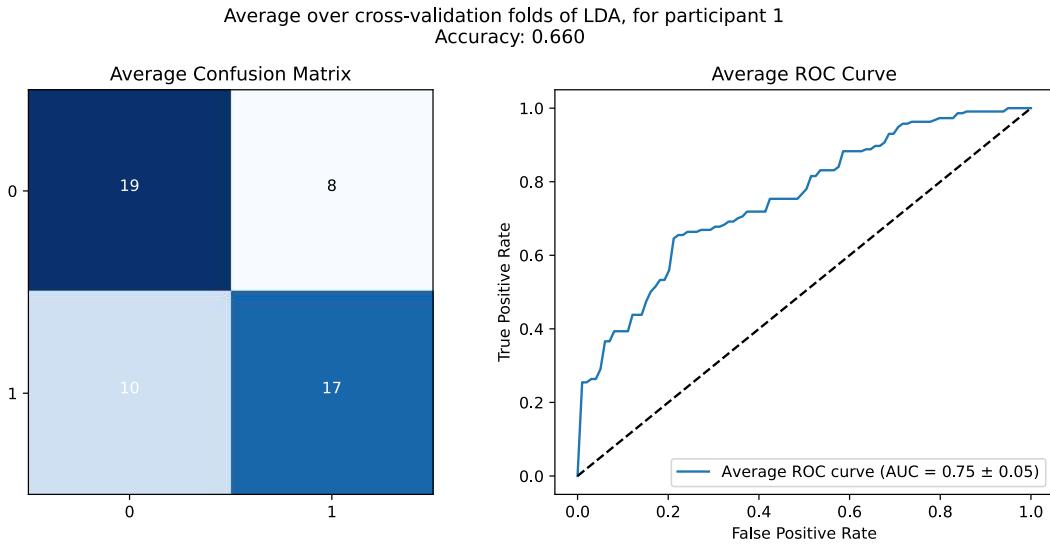


Figure 3.7: Shows the results of the classification model trained on the pre-movement signals for participant 1. The left hand side shows the confusion matrix, with the light cells being predicted correctly and the darker ones incorrectly. On the right side the ROC curve is plotted.

As mentioned before, the fully trained models are tested on the holdout data as a final step. This will validate the models on unseen data. After applying the parameters and pre-trained models, it was found that both of the models perform above chance level for the majority of participants. In figure 3.8, the significance values can be observed. Where the classification model is significant for 12/15 participants and the regression model for 9/15 participants.

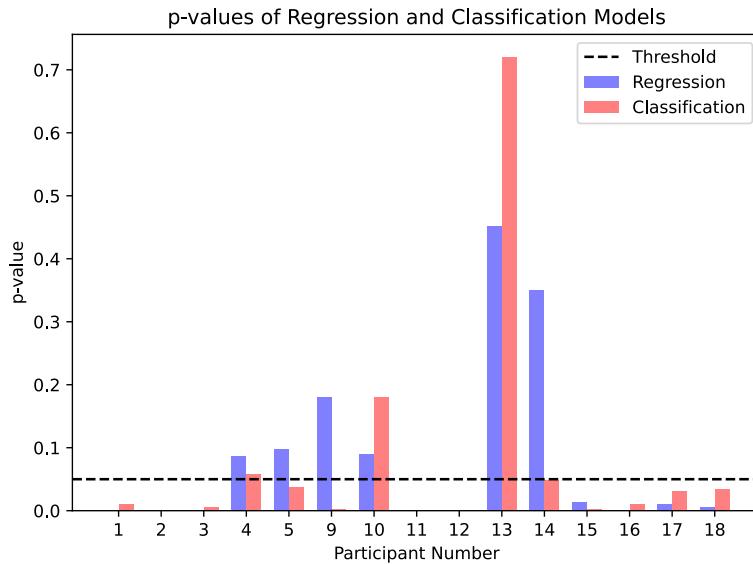


Figure 3.8: Shows the p-values for each participant, for both the classification and regression models.

Chapter 4

Discussion

The following chapter presents a detailed discussion on the presented work. It starts with two sections discussing the results obtained during the pre-trial and pre-movement analysis, and relating these findings to the underlying scientific literature. Subsequently, the chapter delves into an exploration of the limitations inherent in the presented work. Finally, the section on further work explores potential avenues for improvement and outlines the next steps to be taken by further research.

4.1 Pre-trial

The analysis on the pre-trial slow cortical potentials did not return any significant results, nor did it find any features that could explain the fluctuations in trial performance. This means that the objective of finding additional neural markers in the form of slow cortical potentials that can be used for predicting upcoming performance is reached. A common factor over all the regression models is that they learn the mean of the reaction times quite well, this corresponds to the intersection in the regression model. When visually inspecting the clean signals from the pre-trial analysis, no significant activation could be observed for any of the participants. The introduction chapter discussed the activations that could potentially be observed in the cleaned signals. This activation was the Contingent Negative Variation CNV, which consisted of an early and late component. The late component is only active after the start of the trial and therefore was not of interest for the pre-trial analysis. The early component, if present, should have been observable. However, it was not present in the analysis. This can have two possible explanations, either the early-like component is not present in the data or some mistakes were made in the analysis. It is not very clear which of the two explanations is correct, due to reasons that will become clear later in this section.

4.2 Pre-movement

The pre-movement slow cortical potentials were additionally analysed, using the same analysis pipeline. The analysis yielded promising results for most of the participants. Even when applying the learned parameters to the holdout data-set, the performance drops by a small margin. Further significance testing showed above chance level performance for 11 out of the 15 participants for the classification model and 9 out of 15 participants for the regression model. Where the group of significant participants for the

regression is a subset of the classification group.

Observing coefficients of the features, gives a strong preference for central and occipital electrodes. This is in line with the activation of the activation of the CNV responds. As for the averaging of windows, it seems that the second window is the most predictive. This time window is consented to the most negative part of the response and corresponds with the peak of electrical neural build-up. This points towards the conclusion CNV-like late response is present in the SVIPT recordings for most of the participants.

4.3 Limitations

The presented work, while providing valuable insights, is accompanied by certain limitations that should be acknowledged. These limitations highlight areas where improvements can be made and caution is warranted in interpreting the results.

One limitation relates to the computation of reaction times. The reaction times are derived from the given marker files, which may introduce potential inaccuracies and missing reaction times. This limitation arises from the specific method used to calculate reaction times. These inconsistencies might have been the result of problems during the recording process, where the threshold on the force sensor might not have been set up correctly. For three of the participants the number of problematic reaction times were too high. It might be possible to mitigate the limitations associated with the computation of reaction times. The next section on further work will further discuss a possible solution.

In the pre-trial analysis, a notable limitation occurs due to the variable length between the "get-ready" and "go" cues. The variability in timing between these cues can result in misalignment of responses during analysis. This misalignment may impact the interpretation of the results and introduce uncertainties. This most likely means that the possible evoked response by the "get-ready" cue was not captured in the analysis. Furthermore, the pre-movement analysis is subject to a limitation concerning the go-cue to first movement interval. This interval serves a dual purpose, as it is used both for calculating reaction times and examining pre-movement activations. However, this overlap between the reaction time window and the window containing pre-movement activations introduces potential confounding factors. Where undesirable activation such as from eye movements could carry significant predictive power for the reaction time. In addition, it is important to observe that the pre-movement analysis is not predicting the reaction times, as they are occurring at the same moment in time.

By recognizing and acknowledging these limitations, it becomes apparent where potential sources of error or imprecision exist within the presented work. Addressing these limitations in future studies will contribute to enhancing the overall accuracy, consistency, and validity of the findings, allowing for more robust interpretations and conclusions.

4.4 Further work

To overcome the limitations identified in the previous section and enhance the overall robustness of the findings, several avenues for further work can be explored. These potential solutions aim to address the challenges associated with the computation of reaction times

and improve the accuracy and reliability of the analysis.

In order to address the challenges associated with calculating reaction times, an alternative method could be employed. Instead of solely relying on the provided marker files, further work could consider directly extracting reaction times from the force sensor recordings themselves. By leveraging the raw force sensor readings, which directly capture participants' responses, it becomes possible to overcome potential inconsistencies or limitations associated with the marker files. This direct measurement of reaction times from the force sensors would offer a more accurate and reliable representation of participants' response timing, thereby significantly bolstering the validity and precision of the analysis. This could possibly enable the three left-out participants to be included.

Next, creating an additional analysis that time-locks specifically to the "get-ready" cue can address the issue of variable length between the "get-ready" and "go" cues. By incorporating this time-locking approach, further work could analyse the activation that occurs due to the "get-ready" cue, as it is currently unclear if this early activation is present. In addition, the predictive power of this early component could be tested, giving a more complete view on the different slow components.

Furthermore, exploring different metrics to measure performance on the SVIPT trials can provide a more comprehensive understanding of participants' task performance. While reaction times serve as a crucial metric, considering additional performance measures such as accuracy, movement time, or error rates can offer a more comprehensive evaluation. Incorporating these metrics in a further analysis could be especially beneficial to the pre-movement analysis, as it would remove the overlap between the recorded features and the performance metric. This would make the pre-movement analysis an actual prediction task, thereby, improving its validity.

By incorporating these potential solutions in future studies, future work can effectively tackle the limitations identified in this work, leading to improved refinement and advancement of the research domain. These efforts will improve the reliability and validity of the findings, enabling more precise interpretations. Additionally, while these advancements may not be entirely satisfactory in improving pre-trial performance, they have demonstrated the presence of predictive slow cortical potentials before movement onset in the SVIPT trials. This observation holds promise and may serve as inspiration for future work in this area.

Chapter 5

Acknowledgments

This thesis was a personal effort, as it should be the culmination of the Artificial Intelligence Bachelor. However, it is important to acknowledge the role my supervisor dr. M.W. Tangermann played during the process. The weekly meetings, and the feedback they provided, were incredibly helpful. Further acknowledgements go to the other students of my thesis group: Jesse Manders, Ognyan Bachvarov, Laurenz Schindler and Ella Has. A number of coding reviews were organised, to discuss our work and help each other with encountered issues. Special thanks to Laurenz Schindler, who suggested the epoch-wise outlier detection, as it is implemented in the analysis.

Chapter 6

Source code

The code used for the analysis and generating the figures was written in Python. The code is made public thought the MIT-license and can be found in the following GitHub reposotory:

https://github.com/MatsuWhatsu/erp_pipeline_slow_potentials

References

- Abou Zeid, E., Sereshkeh, A. R., & Chau, T. (2016). A pipeline of spatio-temporal filtering for predicting the laterality of self-initiated fine movements from single trial readiness potentials. *Journal of Neural Engineering*, 13(6), 066012.
- Chaumon, M., Bishop, D. V., & Busch, N. A. (2015). A practical guide to the selection of independent components of the electroencephalogram for artifact correction. *Journal of neuroscience methods*, 250, 47–63.
- Delorme, A., Palmer, J., Onton, J., Oostenveld, R., & Makeig, S. (2012). Independent eeg sources are dipolar. *PloS one*, 7(2), e30135.
- Dharmaprani, D., Nguyen, H. K., Lewis, T. W., DeLosAngeles, D., Willoughby, J. O., & Pope, K. J. (2016). A comparison of independent component analysis algorithms and measures to discriminate between eeg and artifact components. In *2016 38th annual international conference of the ieee engineering in medicine and biology society (embs)* (pp. 825–828).
- Gramfort, A., Luessi, M., Larson, E., Engemann, D. A., Strohmeier, D., Brodbeck, C., ... Härmäläinen, M. S. (2013). MEG and EEG data analysis with MNE-Python. *Frontiers in Neuroscience*, 7(267), 1–13. doi: 10.3389/fnins.2013.00267
- Hallett, M. (2005). Neuroplasticity and rehabilitation. *Journal of Rehabilitation Research and Development*, 42(4), R17.
- Hanna, J., Kim, C., & Müller-Voggel, N. (2020). External noise removed from magnetoencephalographic signal using independent component analyses of reference channels. *Journal of Neuroscience Methods*, 335, 108592.
- Hyvärinen, A., & Oja, E. (2000). Independent component analysis: algorithms and applications. *Neural networks*, 13(4-5), 411–430.
- Komosar, M., Fiedler, P., & Haueisen, J. (2022). Bad channel detection in eeg recordings. *Current Directions in Biomedical Engineering*, 8(2), 257–260.
- Kormylo, J., & Jain, V. (1974). Two-pass recursive digital filter with zero phase shift. *IEEE Transactions on Acoustics, Speech, and Signal Processing*, 22(5), 384–387.
- Kornhuber, H. H., & Deecke, L. (1965). Hirnpotentialänderungen bei willkürbewegungen und passiven bewegungen des menschen: Bereitschaftspotential und reafferente potentielle. *Pflüger's Archiv für die gesamte Physiologie des Menschen und der Tiere*, 284, 1–17.
- Makeig, S., Bell, A., Jung, T.-P., & Sejnowski, T. J. (1995). Independent component analysis of electroencephalographic data. *Advances in neural information processing systems*, 8.
- Masi, M. (2021). Spirit calls nature: A comprehensive guide to science and spirituality, consciousness and evolution in a synthesis of knowledge.
- Meinel, A., Castaño-Candamil, J. S., Dähne, S., Reis, J., & Tangermann, M. (2015). Eeg band power predicts single-trial reaction time in a hand motor task. In *2015 7th international ieee/embs conference on neural engineering (ner)* (pp. 182–185).

- Meinel, A., Castaño-Candamil, S., Reis, J., & Tangermann, M. (2016). Pre-trial eeg-based single-trial motor performance prediction to enhance neuroergonomics for a hand force task. *Frontiers in Human Neuroscience*, 10, 170.
- Ofner, P., Schwarz, A., Pereira, J., & Müller-Putz, G. R. (2017). Upper limb movements can be decoded from the time-domain of low-frequency eeg. *PloS one*, 12(8), e0182578.
- Ofner, P., Schwarz, A., Pereira, J., Wyss, D., Wildburger, R., & Müller-Putz, G. R. (2019). Attempted arm and hand movements can be decoded from low-frequency eeg from persons with spinal cord injury. *Scientific reports*, 9(1), 1–15.
- Santosa, F., & Symes, W. W. (1986). Linear inversion of band-limited reflection seismograms. *SIAM journal on scientific and statistical computing*, 7(4), 1307–1330.
- Schurger, A., Pak, J., Roskies, A. L., & et al. (2021). What is the readiness potential? *Trends in cognitive sciences*, 25(7), 558–570.
- Shakeel, A., Navid, M. S., Anwar, M. N., Mazhar, S., Jochumsen, M., & Niazi, I. K. (2015). A review of techniques for detection of movement intention using movement-related cortical potentials. *Computational and mathematical methods in medicine*, 2015.
- Shinmura, S. (2011). Beyond fisher's linear discriminant analysis-new world of discriminant analysis. *ISI2011 CD-ROM*, 1–6.
- Suleiman, A.-B. R., Fatehi, T. A.-H., & et al. (2007). Features extraction techniques of eeg signal for bci applications. *Faculty of Computer and Information Engineering Department College of Electronics Engineering, University of Mosul, Iraq*.
- Viola, F. C., Thorne, J., Edmonds, B., Schneider, T., Eichele, T., & Debener, S. (2009). Semi-automatic identification of independent components representing eeg artifact. *Clinical Neurophysiology*, 120(5), 868–877.
- Walter, W. G., Cooper, R., Aldridge, V., McCallum, W., & Winter, A. (1964). Contingent negative variation: an electric sign of sensori-motor association and expectancy in the human brain. *nature*, 203, 380–384.
- Winkler, I., Debener, S., Müller, K.-R., & Tangermann, M. (2015). On the influence of high-pass filtering on ica-based artifact reduction in eeg-erp. In *2015 37th annual international conference of the ieee engineering in medicine and biology society (embc)* (pp. 4101–4105).

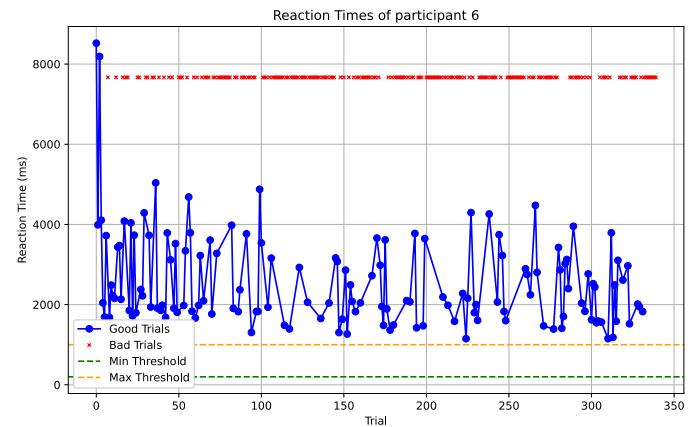
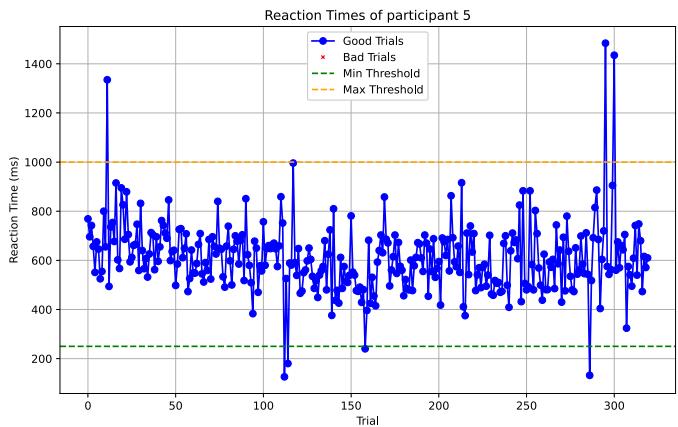
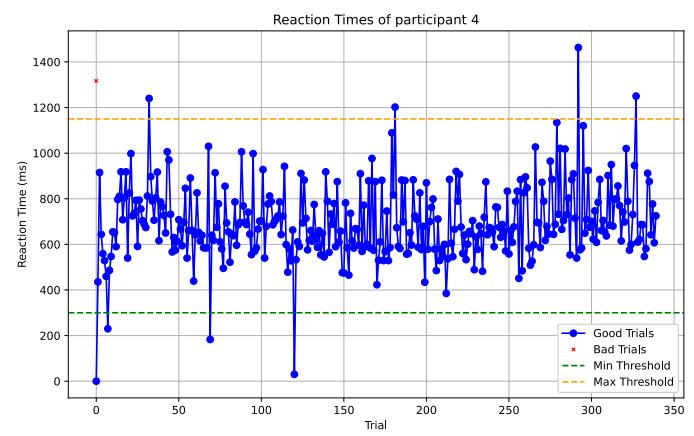
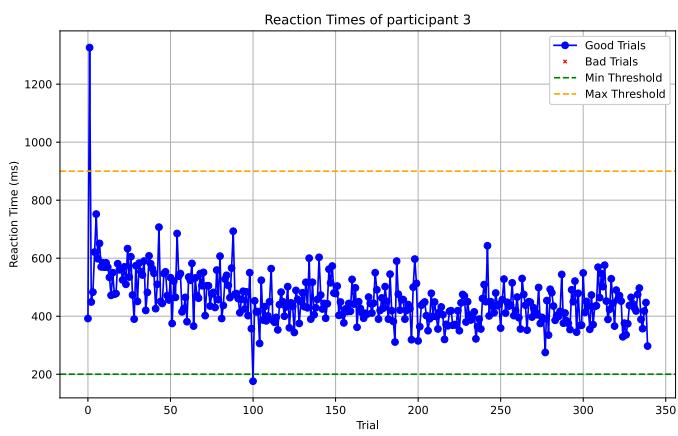
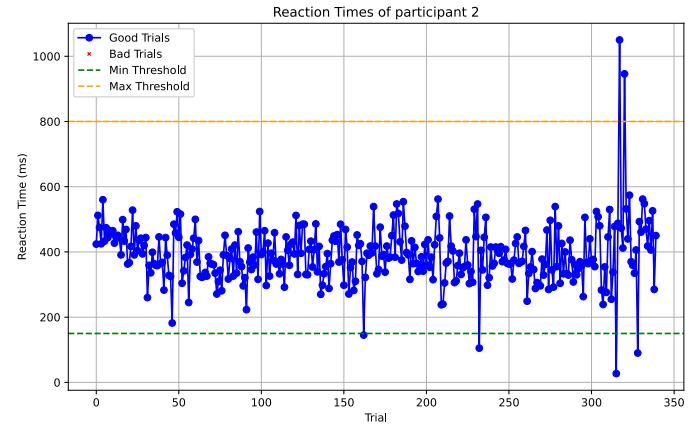
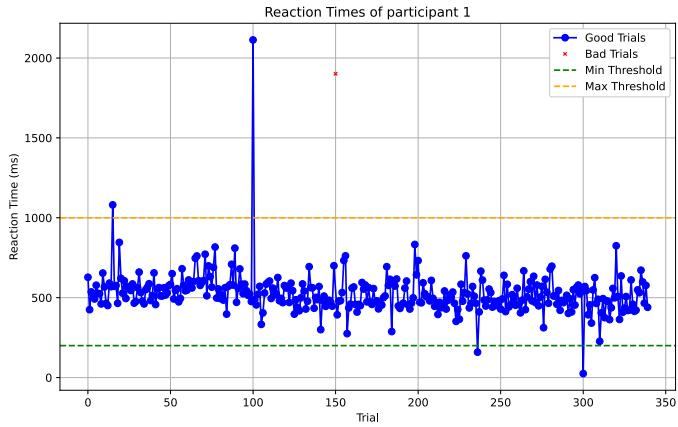
Appendix A

Appendix

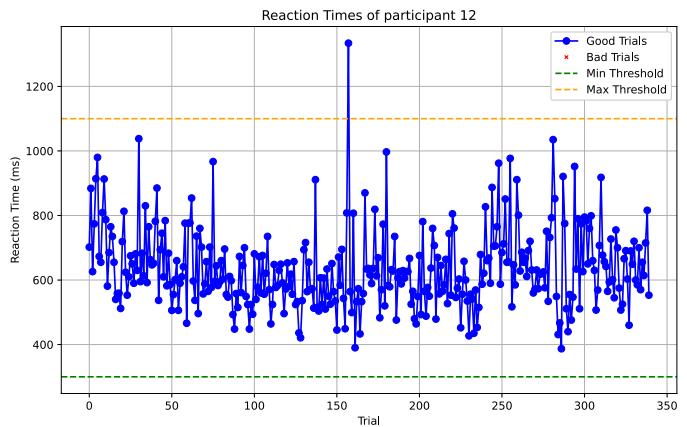
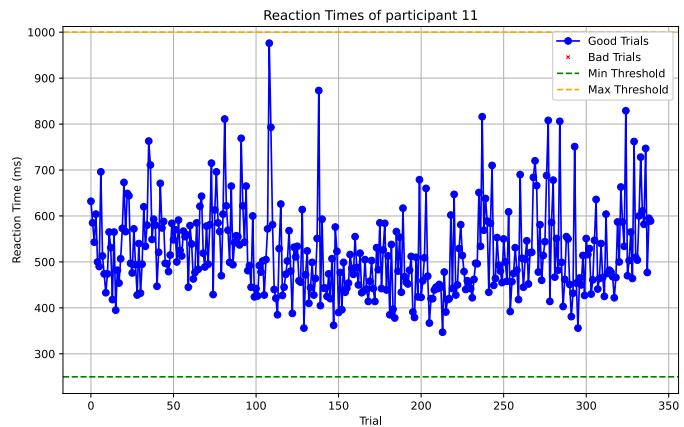
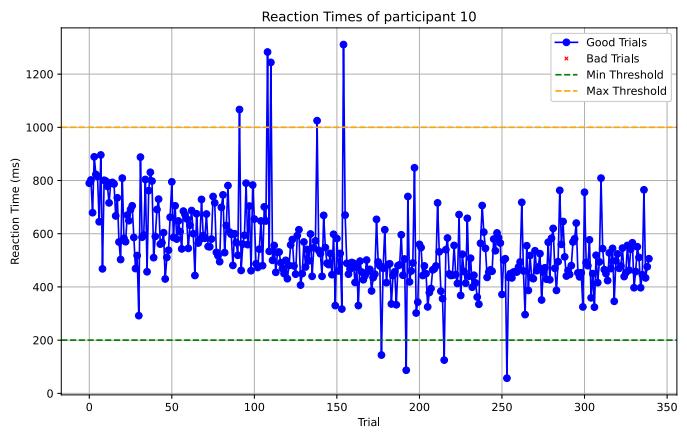
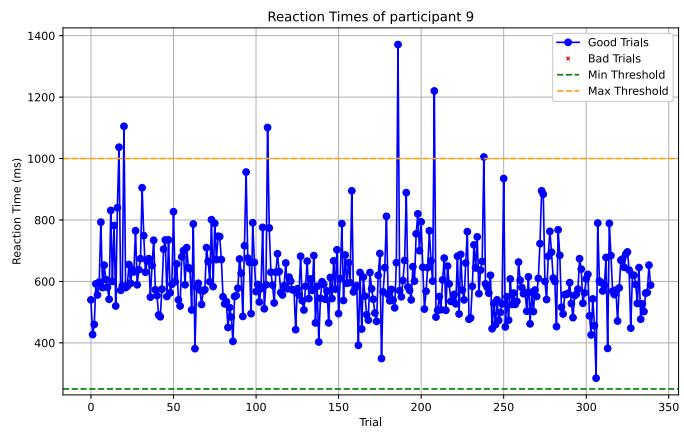
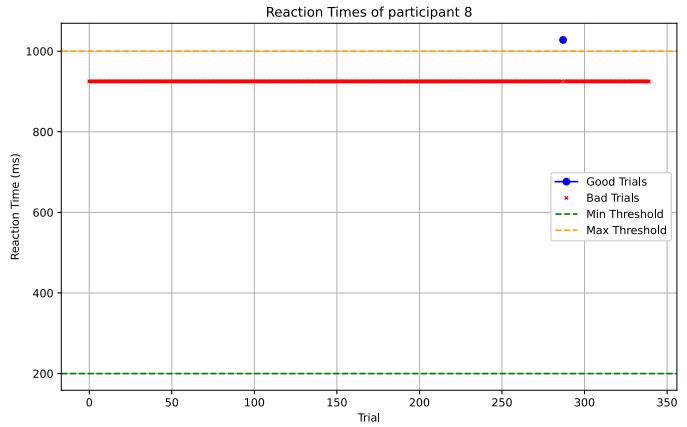
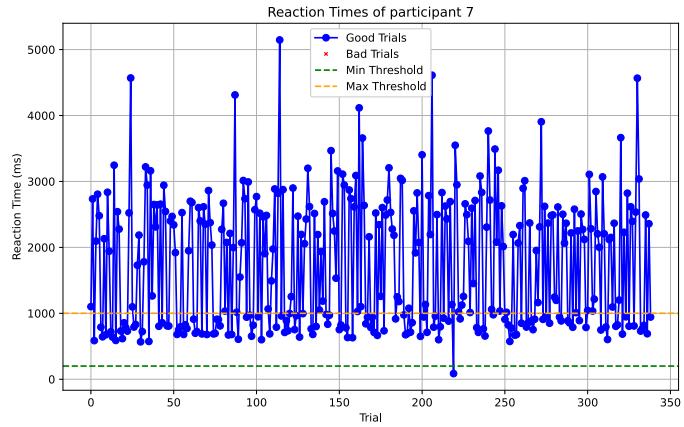
The appendix includes all the plots generated during the analysis. It contains two subsections, one for the pre-trial figures and one for the pre-movement figures. In addition to the reaction time plots. Both sub-directories contain the same 9 plot types, which in turn contain the figures of the participants. Here follows a short description of the 9 types of plots and the reaction time plots:

- Reaction times: The plots display the reaction times for each of the participants. Where the trials marked with a red 'x' marker were not commutable, and those with a blue 'o' marker were. The orange and green dashed lines represent the minimum and maximum thresholds. Reaction times that fall outside of the given thresholds are considered outliers.
- Average signal - train & holdout sets: The averaged activation over the channels after pre-processing and cleaning the signals. The grey slices represent the windows from which the average activity is extracted to form the features.
- Classification results - train set: The results of the classification model on the training data. The figures contain the confusion matrix and ROC curve, both averaged over the folds of the cross-validation.
- Classification results - holdout set: The results of the classification model on the holdout data. The figures contain the confusion matrix and ROC curve. As Well as the calculated p-value.
- Regression results - train sets: The results of the regression model on the train data. The figures plot the real reaction times and the predicted ones. The data is split up into a train and validation set, which are both shown as sub-plots.
- Regression results scatter plot - train sets: Scatter plot of the real reaction times against the predicted reaction times for the train data. These figures show the correlation between the real and predicted reaction times.
- Regression results - holdout set: The results of the regression model on the holdout data. The figures plot the real reaction times and the predicted ones.
- Regression results scatter plot - holdout sets: Scatter plot of the real reaction times against the predicted reaction times for the holdout data.
- Feature importance - holdout set: Bar graph of the importance of the selected features, where importance is chosen to be the coefficients of the features.

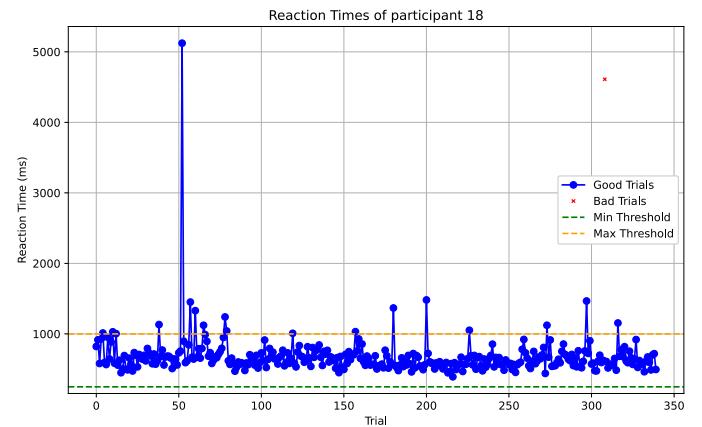
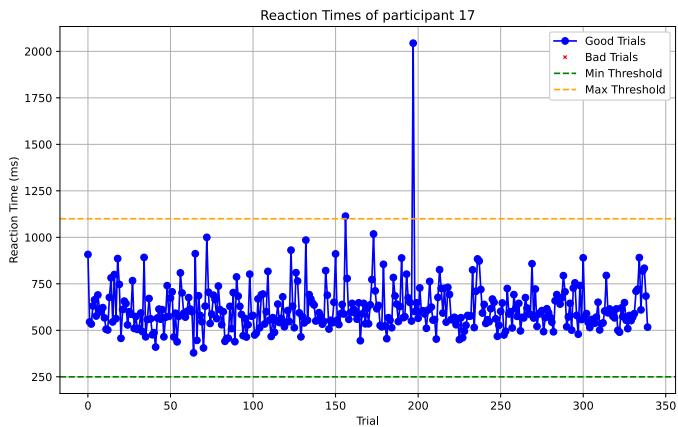
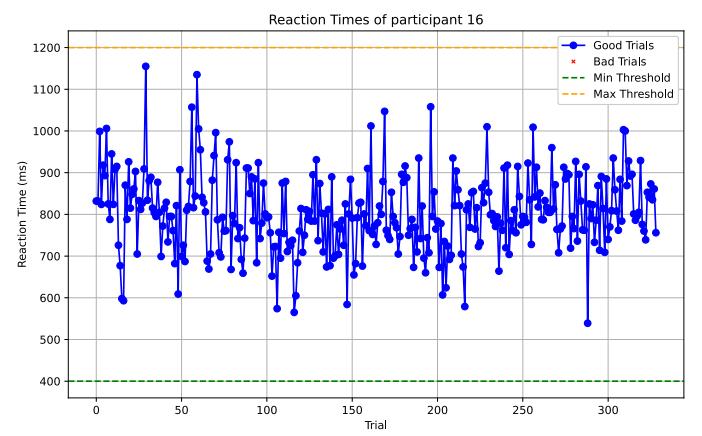
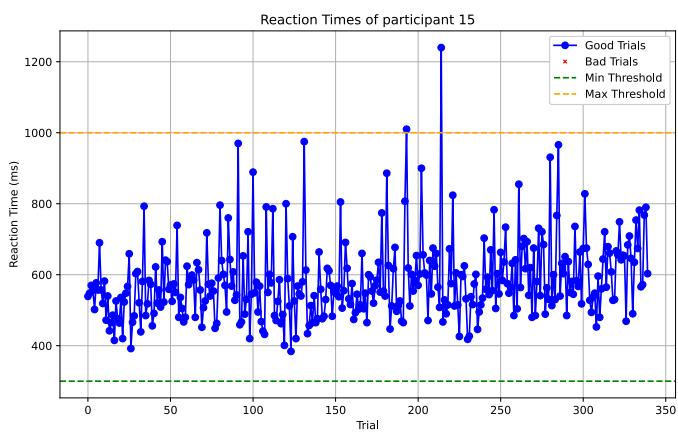
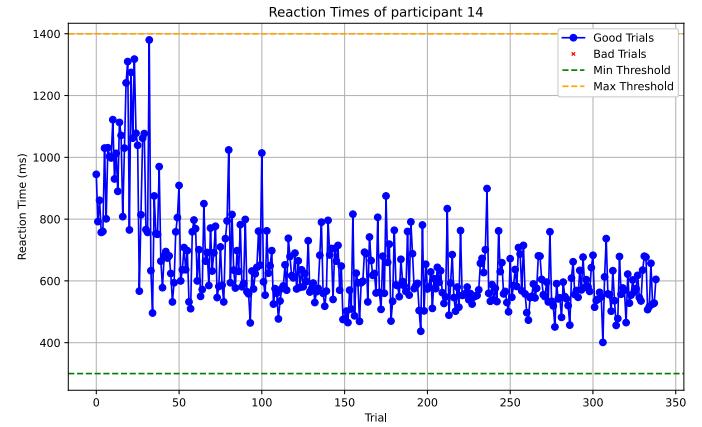
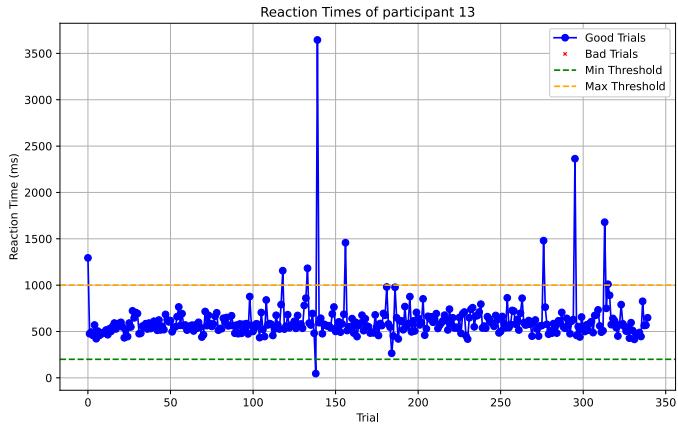
Reaction times



Reaction times

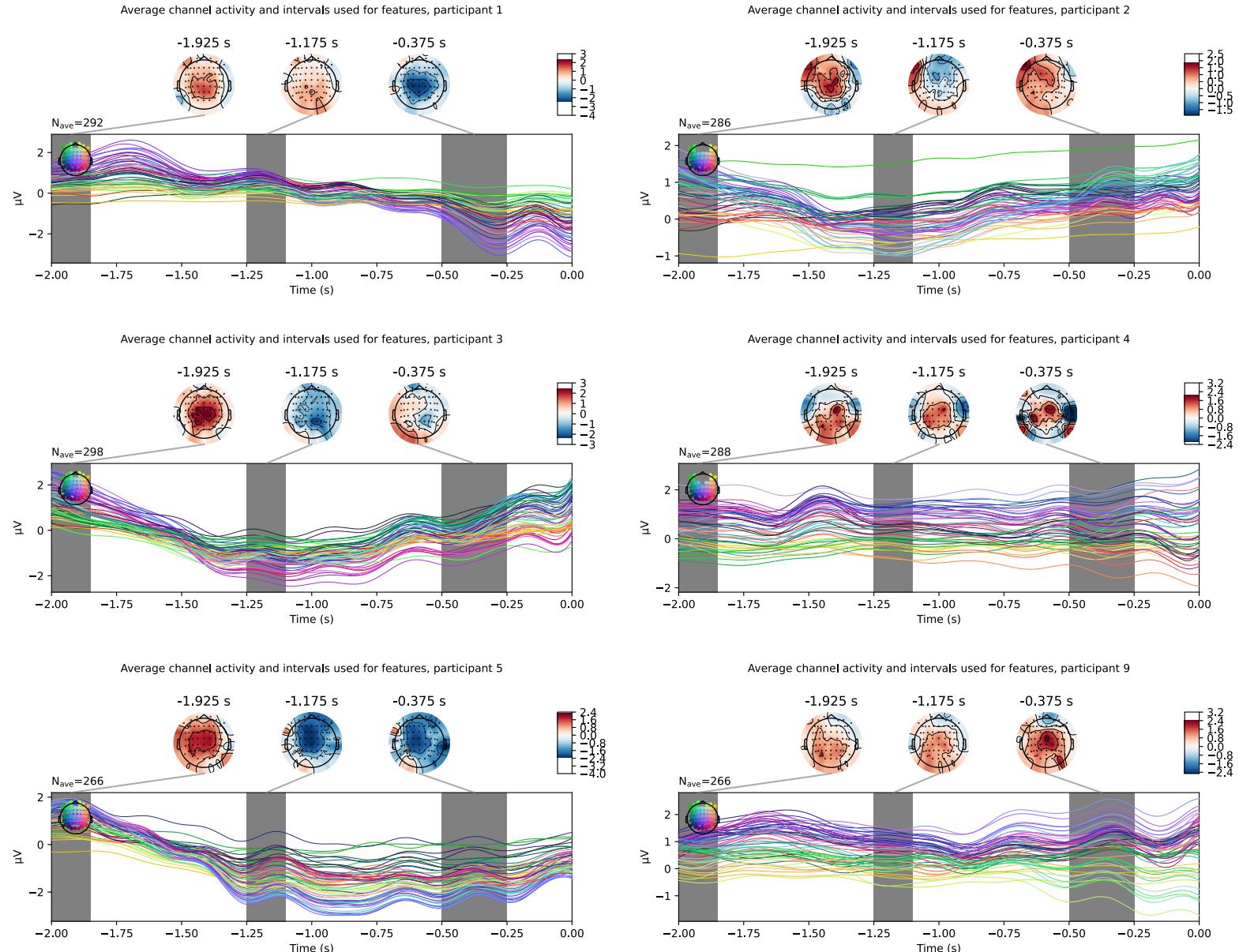


Reaction times



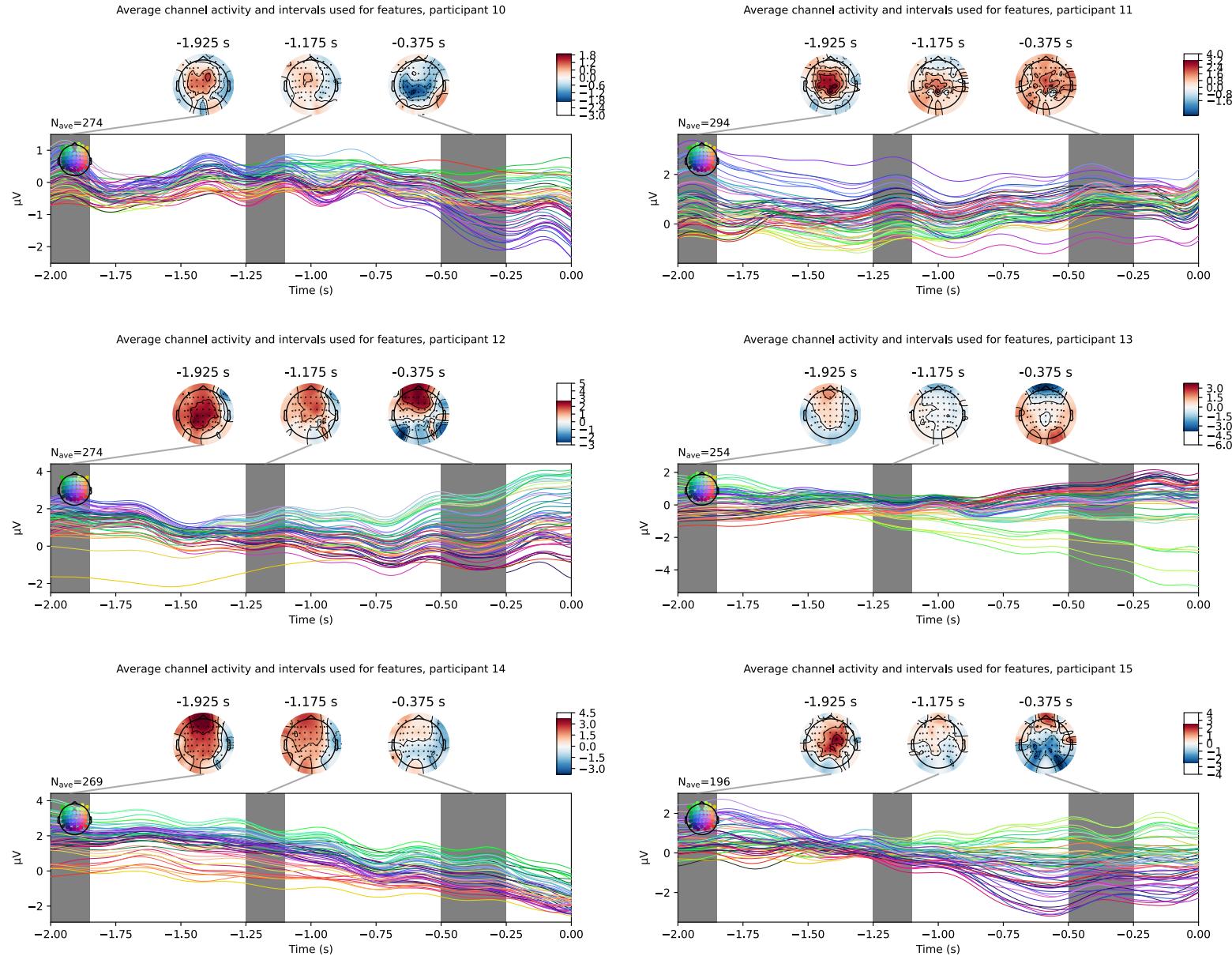
Pre-trial analysis

Averaged signals - train set



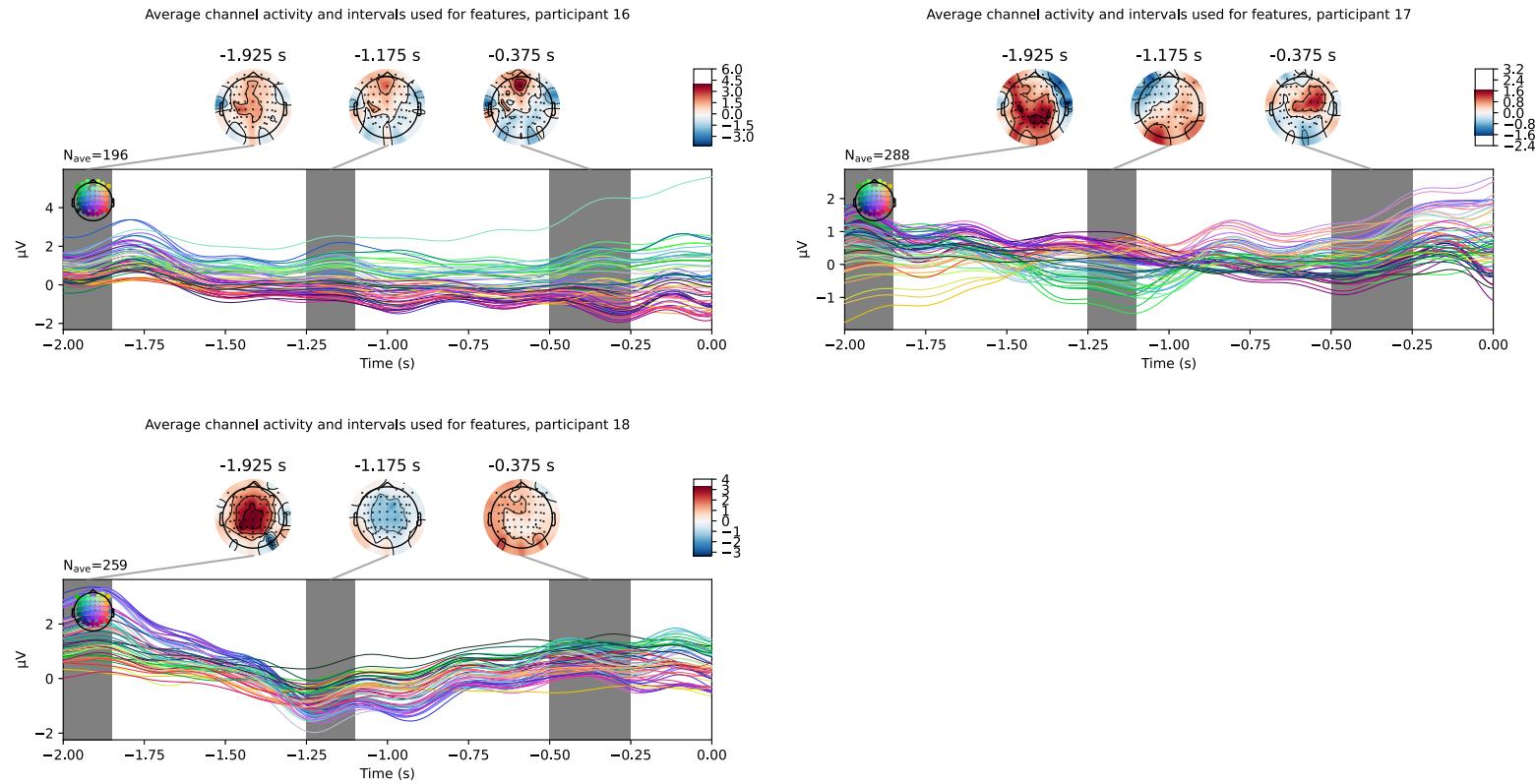
Pre-trial analysis

Averaged signals - train set



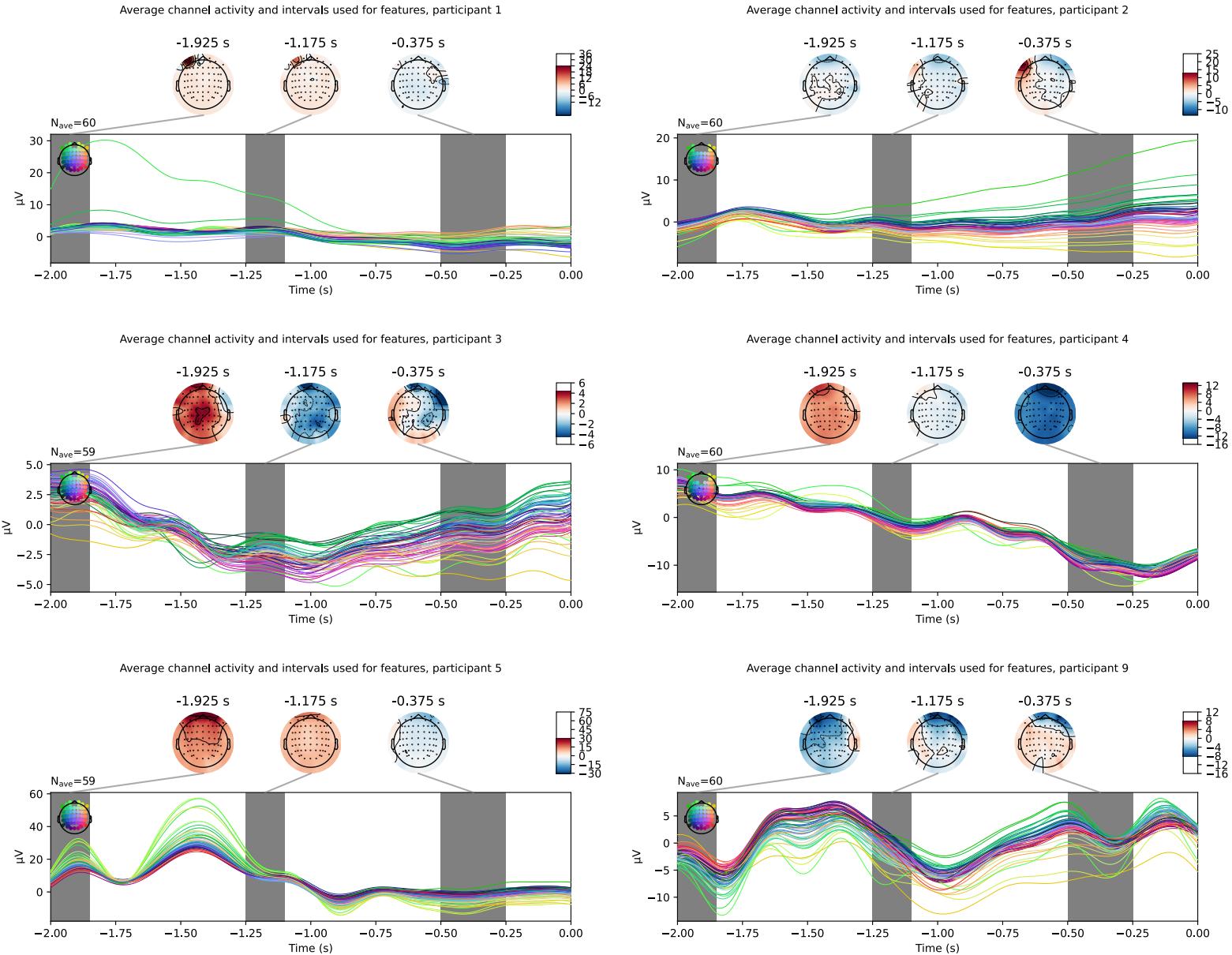
Pre-trial analysis

Averaged signals - train set



Pre-trial analysis

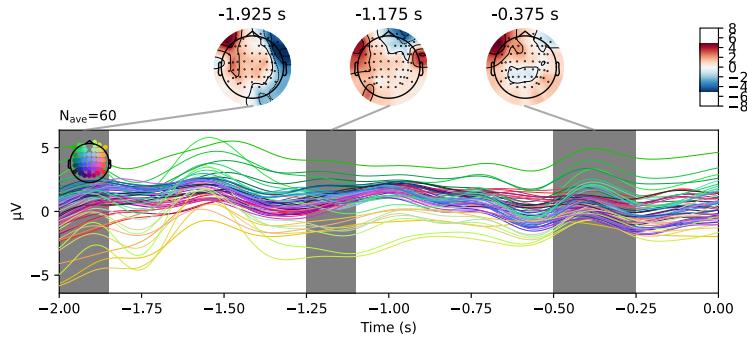
Averaged signals - holdout set



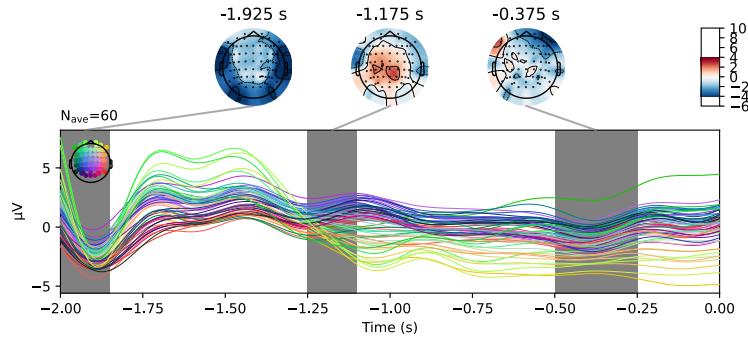
Pre-trial analysis

Averaged signals - holdout set

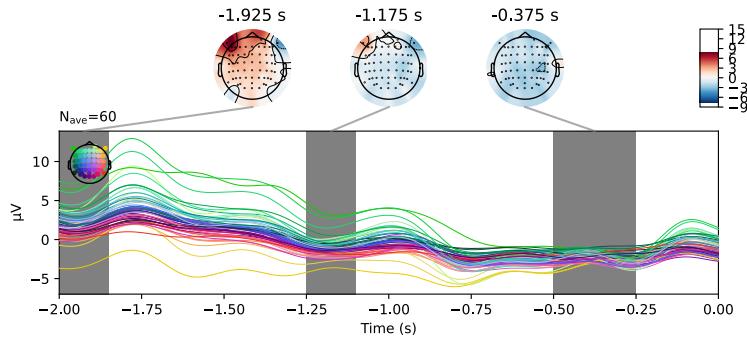
Average channel activity and intervals used for features, participant 10



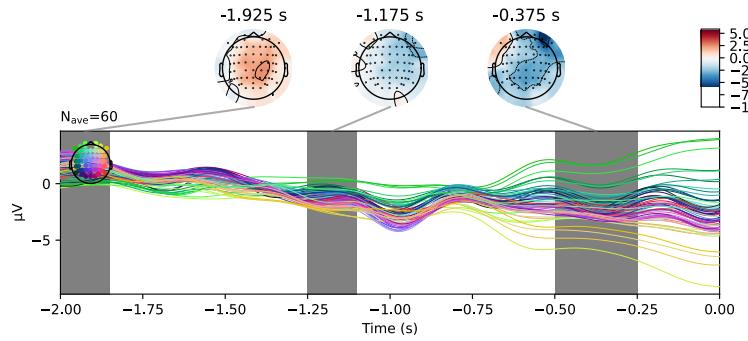
Average channel activity and intervals used for features, participant 11



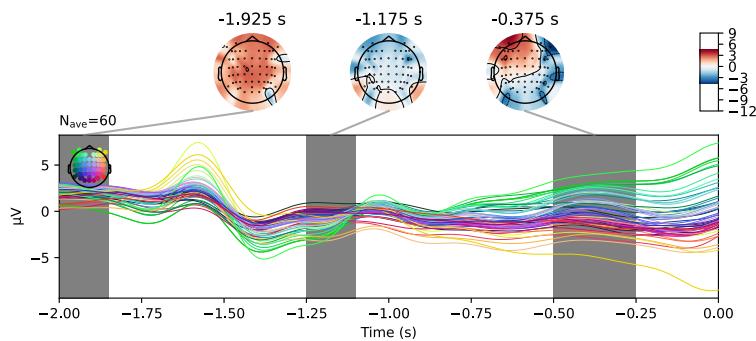
Average channel activity and intervals used for features, participant 12



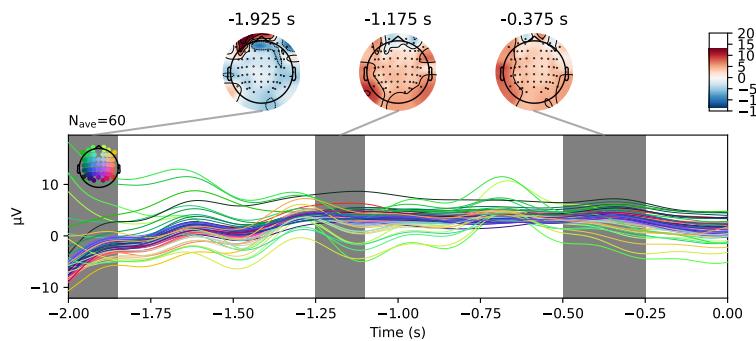
Average channel activity and intervals used for features, participant 13



Average channel activity and intervals used for features, participant 14



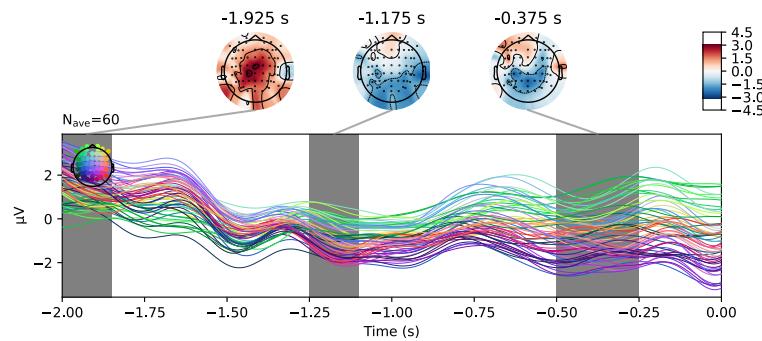
Average channel activity and intervals used for features, participant 15



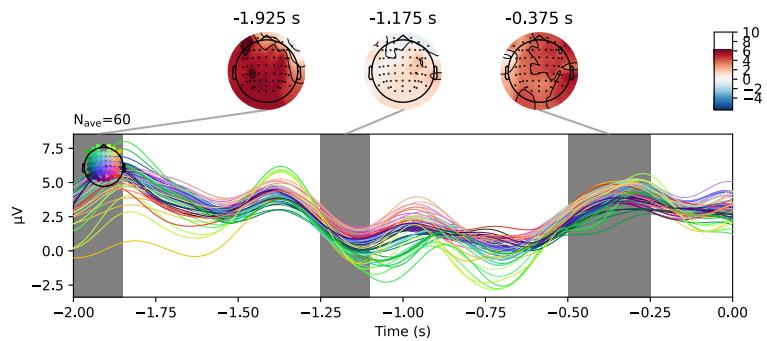
Pre-trial analysis

Averaged signals - holdout set

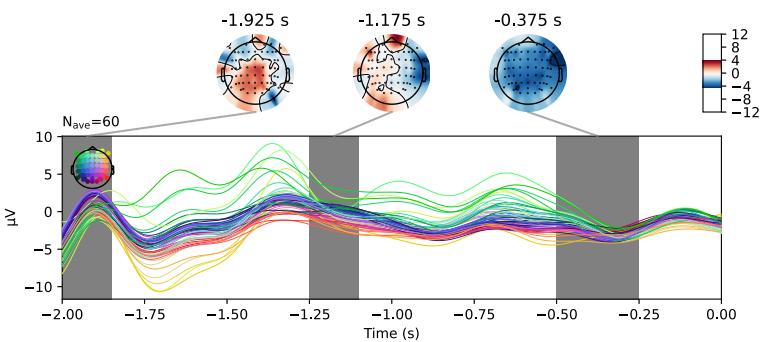
Average channel activity and intervals used for features, participant 16



Average channel activity and intervals used for features, participant 17

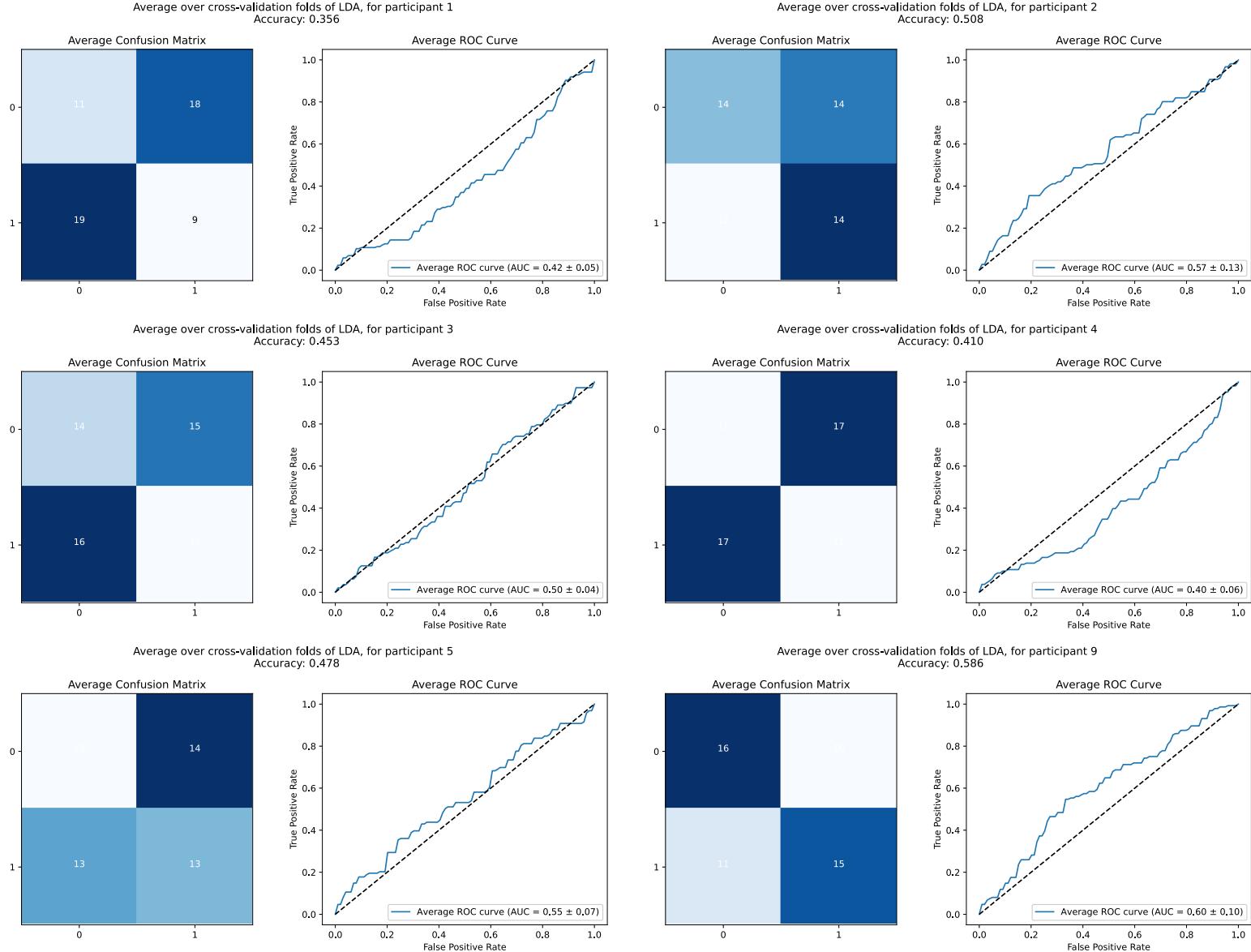


Average channel activity and intervals used for features, participant 18



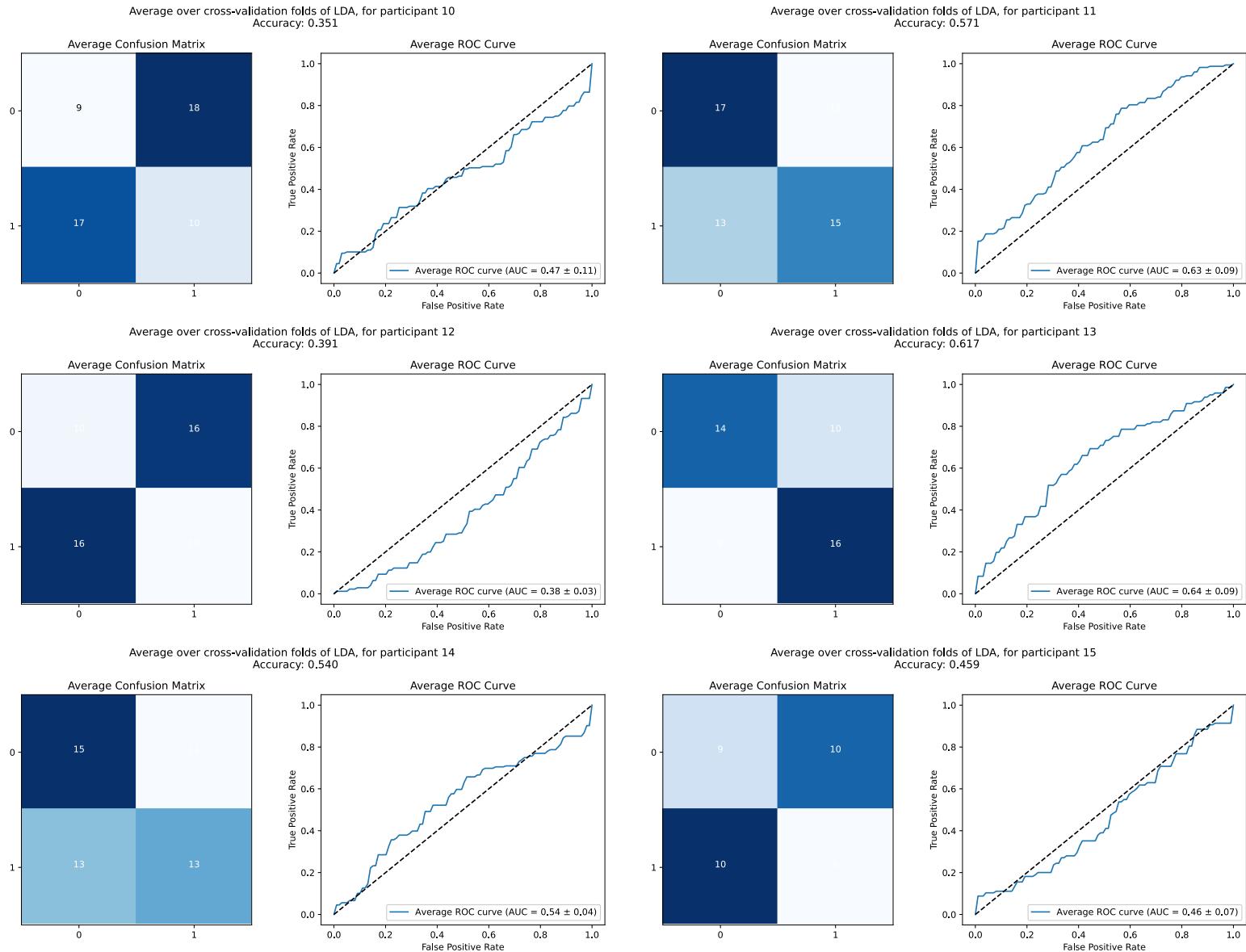
Pre-trial analysis

Classification results - train set



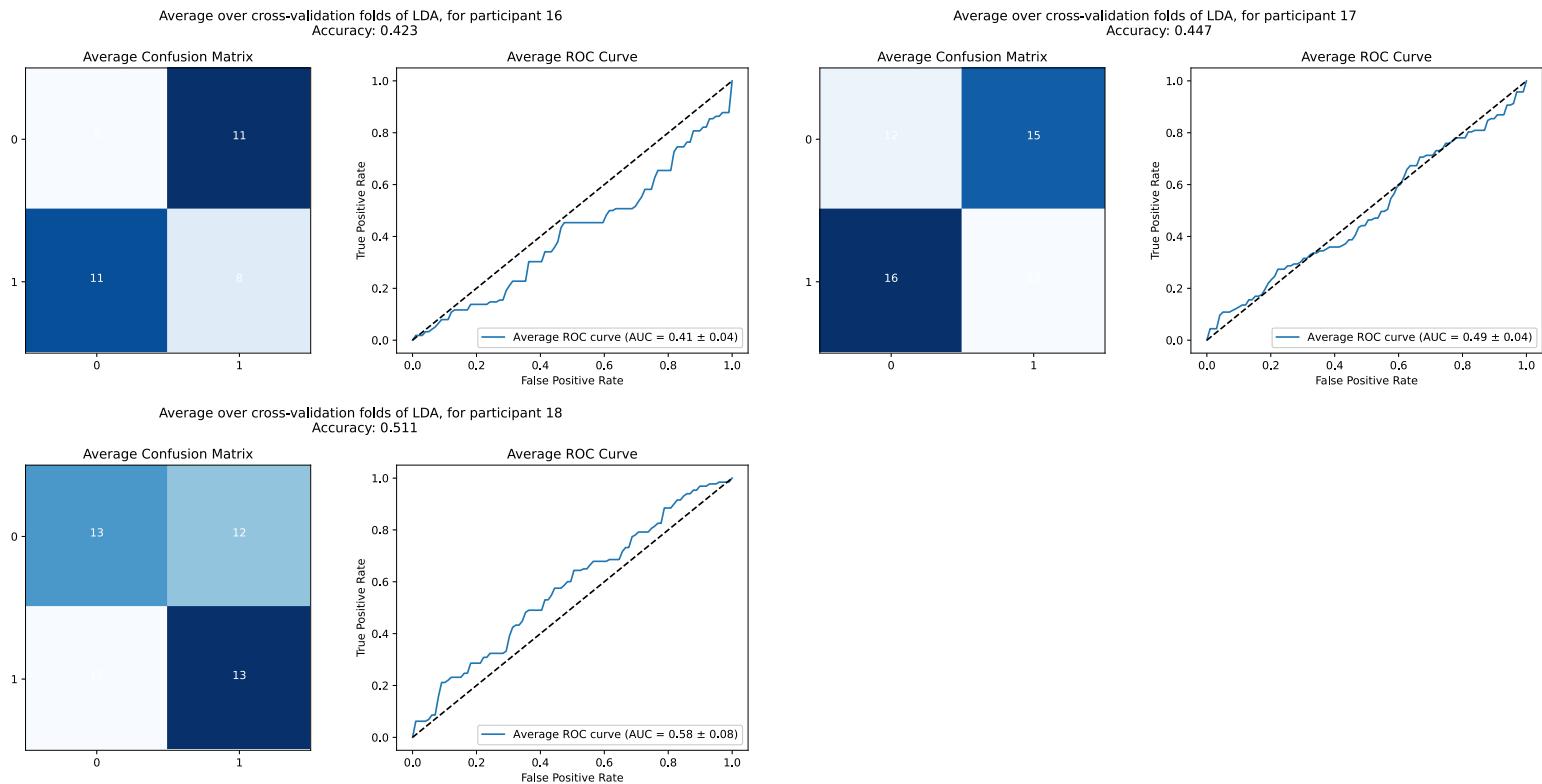
Pre-trial analysis

Classification results - train set



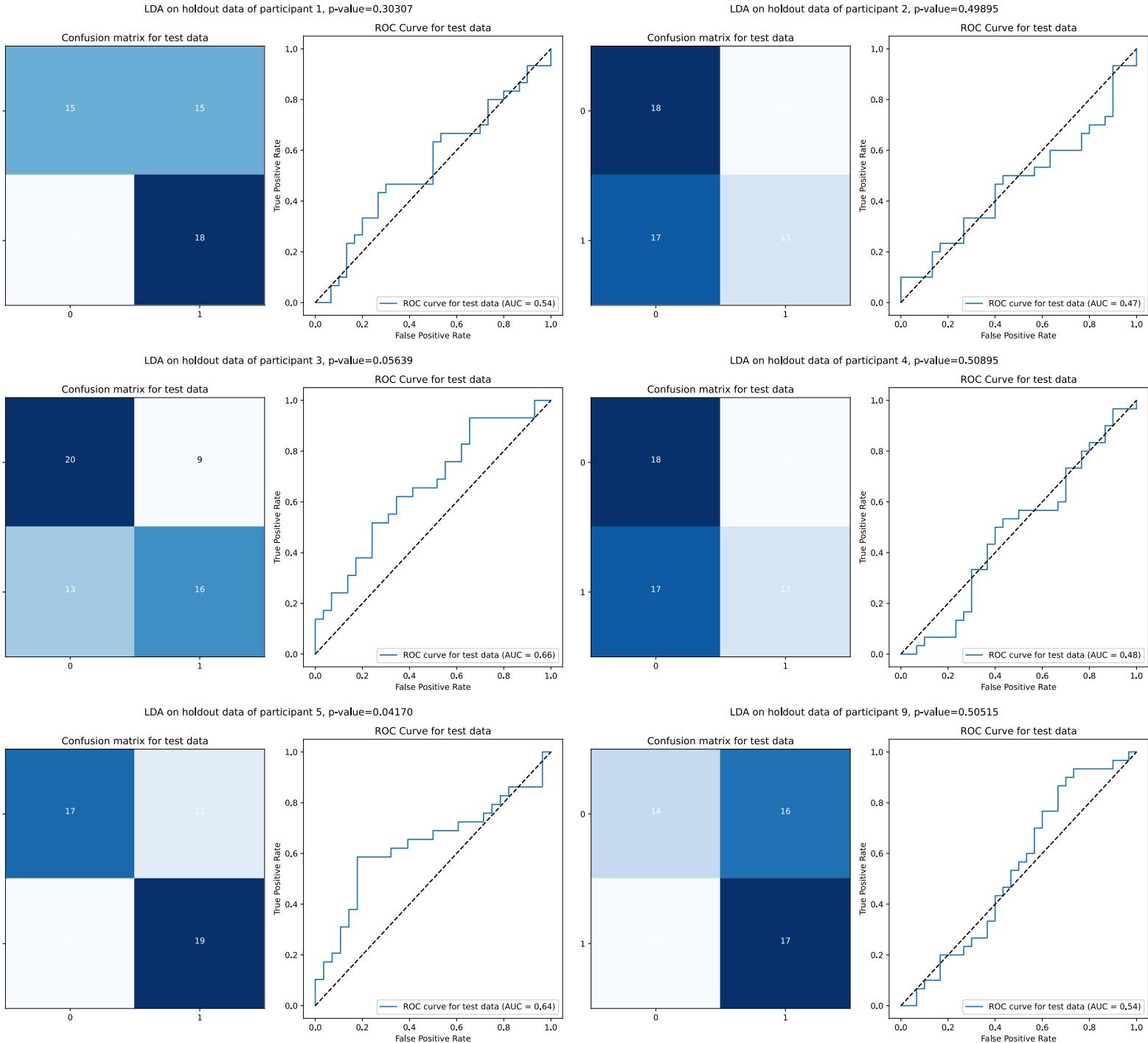
Pre-trial analysis

Classification results - train set



Pre-trial analysis

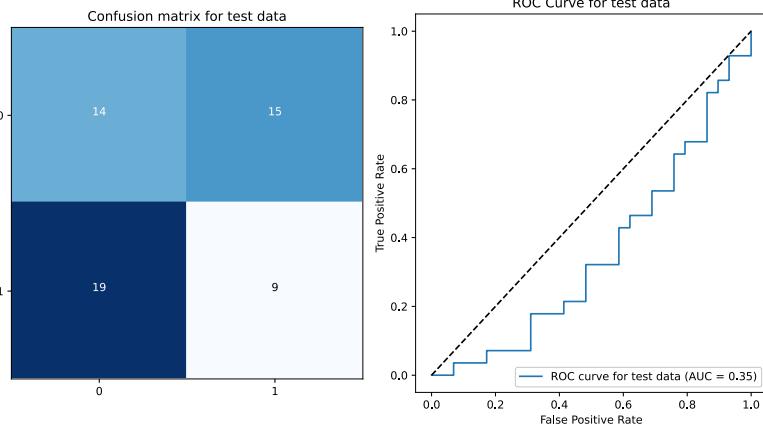
Classification results - holdout set



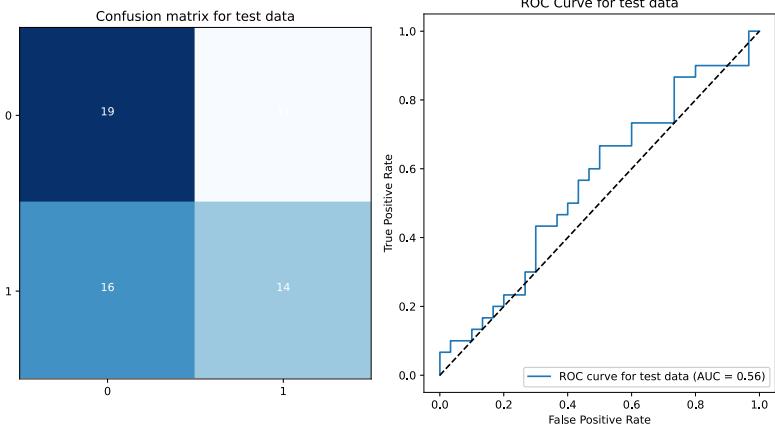
Pre-trial analysis

Classification results - holdout set

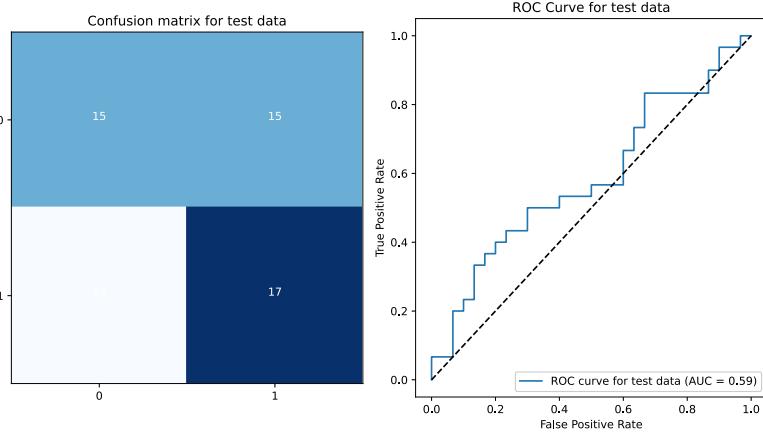
LDA on holdout data of participant 10, p-value=0.95800



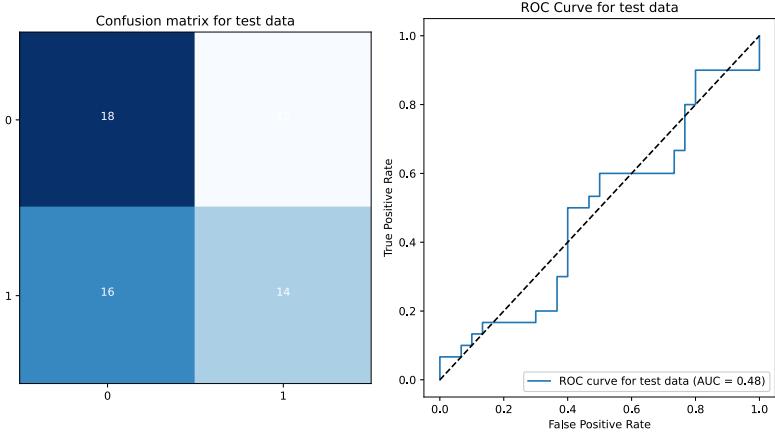
LDA on holdout data of participant 11, p-value=0.30307



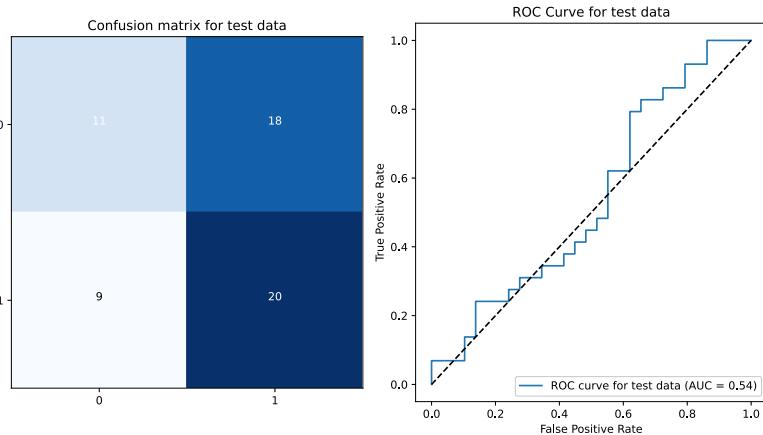
LDA on holdout data of participant 12, p-value=0.39446



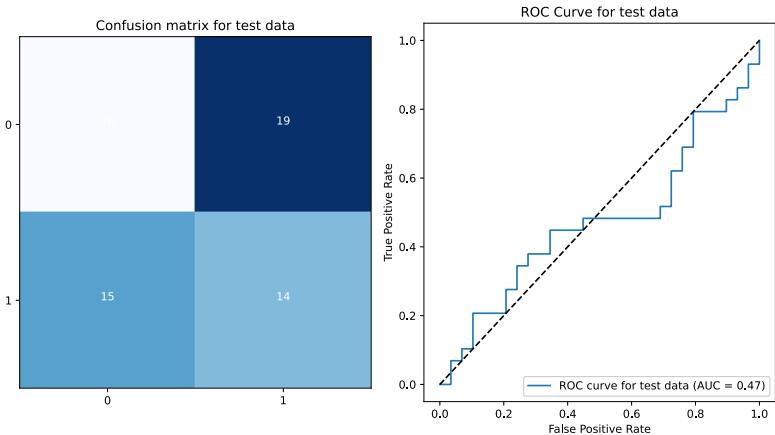
LDA on holdout data of participant 13, p-value=0.39106



LDA on holdout data of participant 14, p-value=0.39316



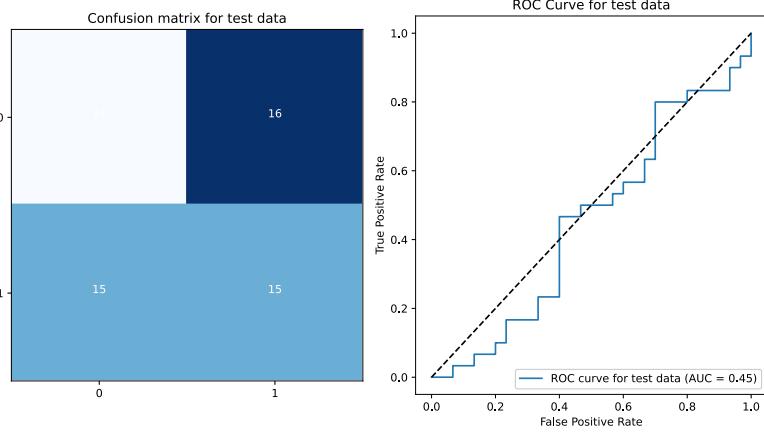
LDA on holdout data of participant 15, p-value=0.94451



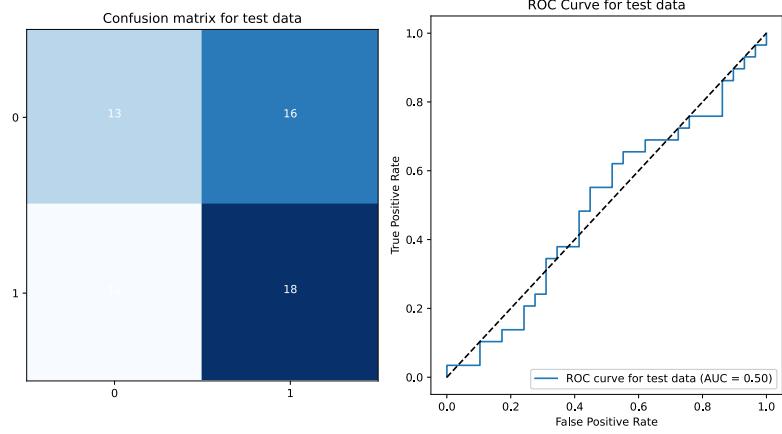
Pre-trial analysis

Classification results - holdout set

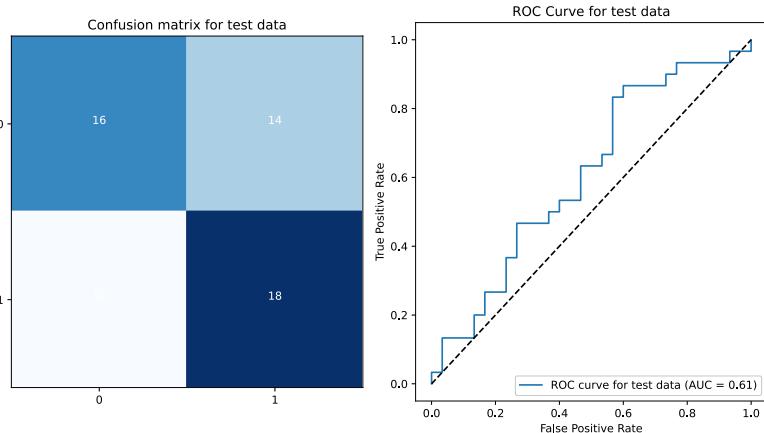
LDA on holdout data of participant 16, p-value=0.69983



LDA on holdout data of participant 17, p-value=0.39386

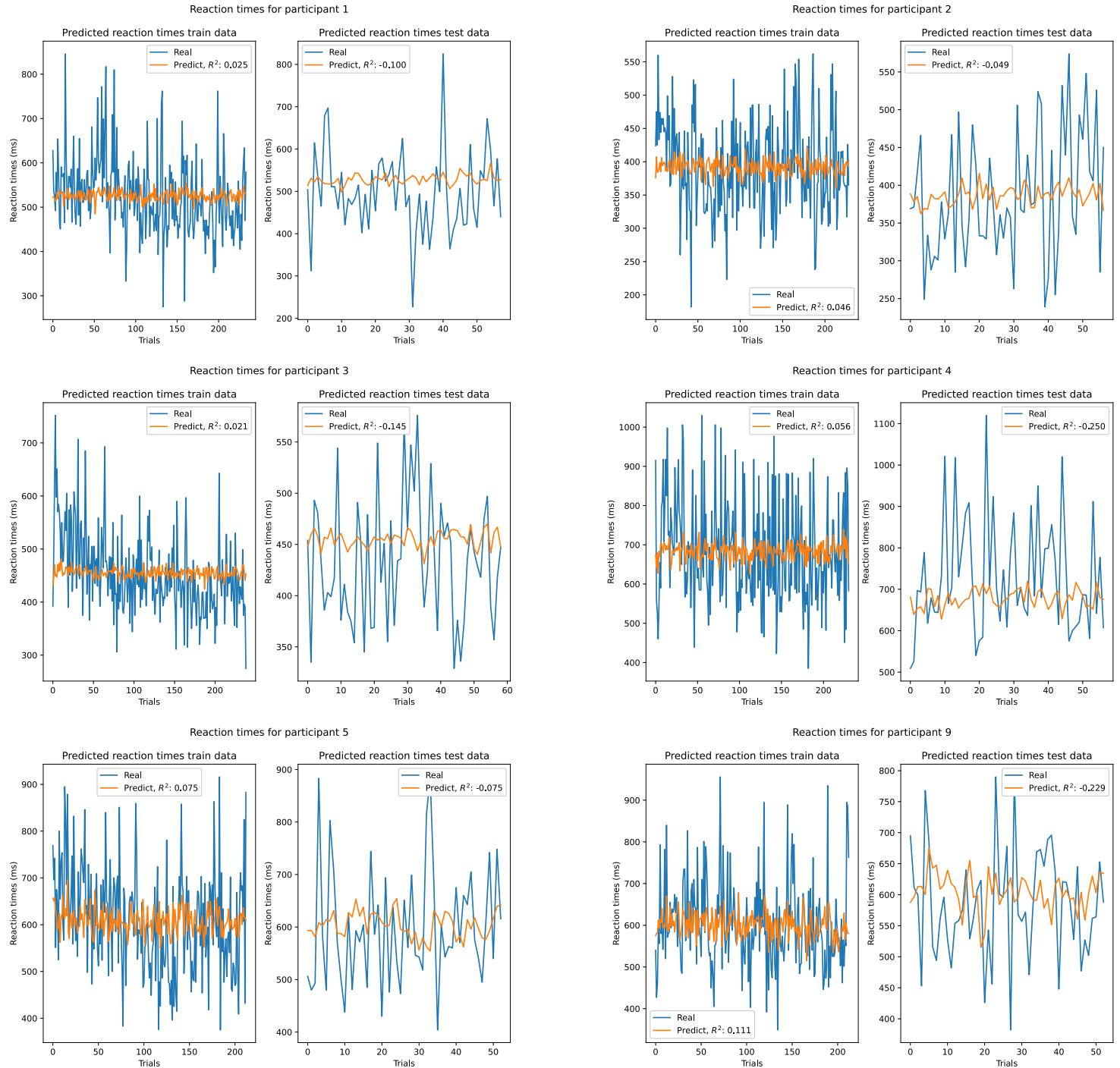


LDA on holdout data of participant 18, p-value=0.22998



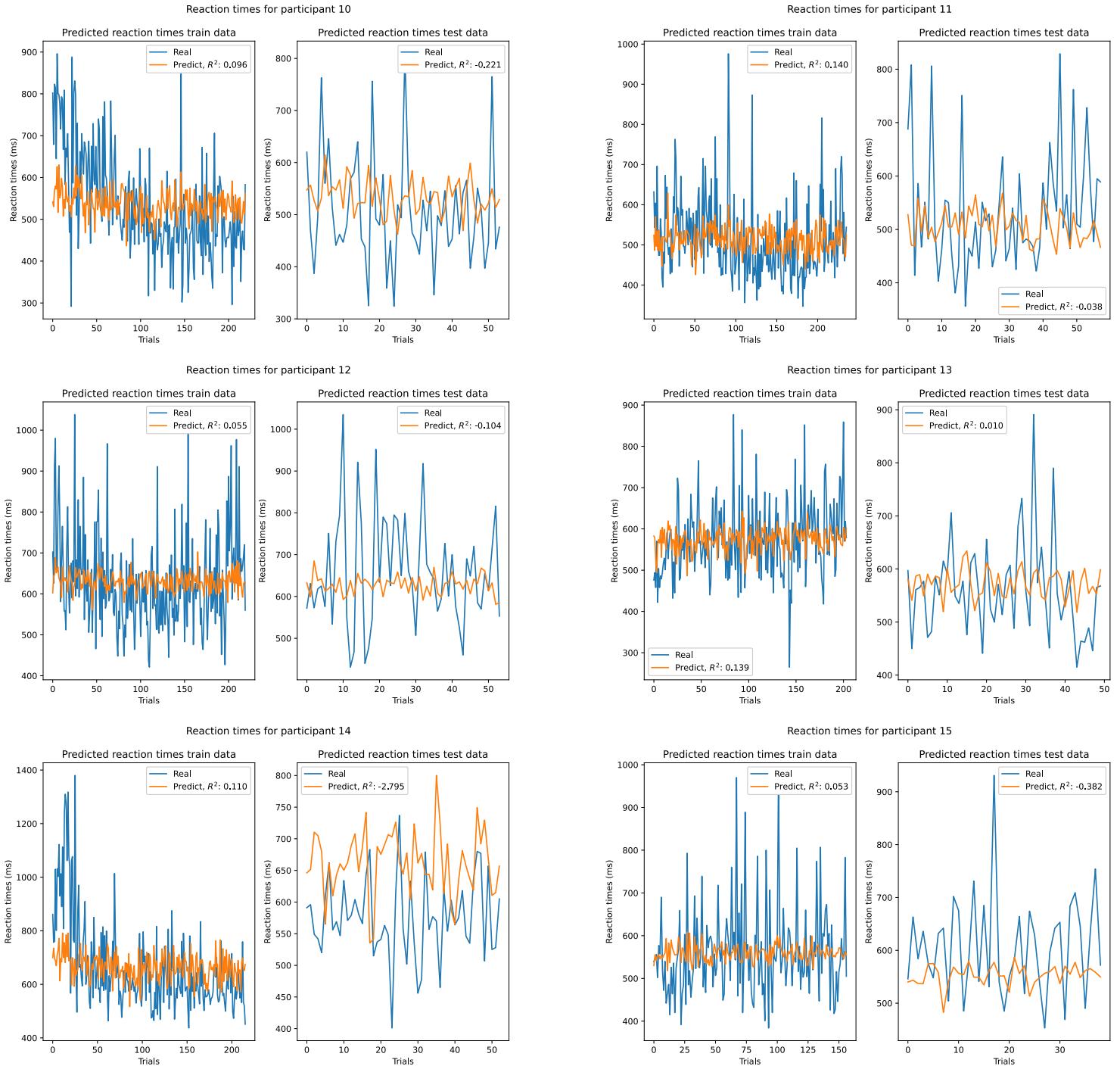
Pre-trial analysis

Regression results - train set



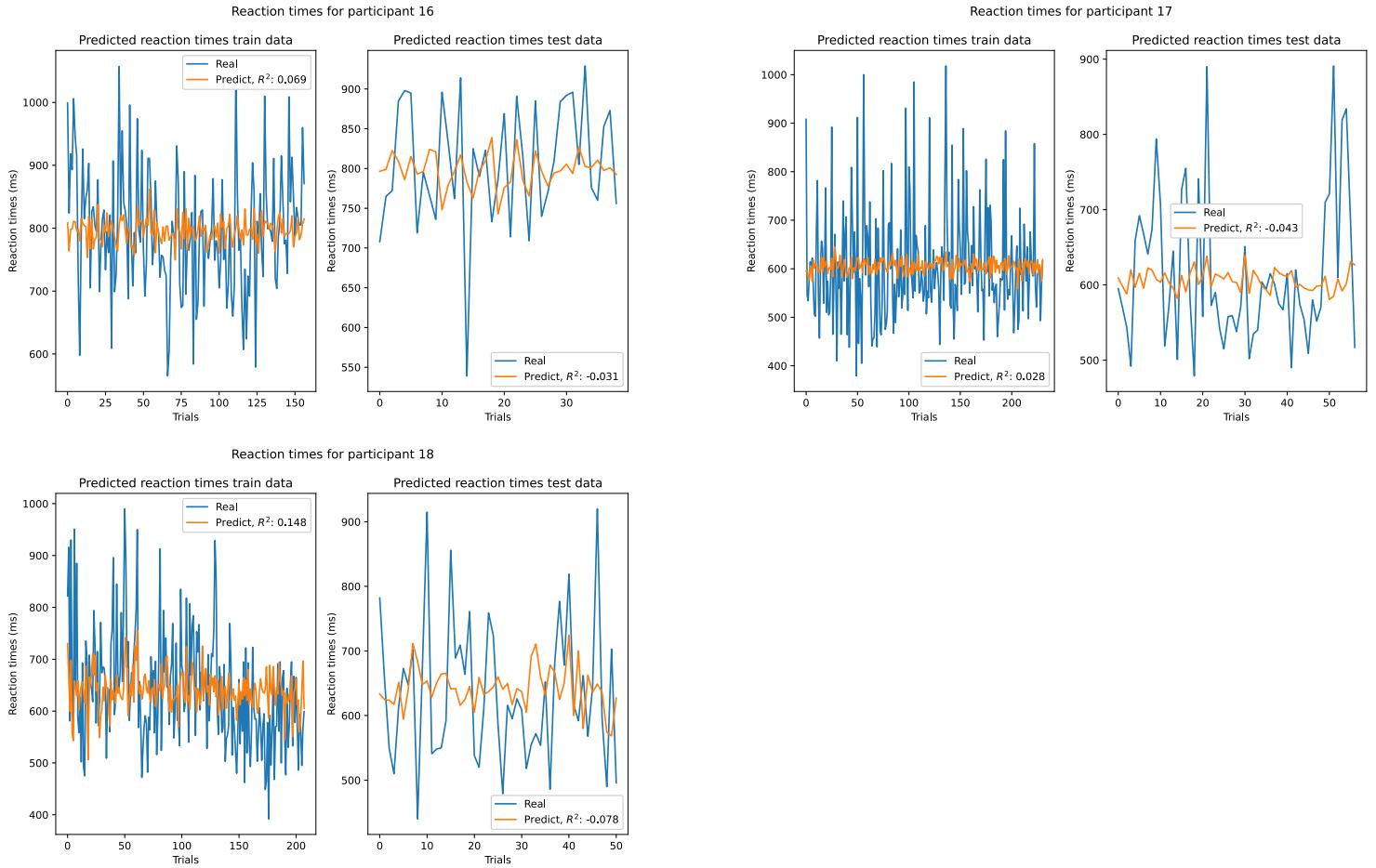
Pre-trial analysis

Regression results - train set



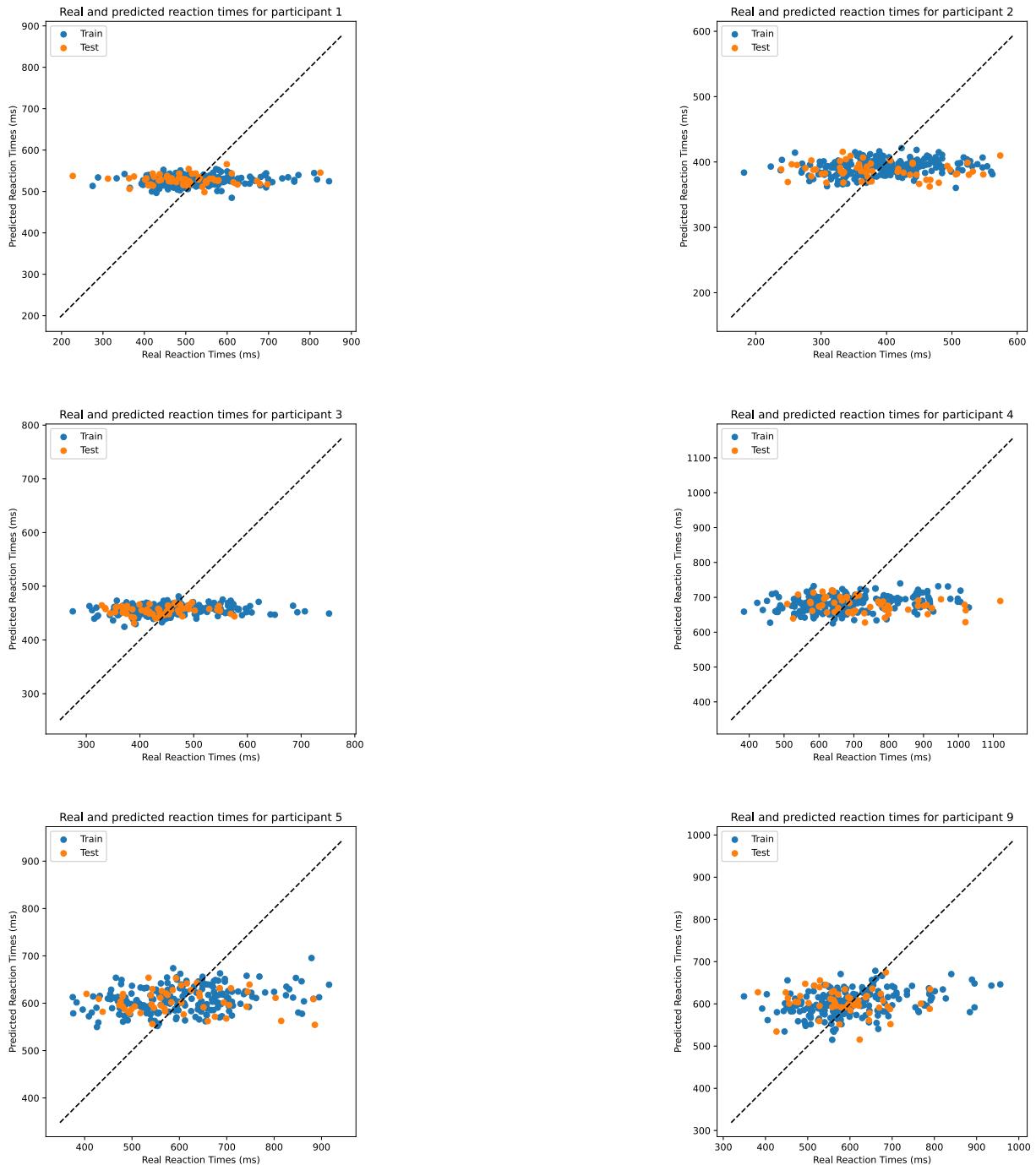
Pre-trial analysis

Regression results - train set



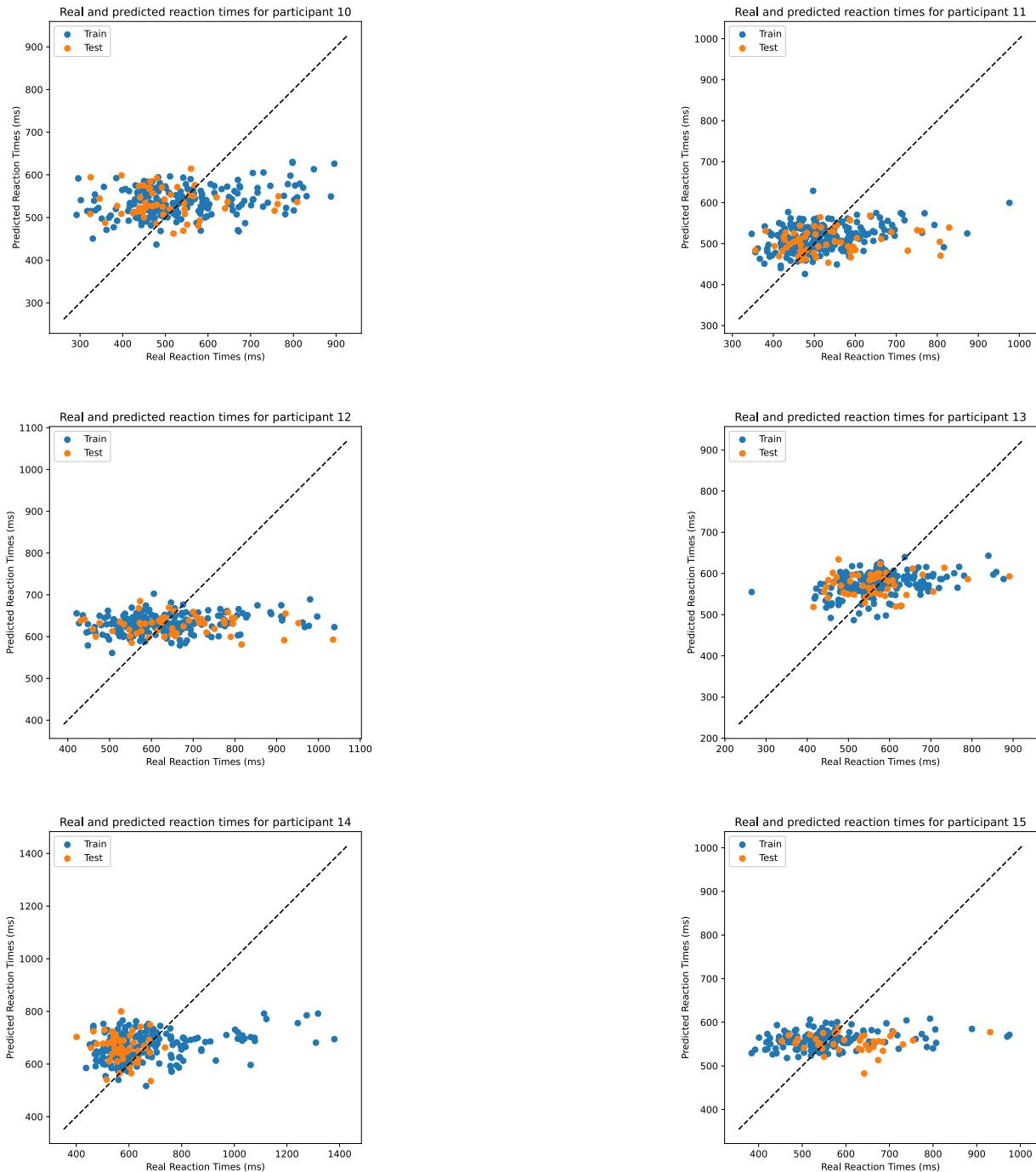
Pre-trial analysis

Regression results scatter plot - train set



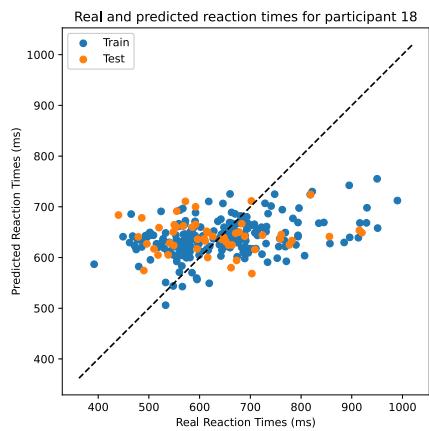
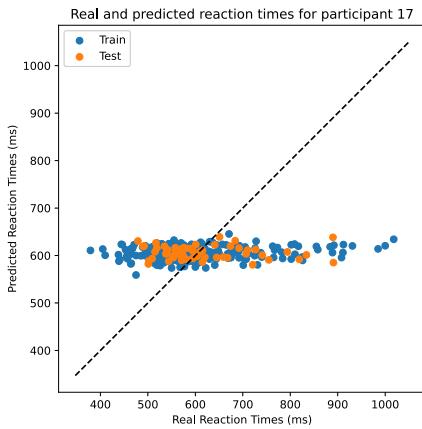
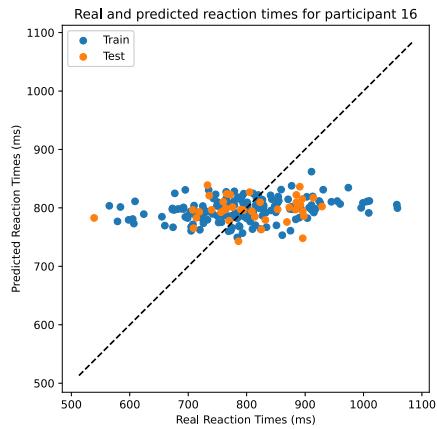
Pre-trial analysis

Regression results scatter plot - train set



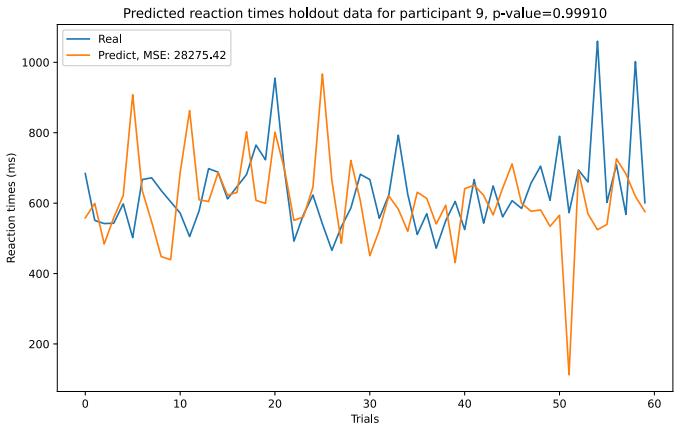
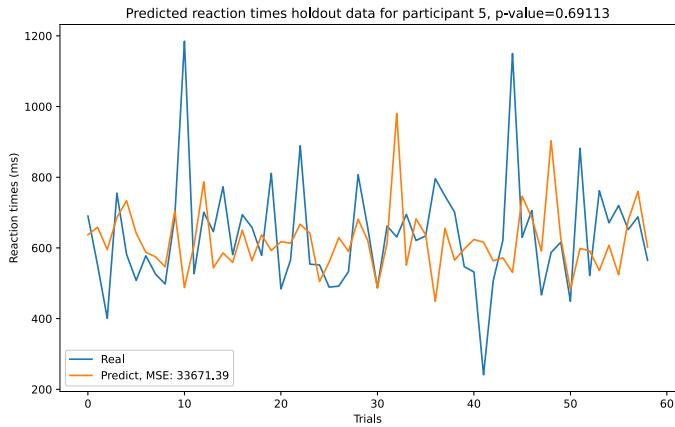
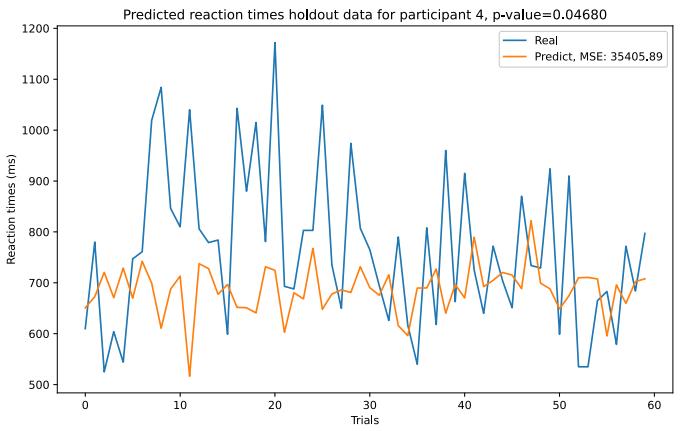
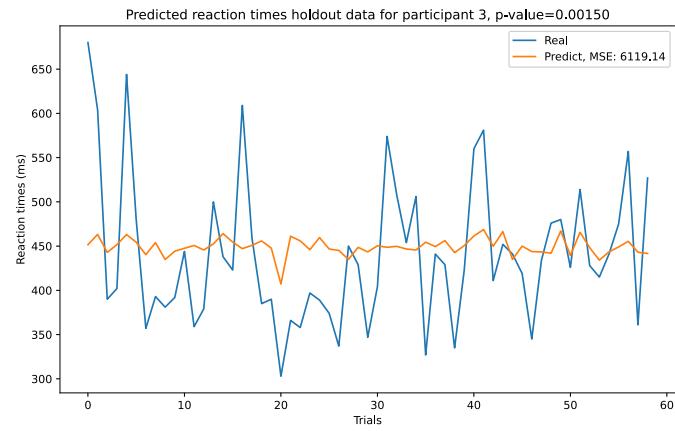
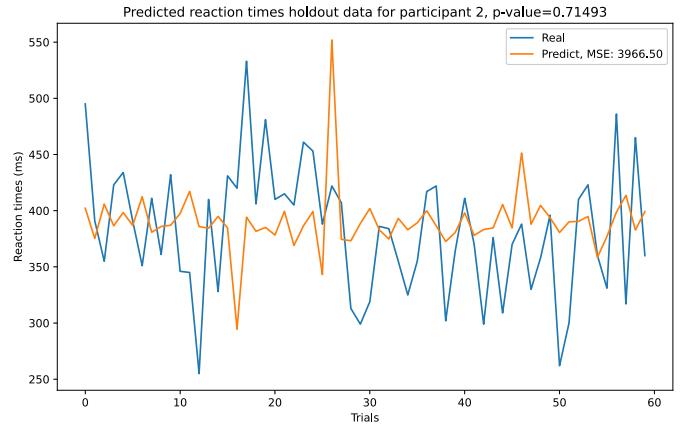
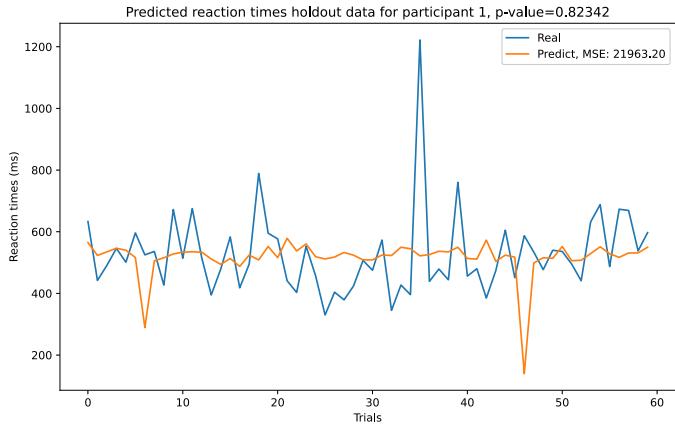
Pre-trial analysis

Regression results scatter plot - train set



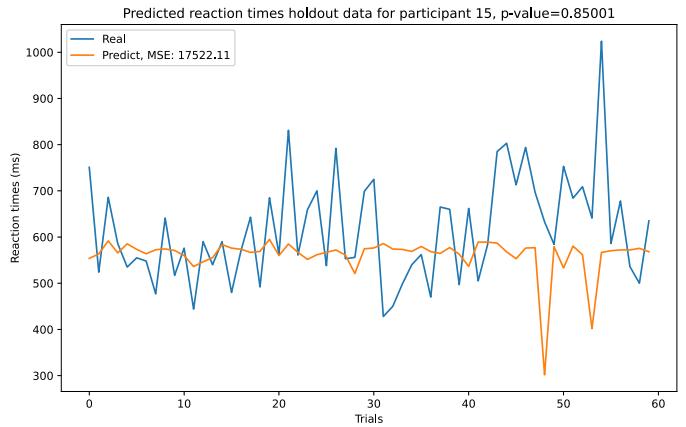
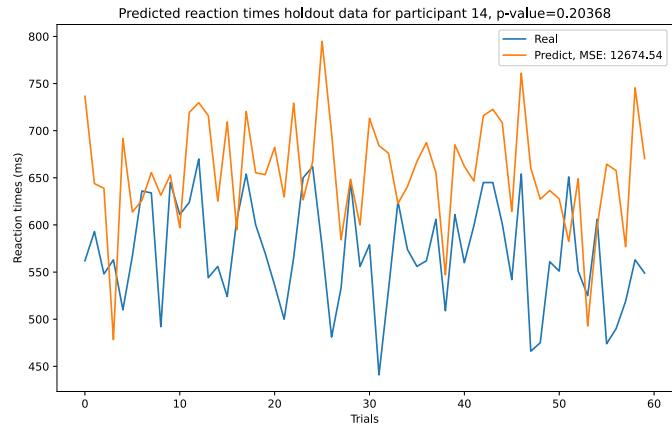
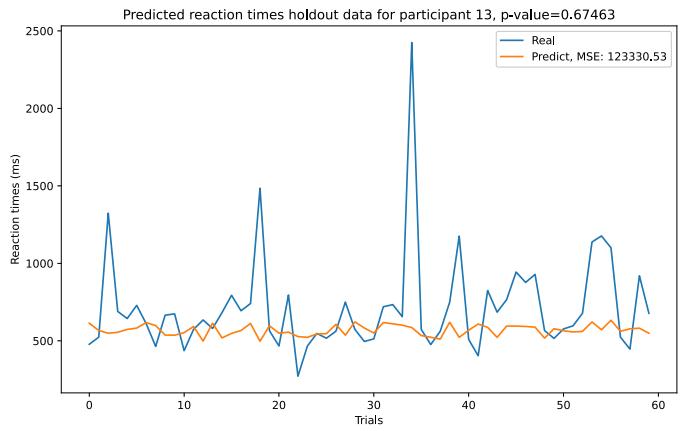
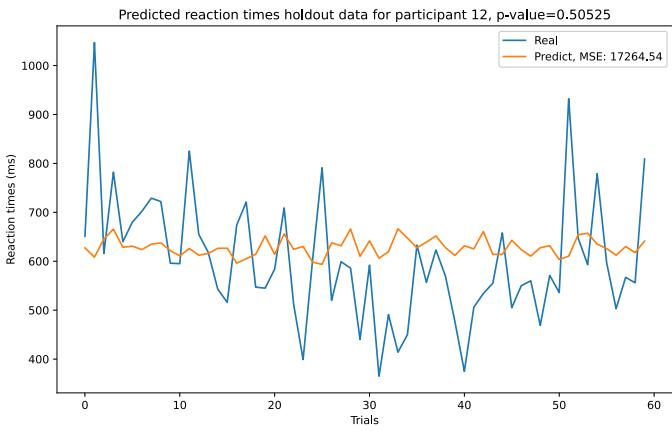
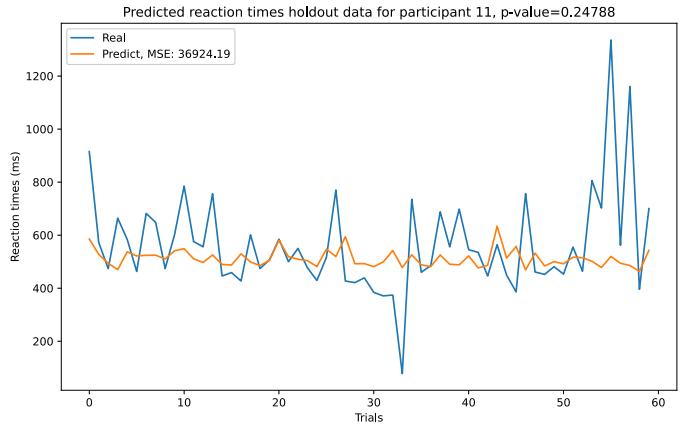
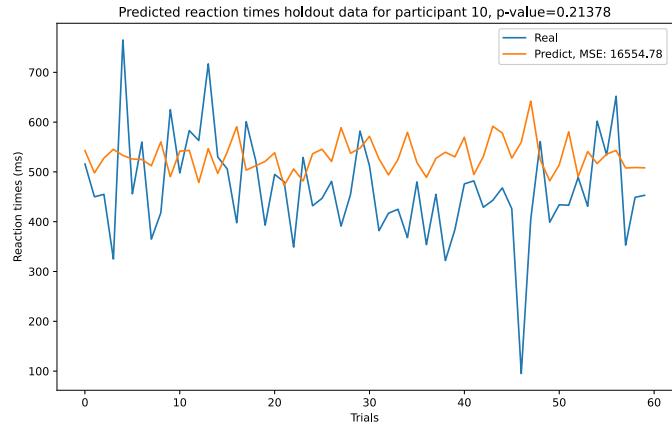
Pre-trial analysis

Regression results - holdout set



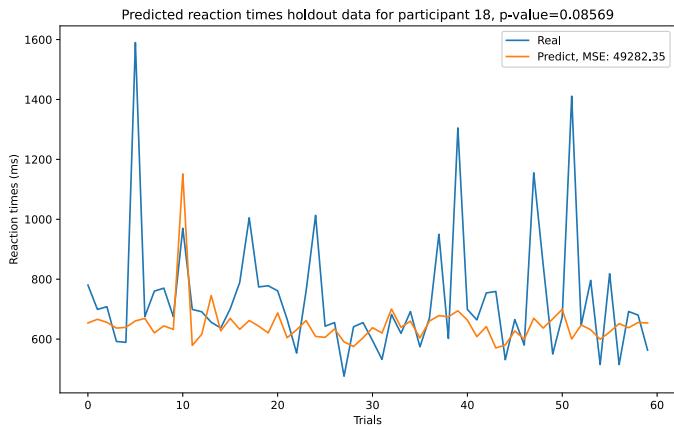
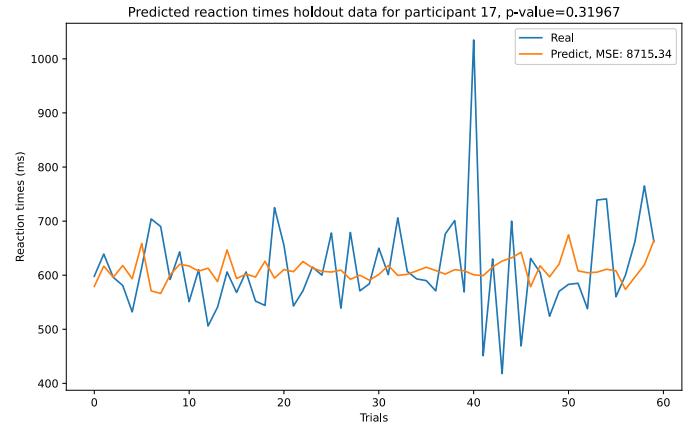
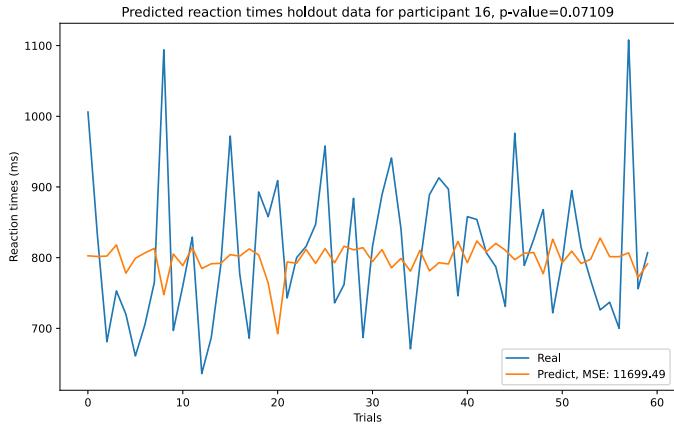
Pre-trial analysis

Regression results - holdout set



Pre-trial analysis

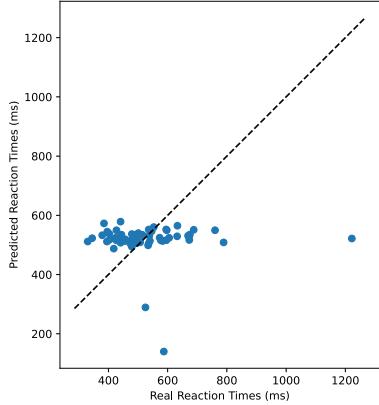
Regression results - holdout set



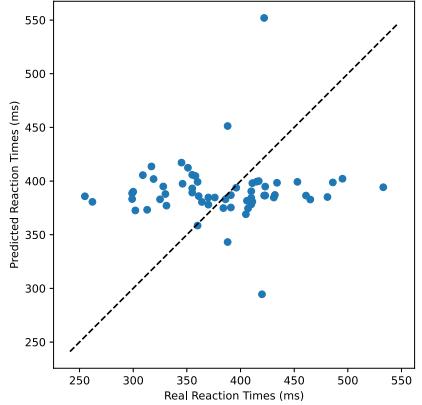
Pre-trial analysis

Regression results scatter plot - holdout set

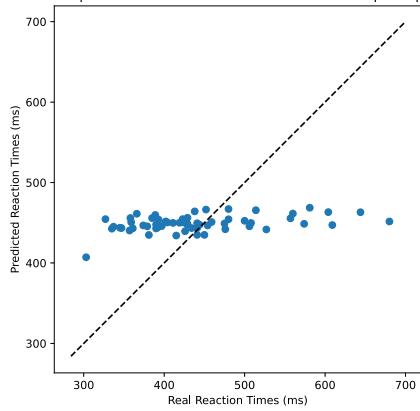
Real and predicted reaction times of holdout data for participant 1



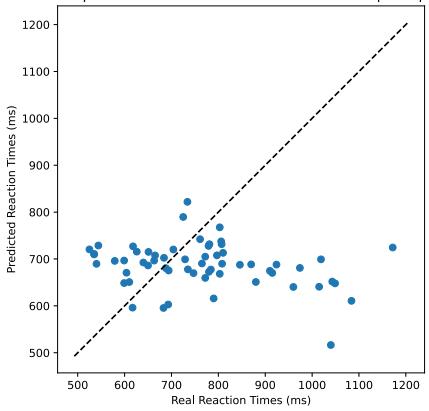
Real and predicted reaction times of holdout data for participant 2



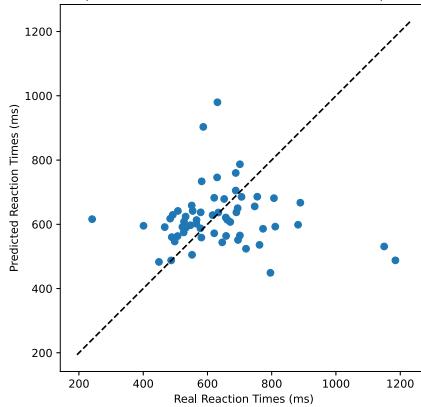
Real and predicted reaction times of holdout data for participant 3



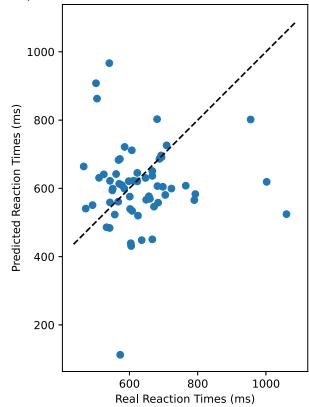
Real and predicted reaction times of holdout data for participant 4



Real and predicted reaction times of holdout data for participant 5

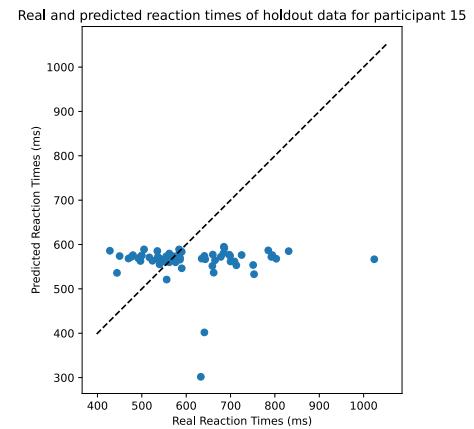
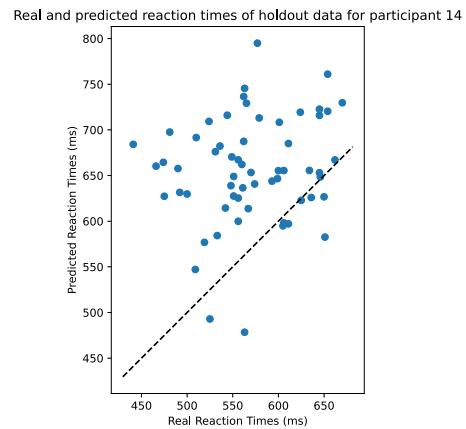
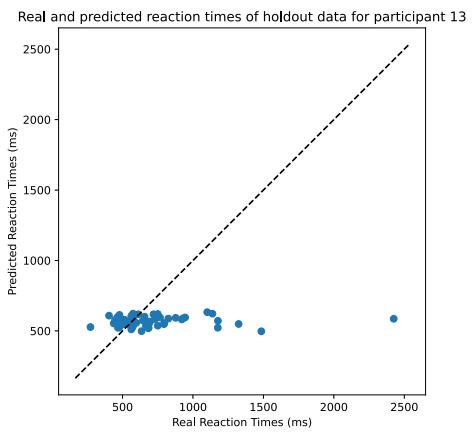
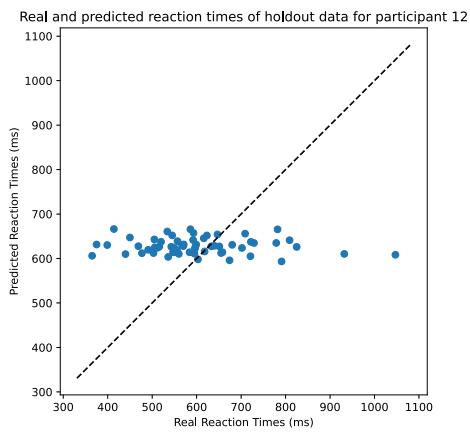
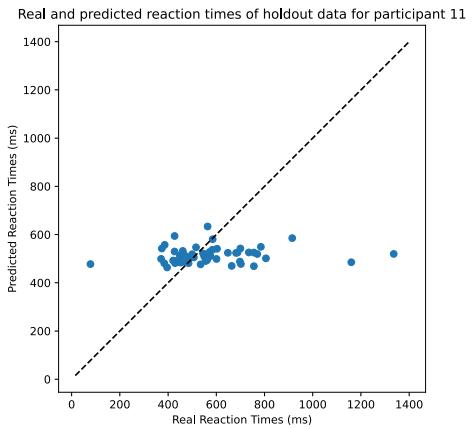
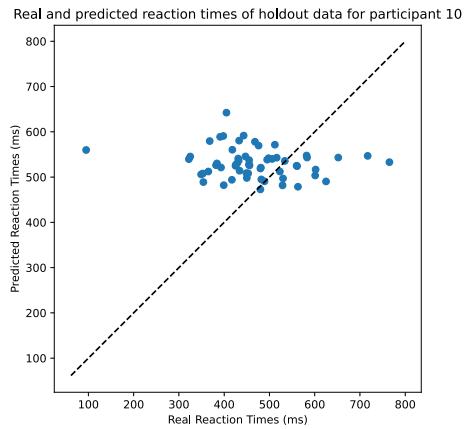


Real and predicted reaction times of holdout data for participant 9



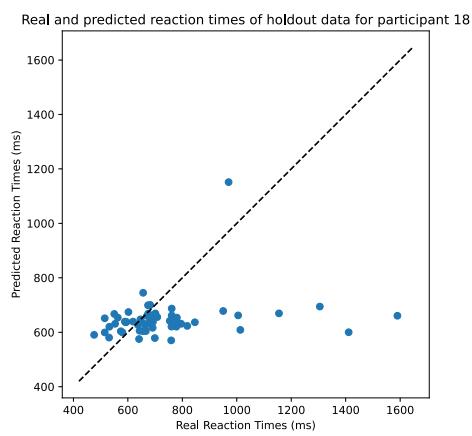
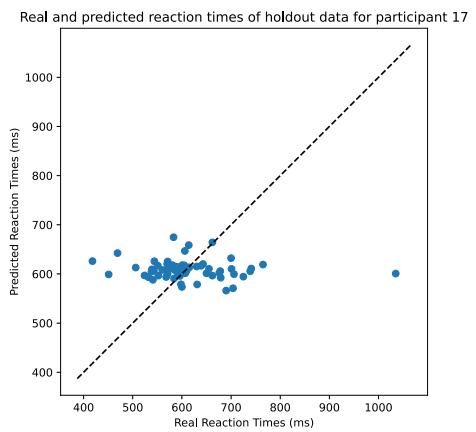
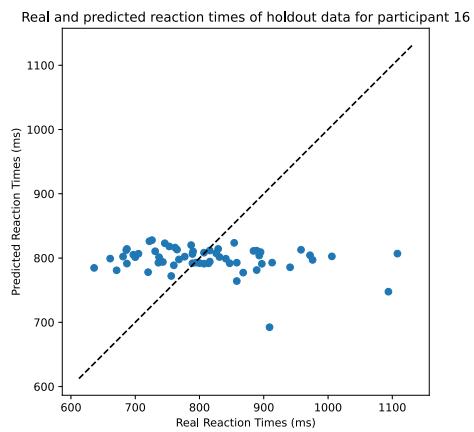
Pre-trial analysis

Regression results scatter plot - holdout set



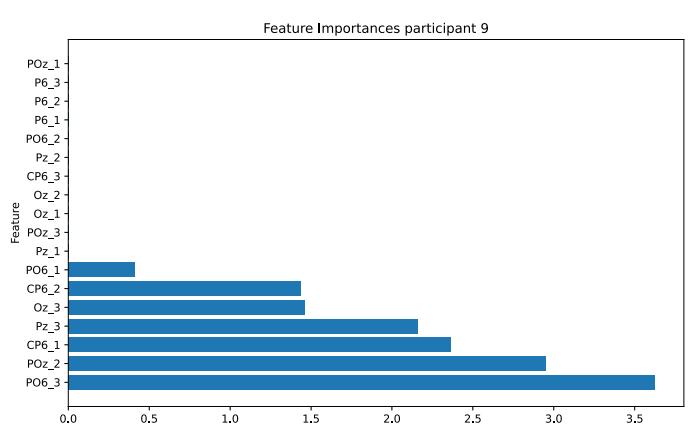
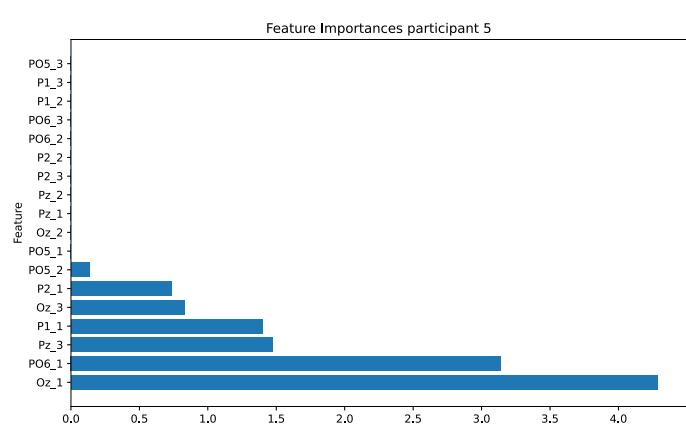
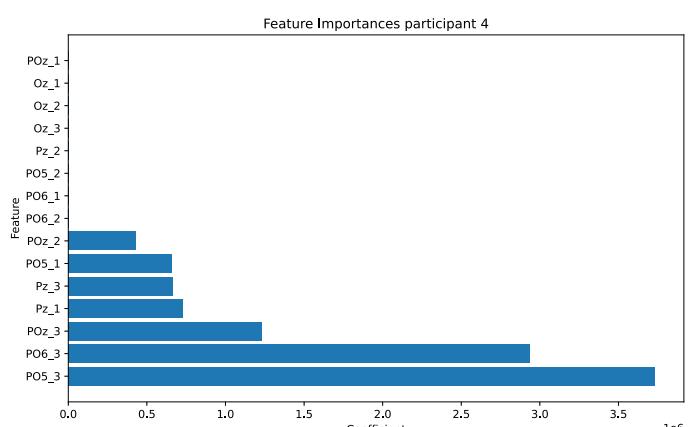
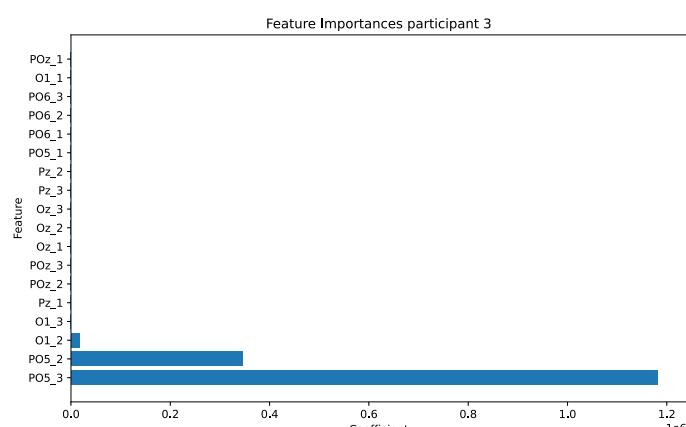
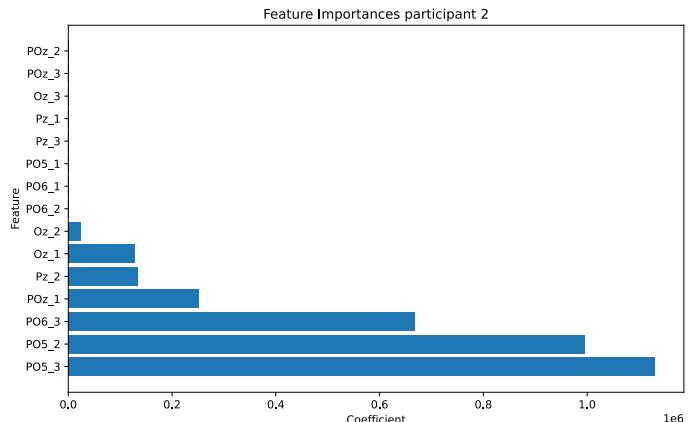
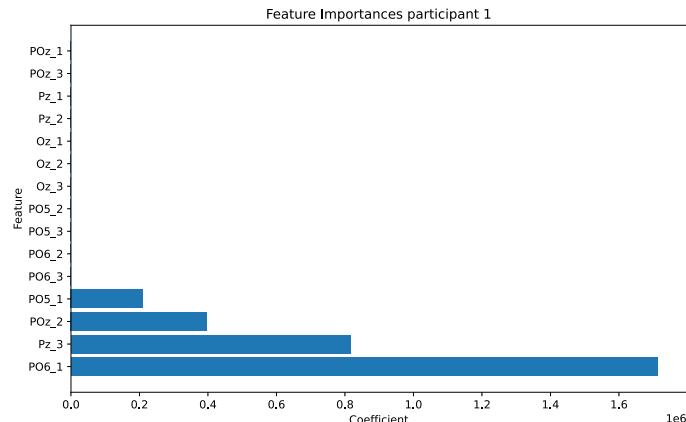
Pre-trial analysis

Regression results scatter plot - holdout set



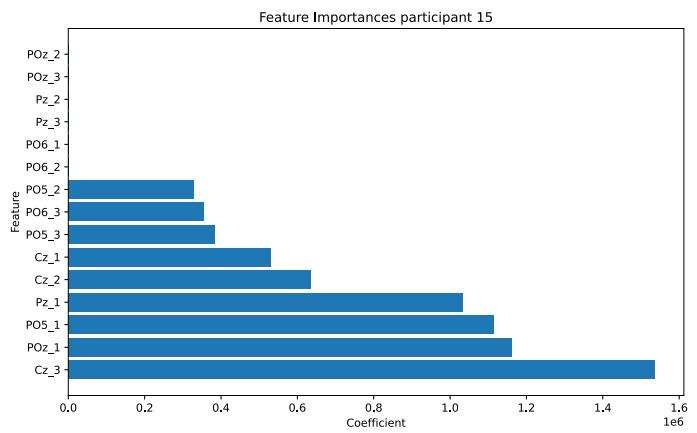
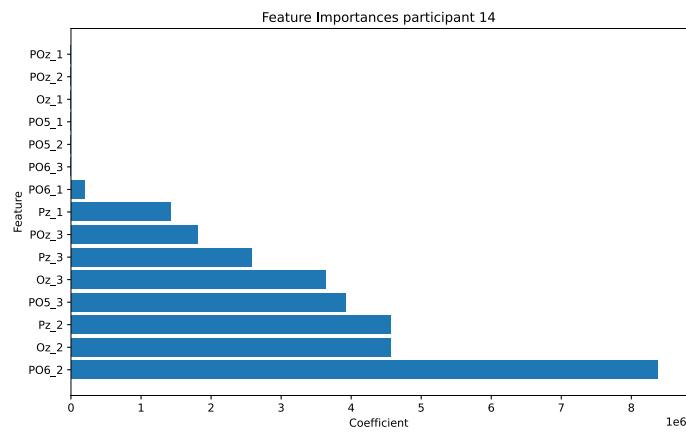
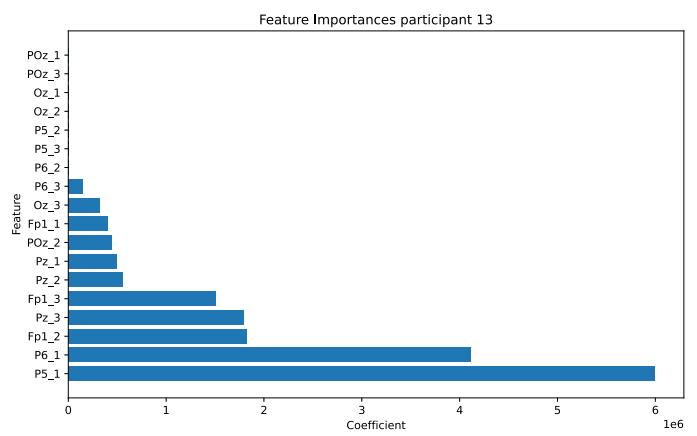
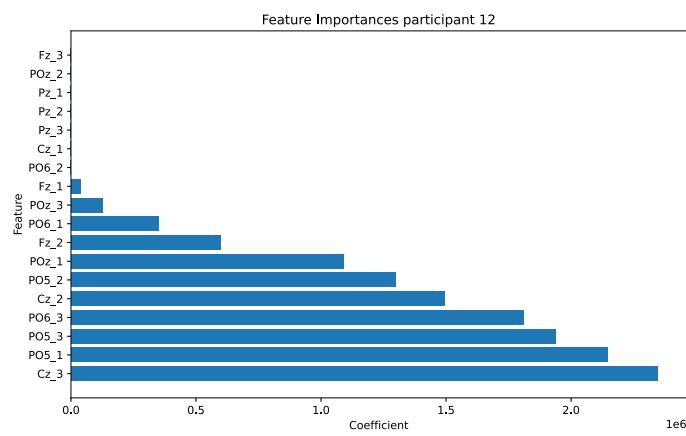
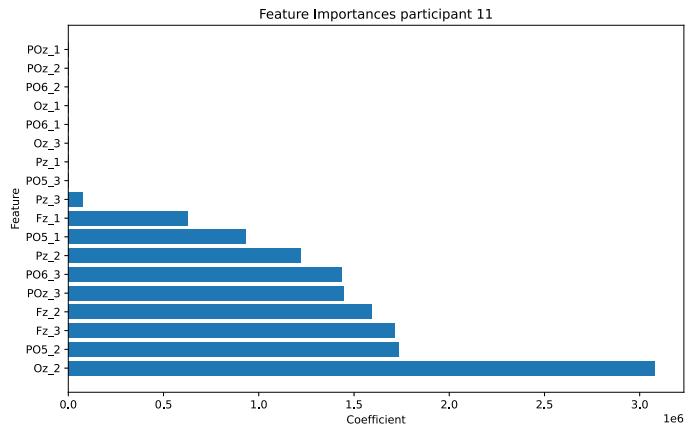
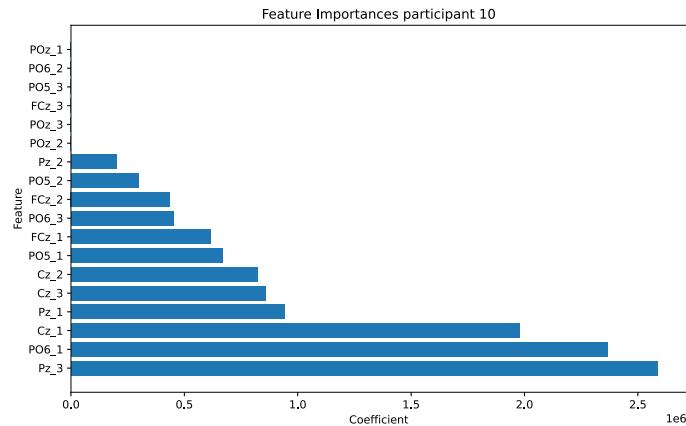
Pre-trial analysis

Feature importance - holdout set



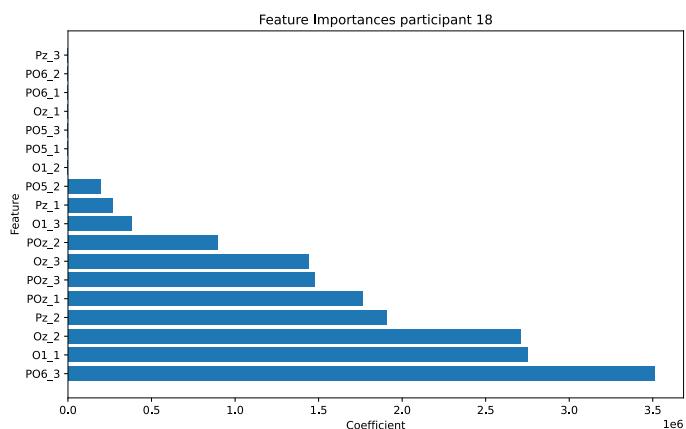
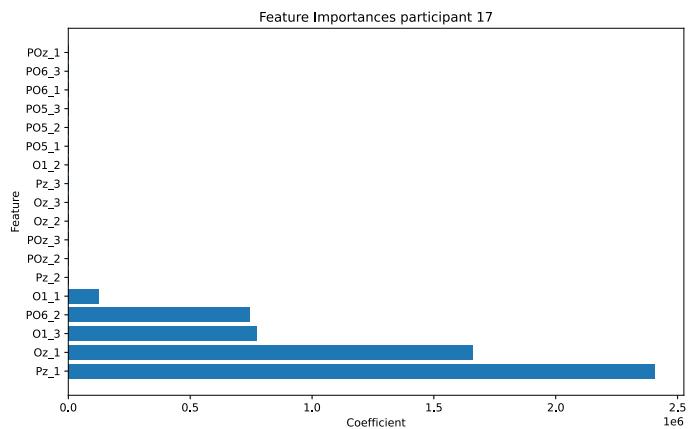
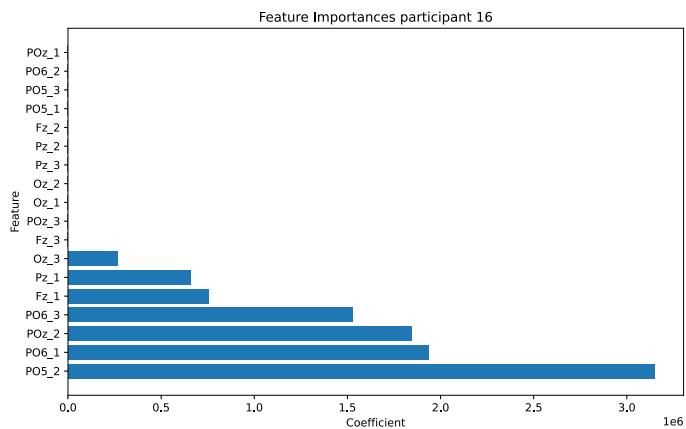
Pre-trial analysis

Feature importance - holdout set



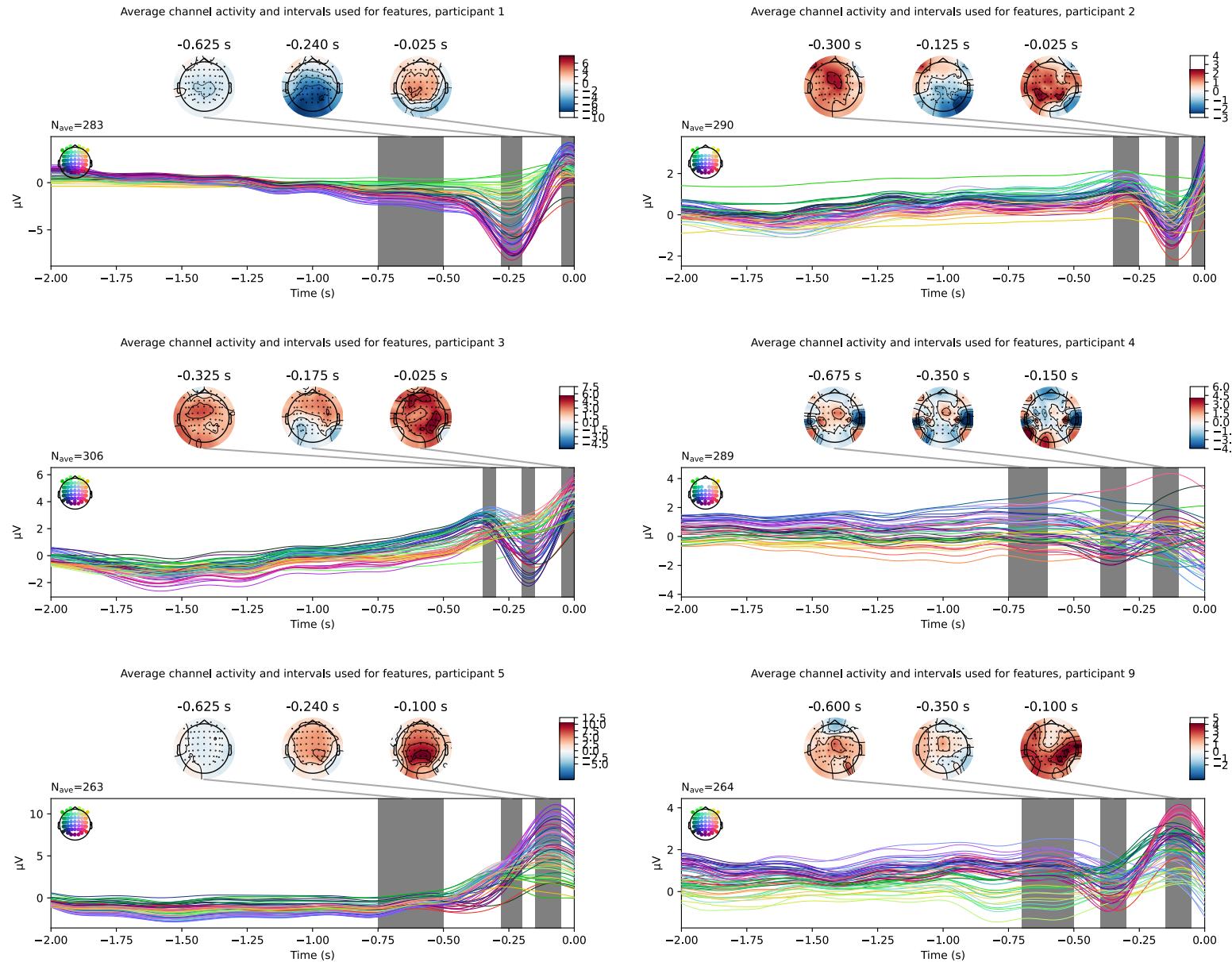
Pre-trial analysis

Feature importance - holdout set



Pre-movement analysis

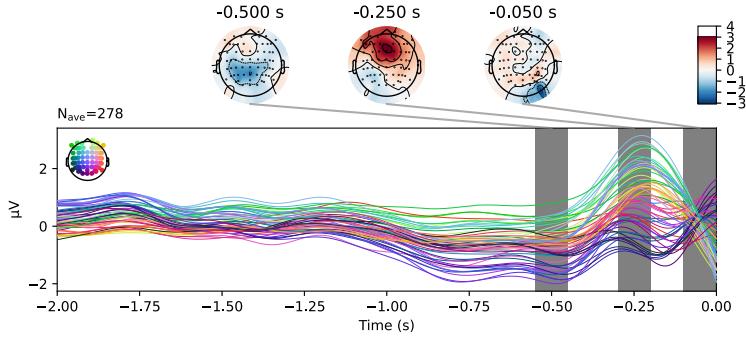
Averaged signals - train set



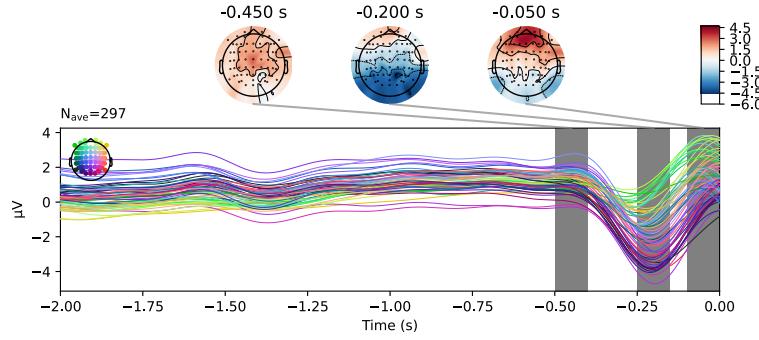
Pre-movement analysis

Averaged signals - train set

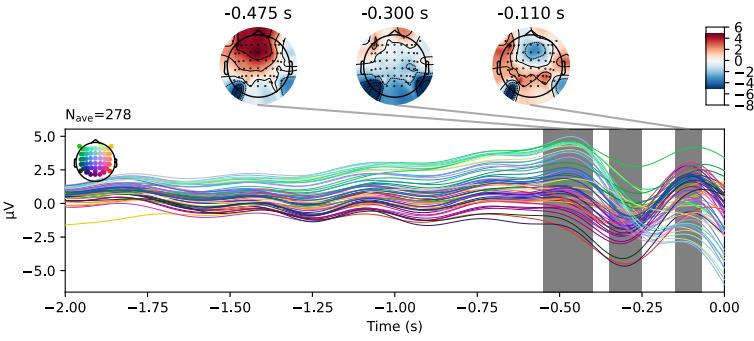
Average channel activity and intervals used for features, participant 10



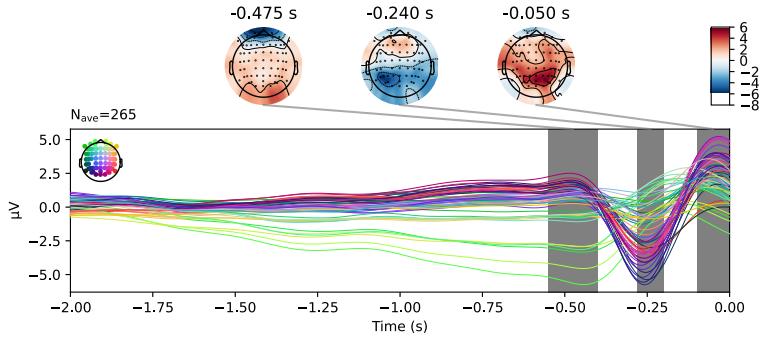
Average channel activity and intervals used for features, participant 11



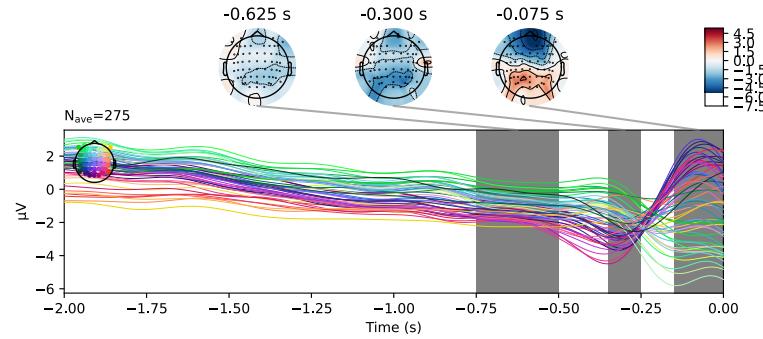
Average channel activity and intervals used for features, participant 12



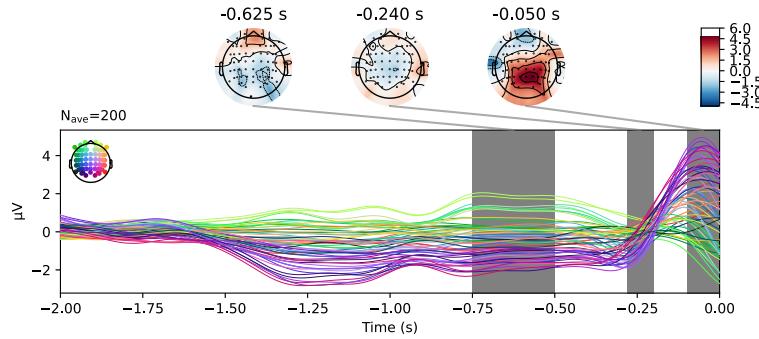
Average channel activity and intervals used for features, participant 13



Average channel activity and intervals used for features, participant 14



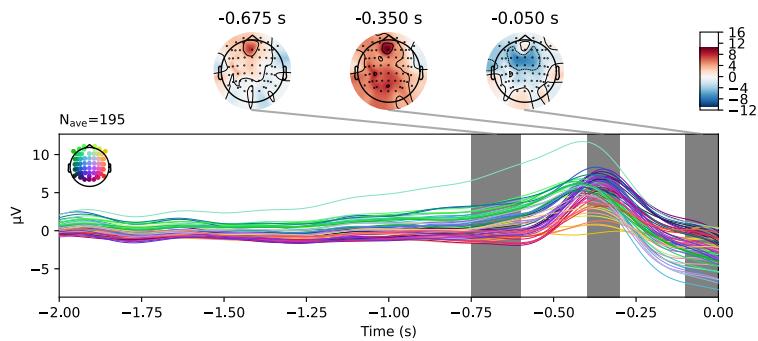
Average channel activity and intervals used for features, participant 15



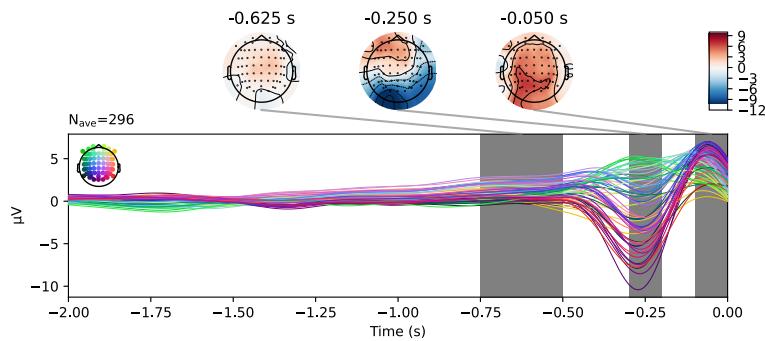
Pre-movement analysis

Averaged signals - train set

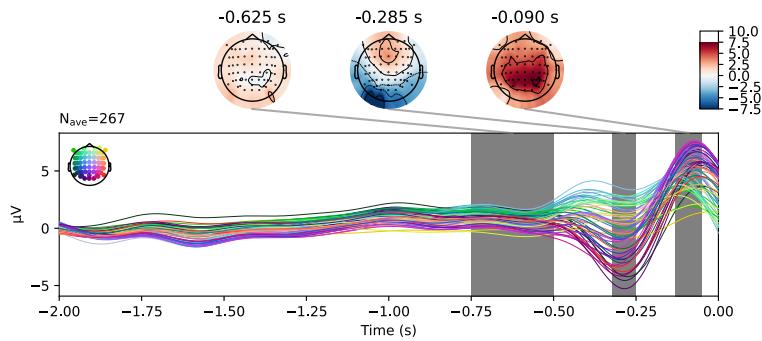
Average channel activity and intervals used for features, participant 16



Average channel activity and intervals used for features, participant 17

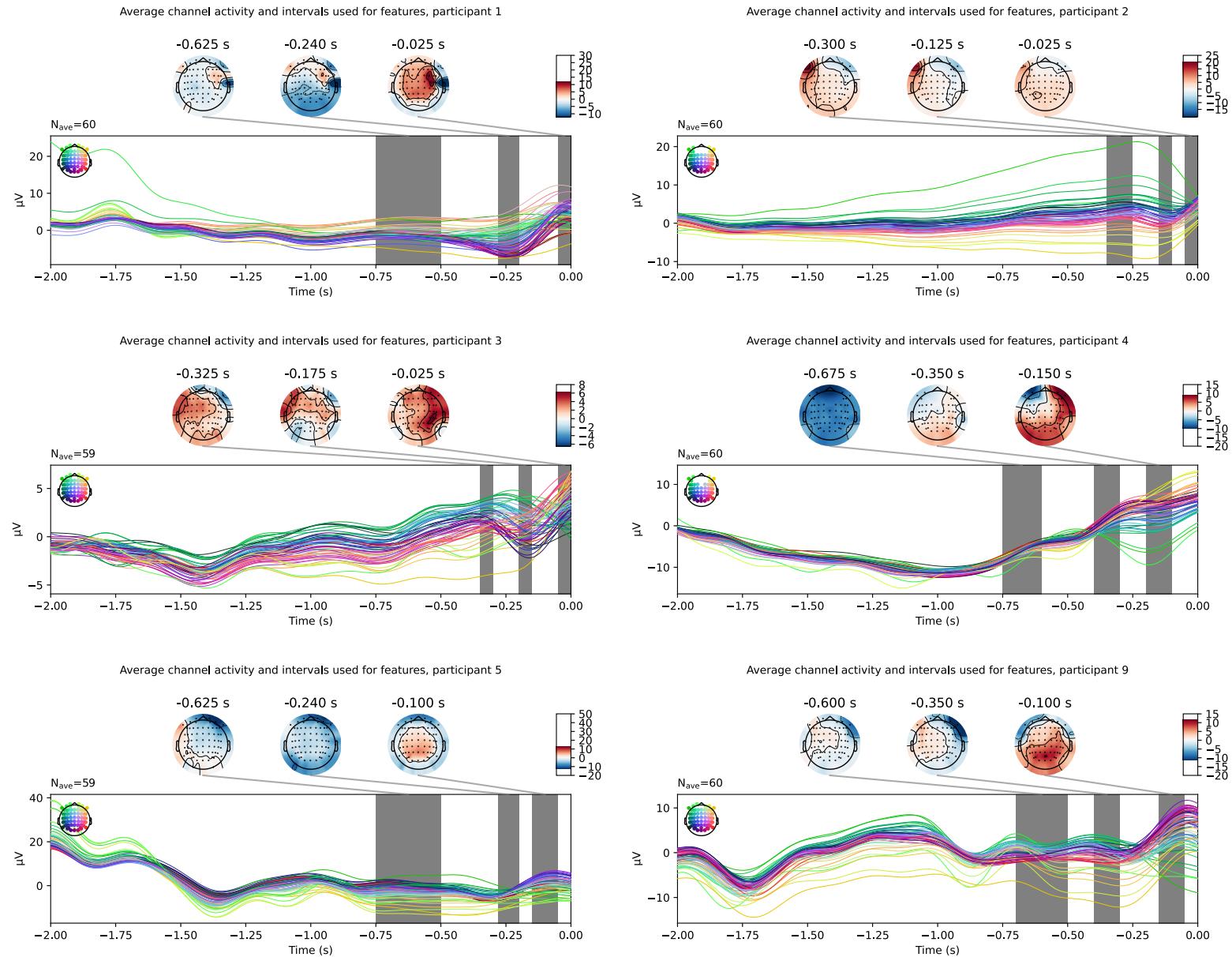


Average channel activity and intervals used for features, participant 18



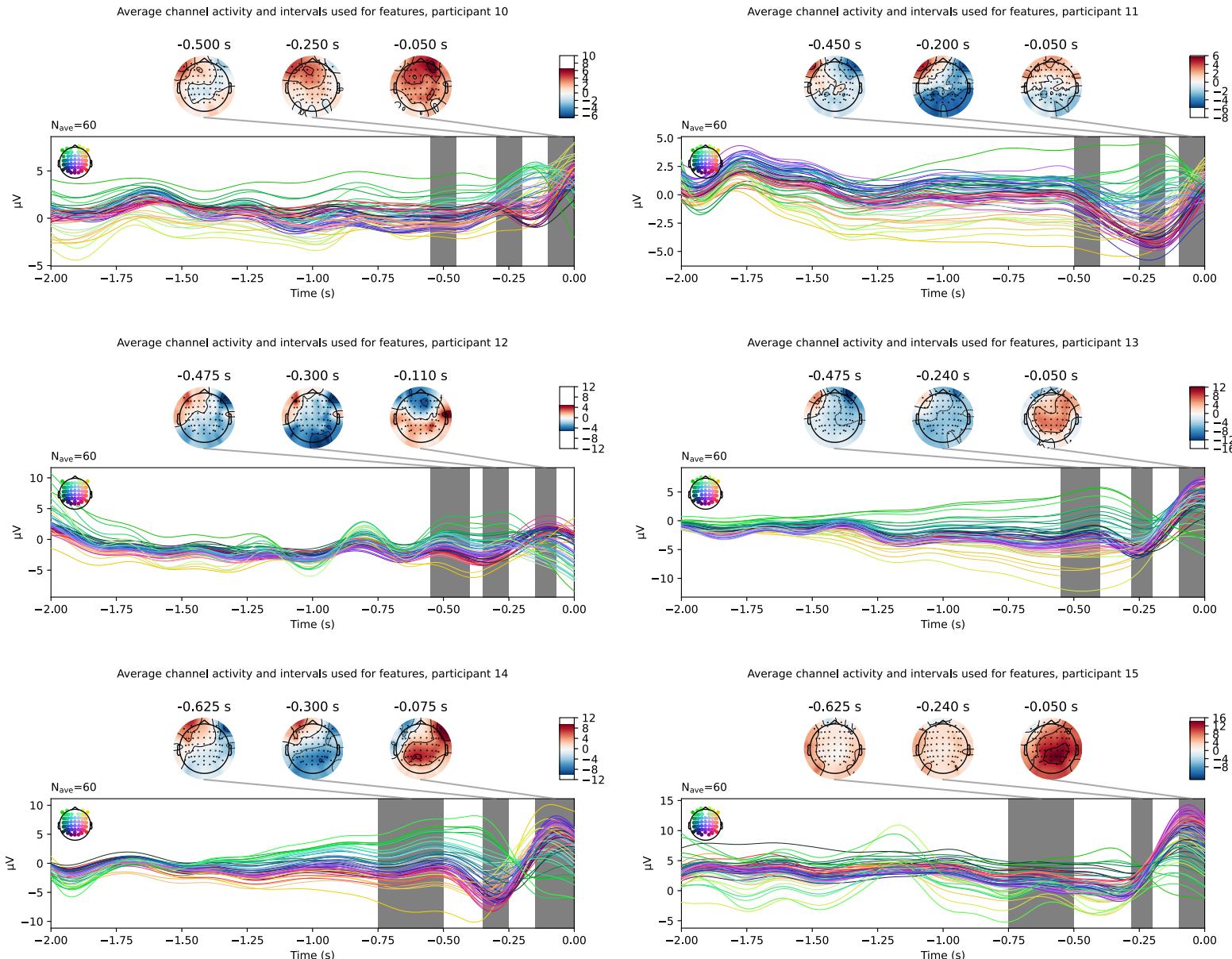
Pre-movement analysis

Averaged signals - holdout set



Pre-movement analysis

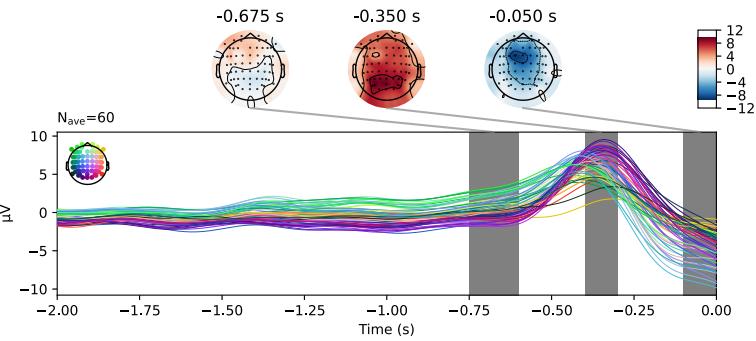
Averaged signals - holdout set



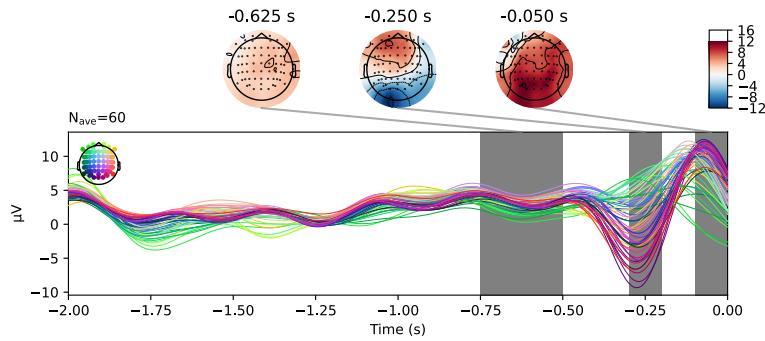
Pre-movement analysis

Averaged signals - holdout set

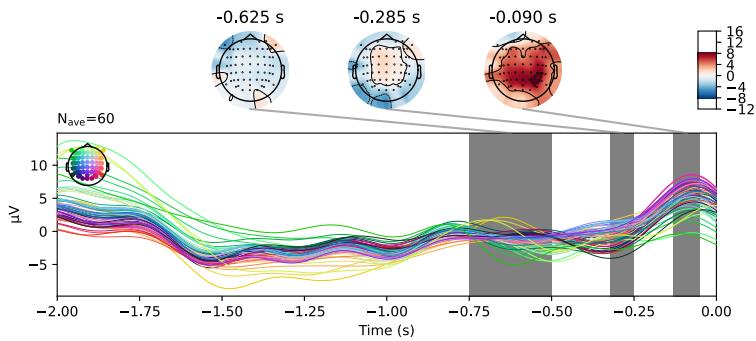
Average channel activity and intervals used for features, participant 16



Average channel activity and intervals used for features, participant 17

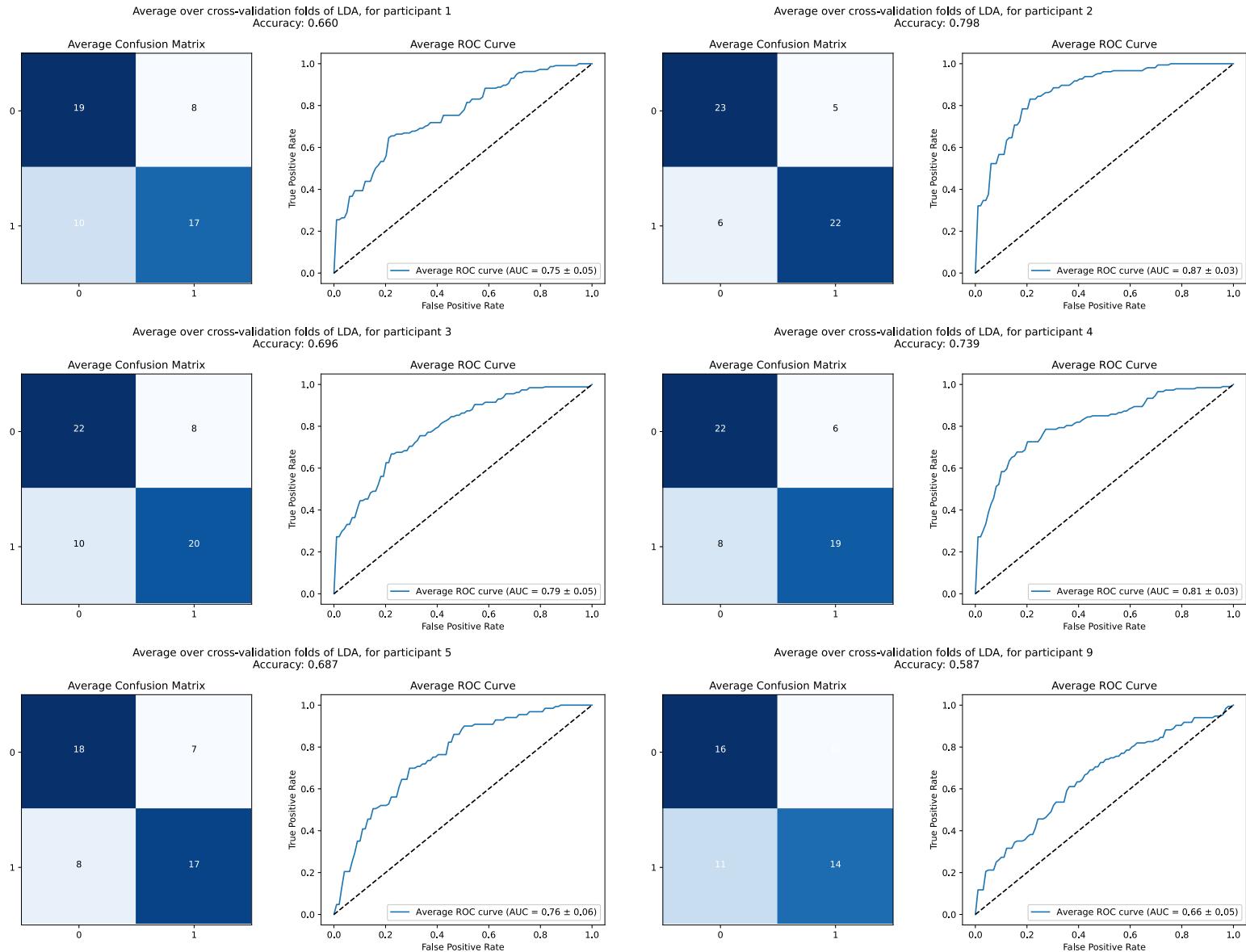


Average channel activity and intervals used for features, participant 18



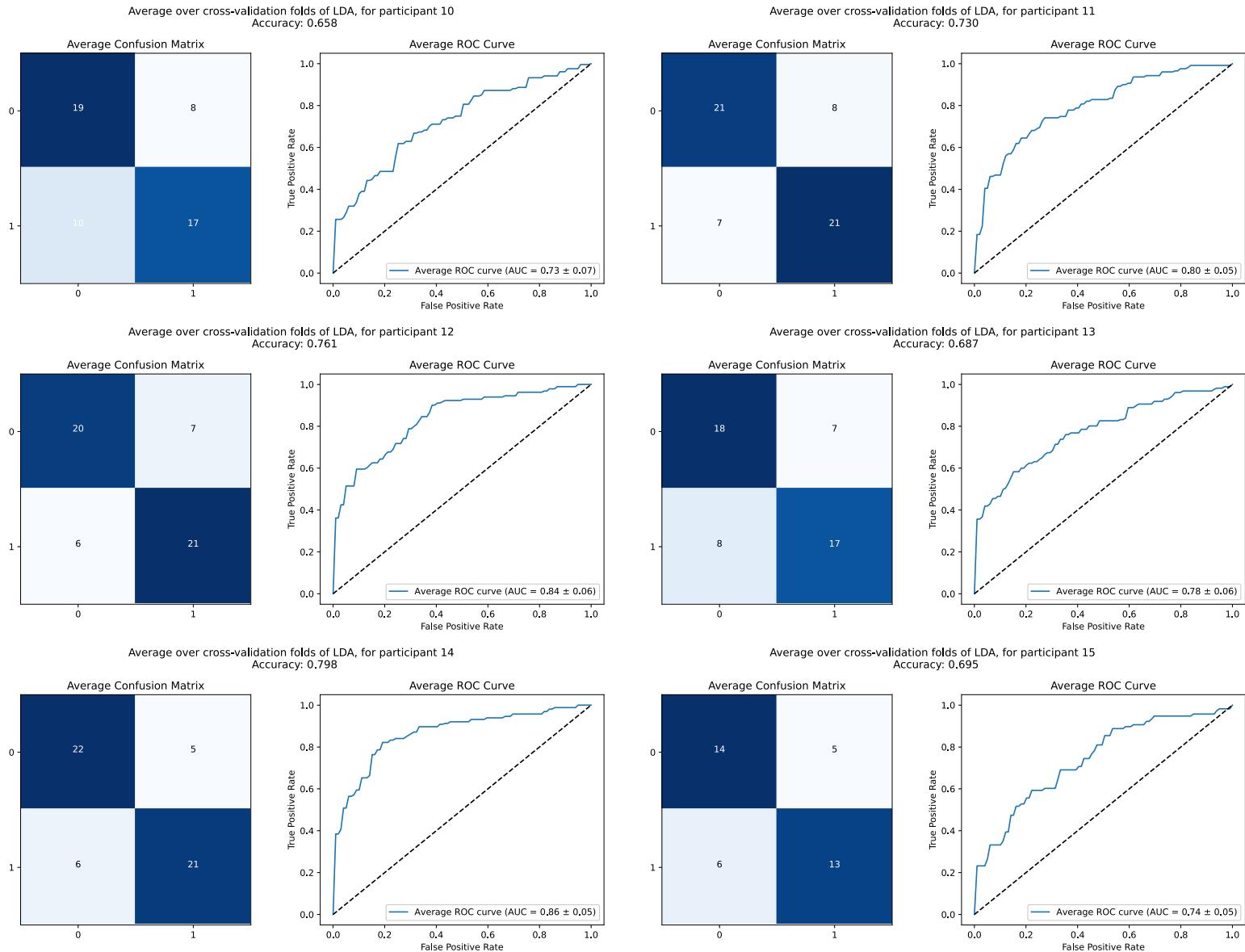
Pre-movement analysis

Classification results - train set



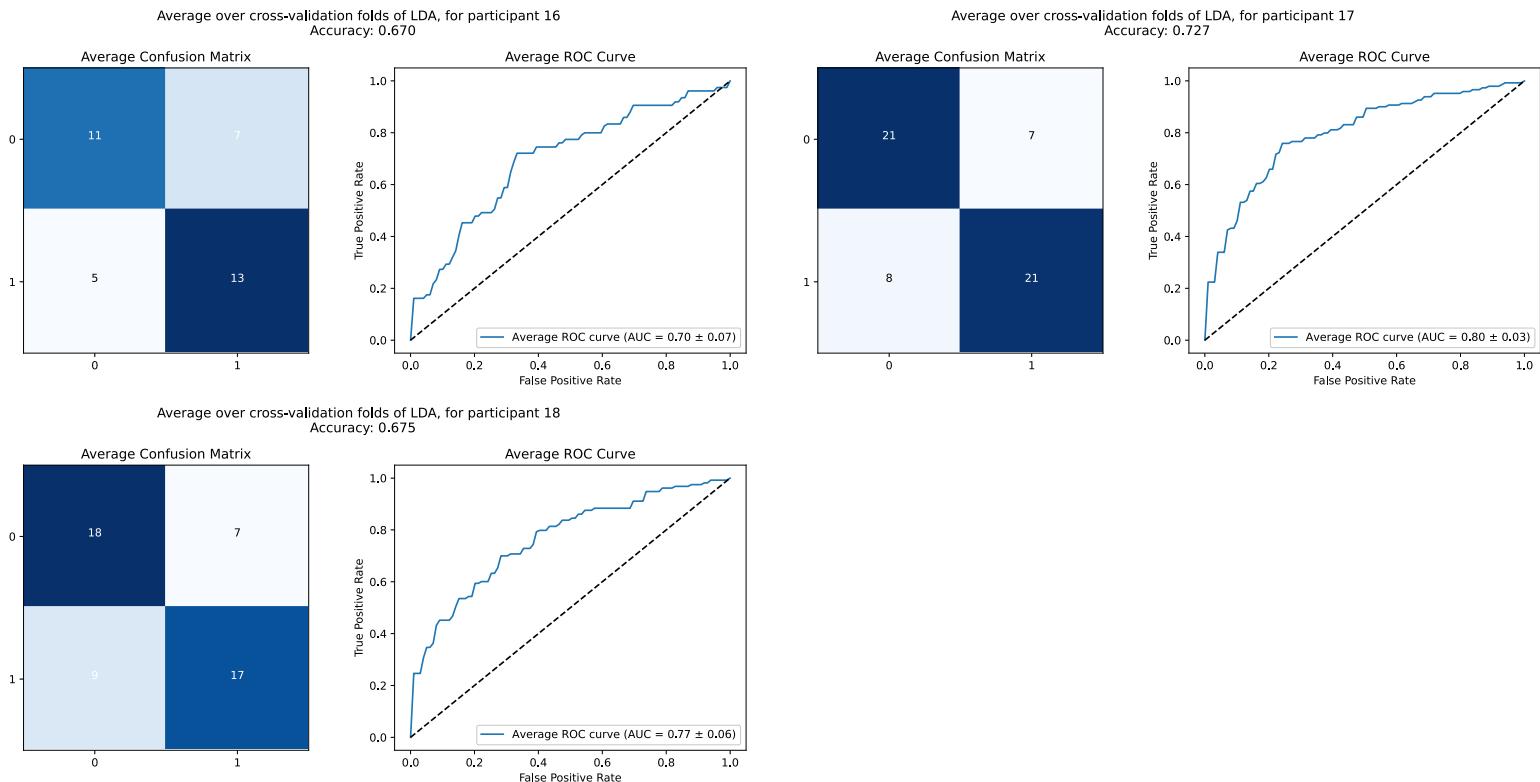
Pre-movement analysis

Classification results - train set



Pre-movement analysis

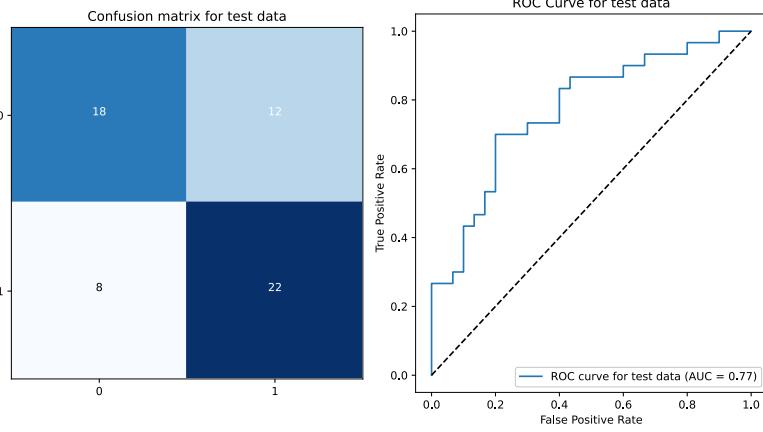
Classification results - train set



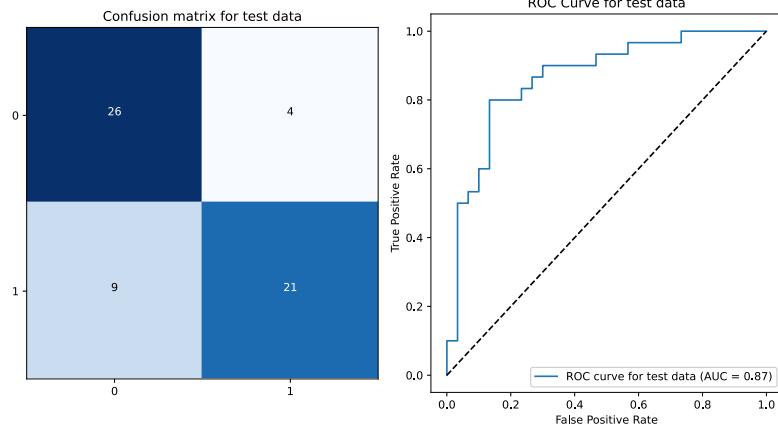
Pre-movement analysis

Classification results - holdout set

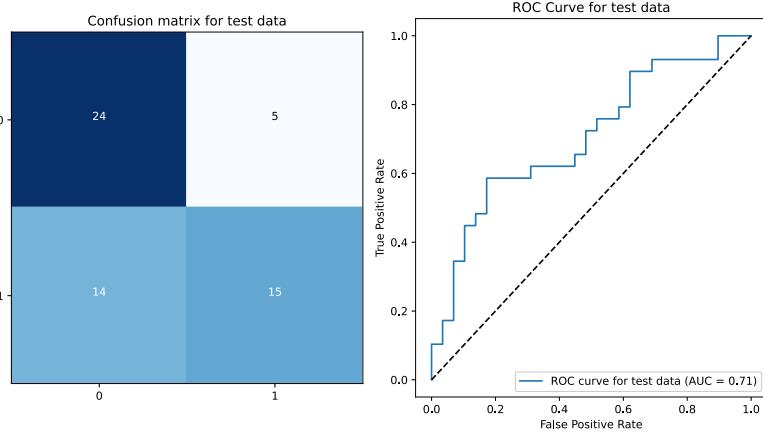
LDA on holdout data of participant 1, p-value=0.00960



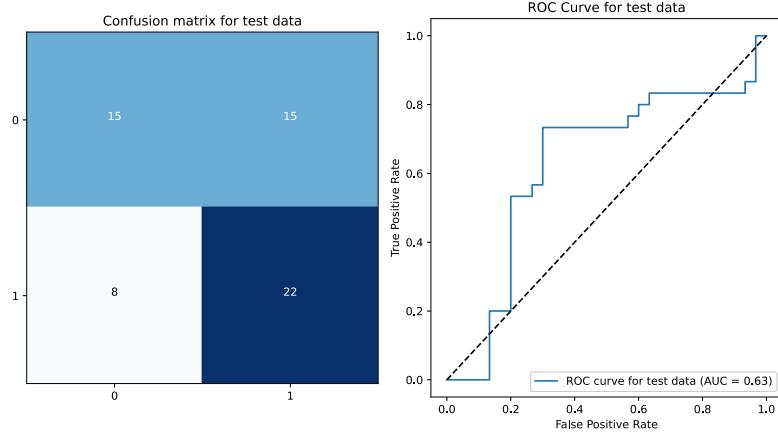
LDA on holdout data of participant 2, p-value=0.00010



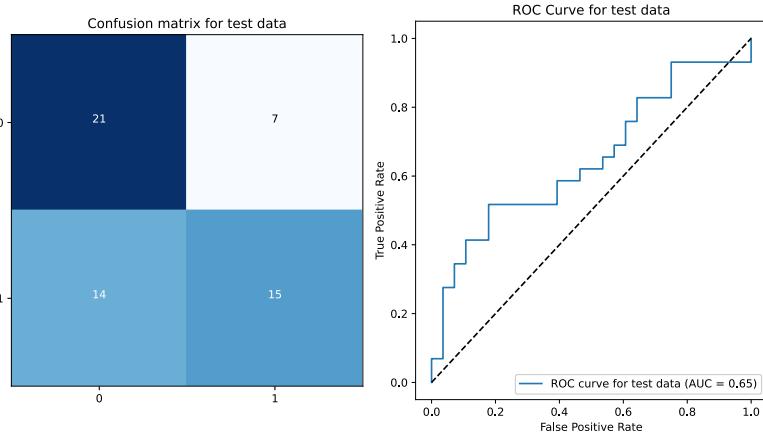
LDA on holdout data of participant 3, p-value=0.00650



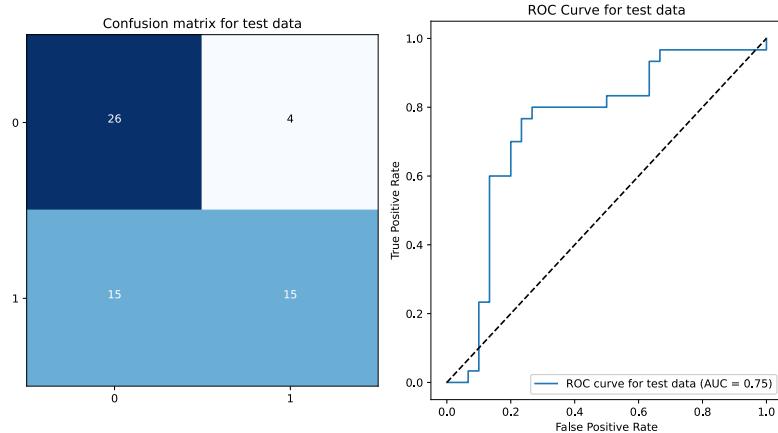
LDA on holdout data of participant 4, p-value=0.05959



LDA on holdout data of participant 5, p-value=0.04170



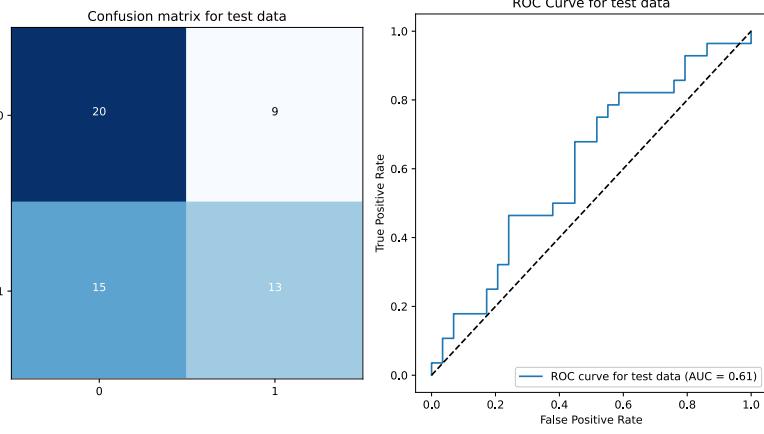
LDA on holdout data of participant 9, p-value=0.00260



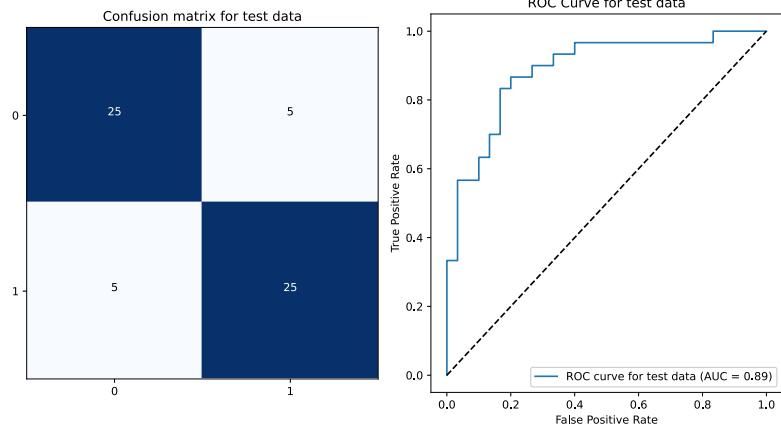
Pre-movement analysis

Classification results - holdout set

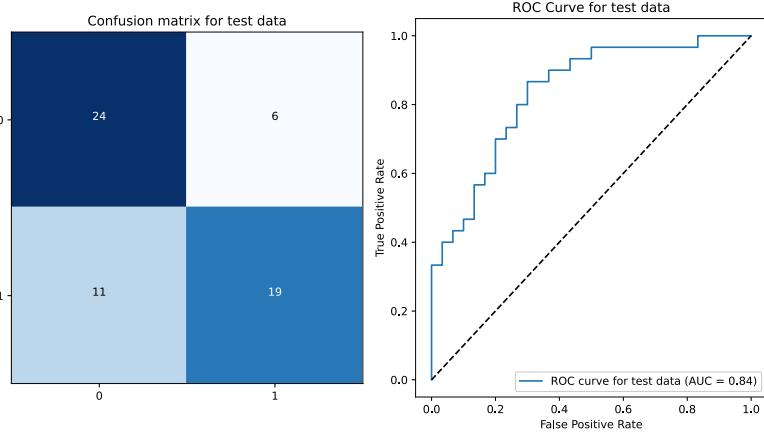
LDA on holdout data of participant 10, p-value=0.17378



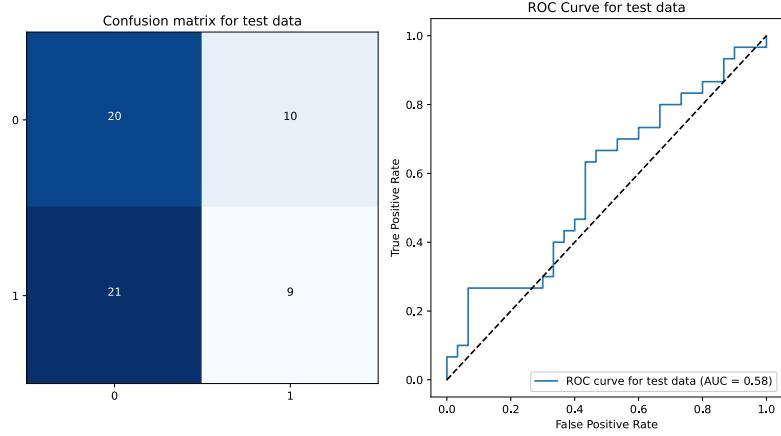
LDA on holdout data of participant 11, p-value=0.00010



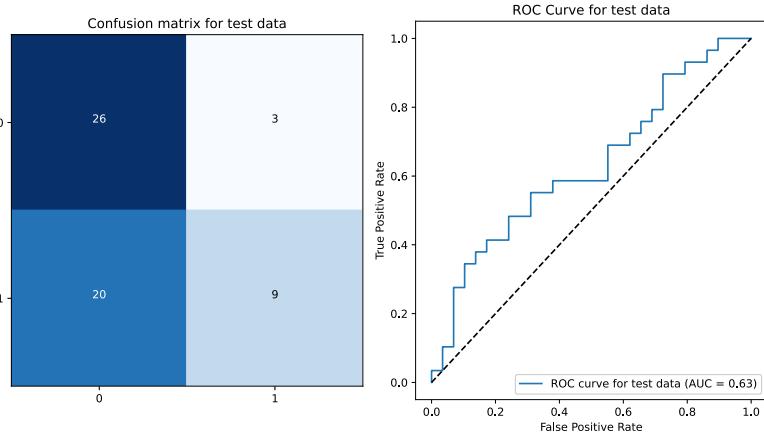
LDA on holdout data of participant 12, p-value=0.00070



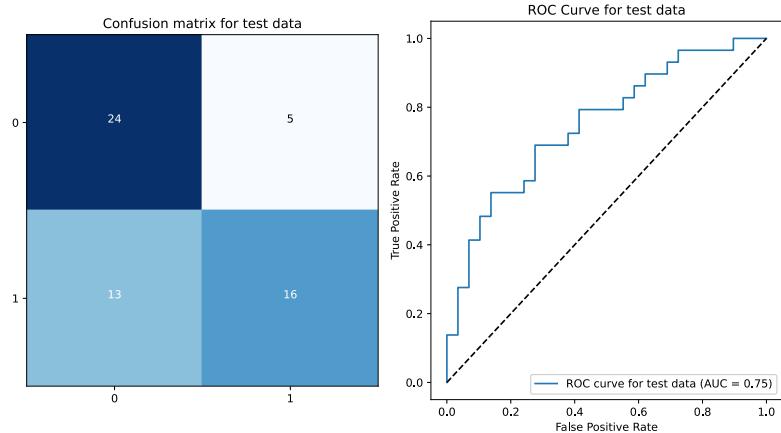
LDA on holdout data of participant 13, p-value=0.71173



LDA on holdout data of participant 14, p-value=0.05379



LDA on holdout data of participant 15, p-value=0.00350

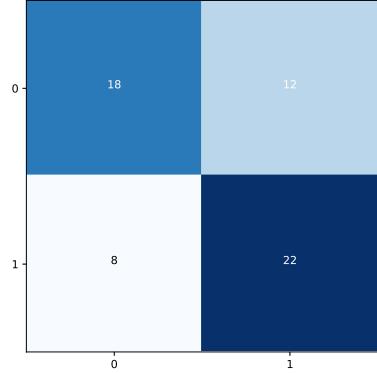


Pre-movement analysis

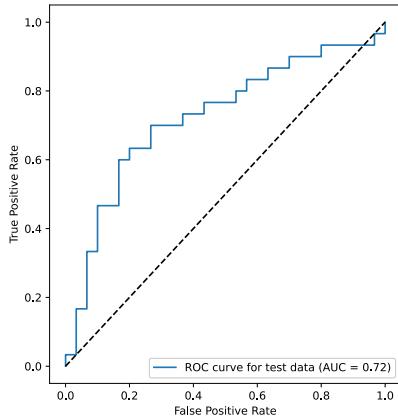
Classification results - holdout set

LDA on holdout data of participant 16, p-value=0.01060

Confusion matrix for test data

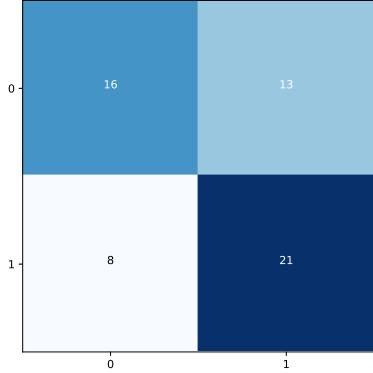


ROC Curve for test data

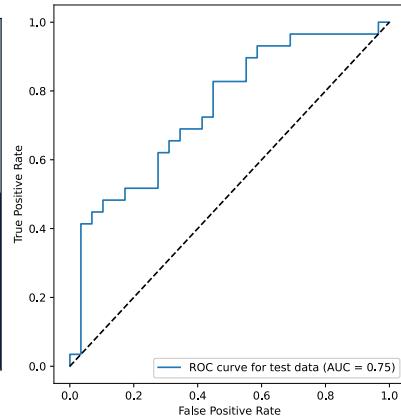


LDA on holdout data of participant 17, p-value=0.03160

Confusion matrix for test data

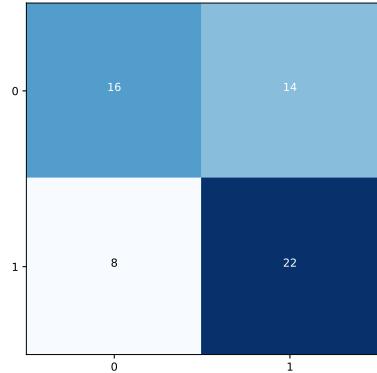


ROC Curve for test data

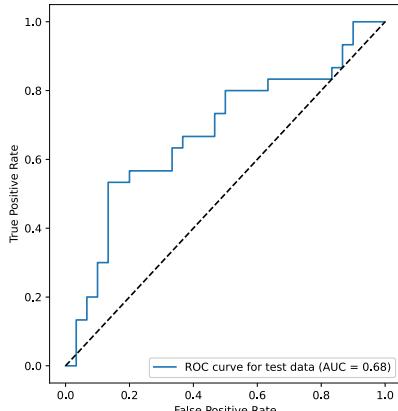


LDA on holdout data of participant 18, p-value=0.03300

Confusion matrix for test data

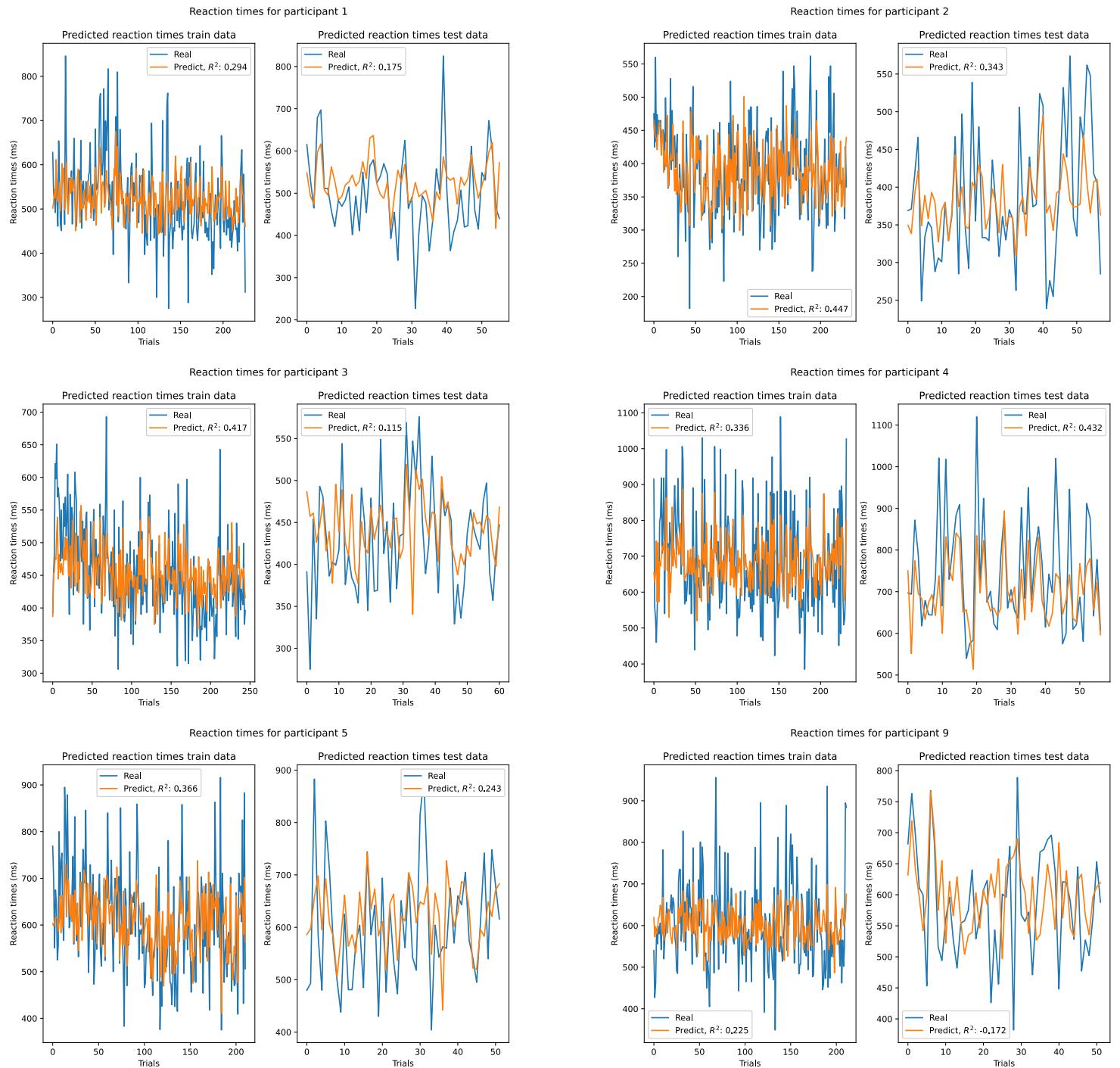


ROC Curve for test data



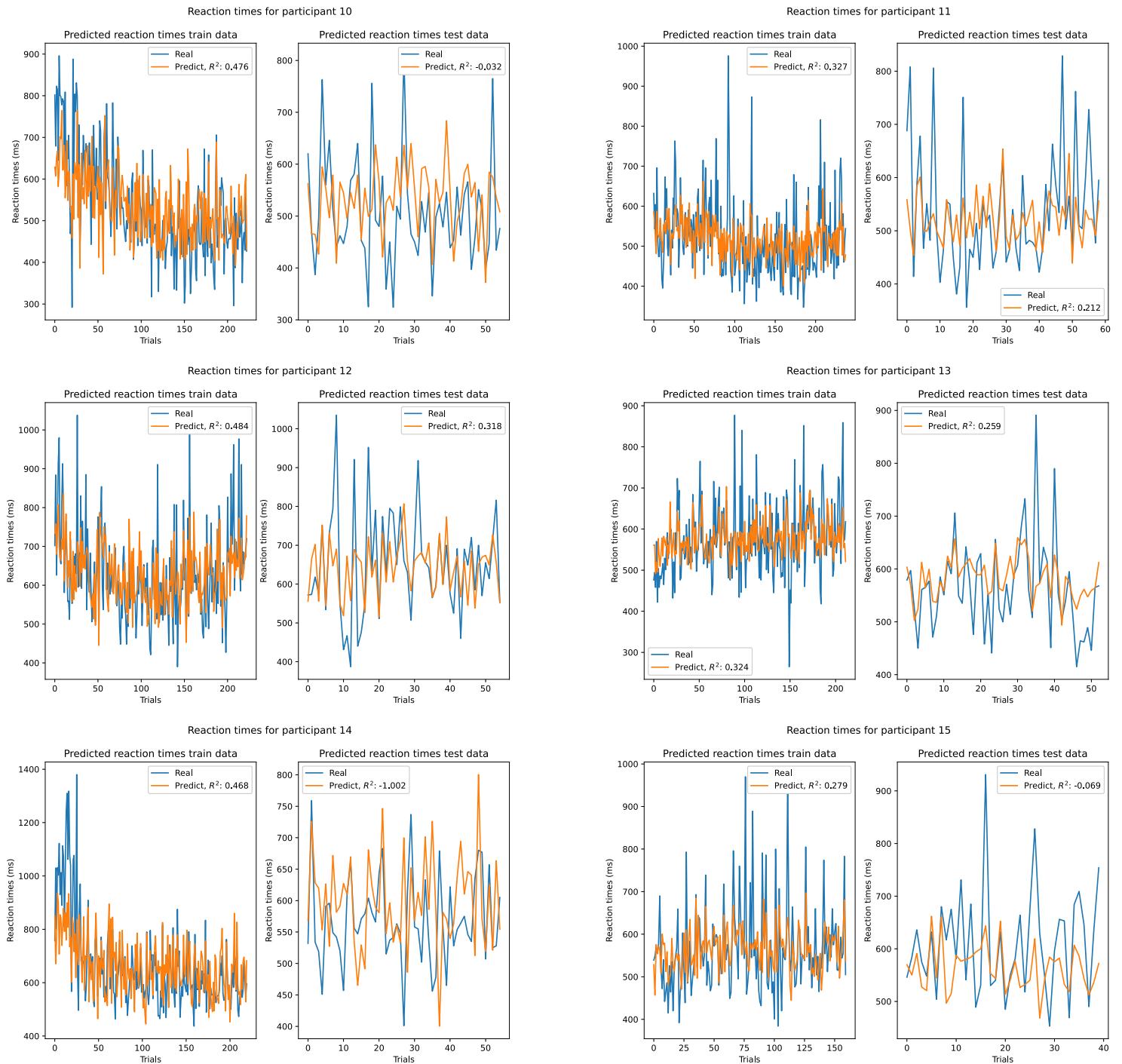
Pre-movement analysis

Regression results - train set



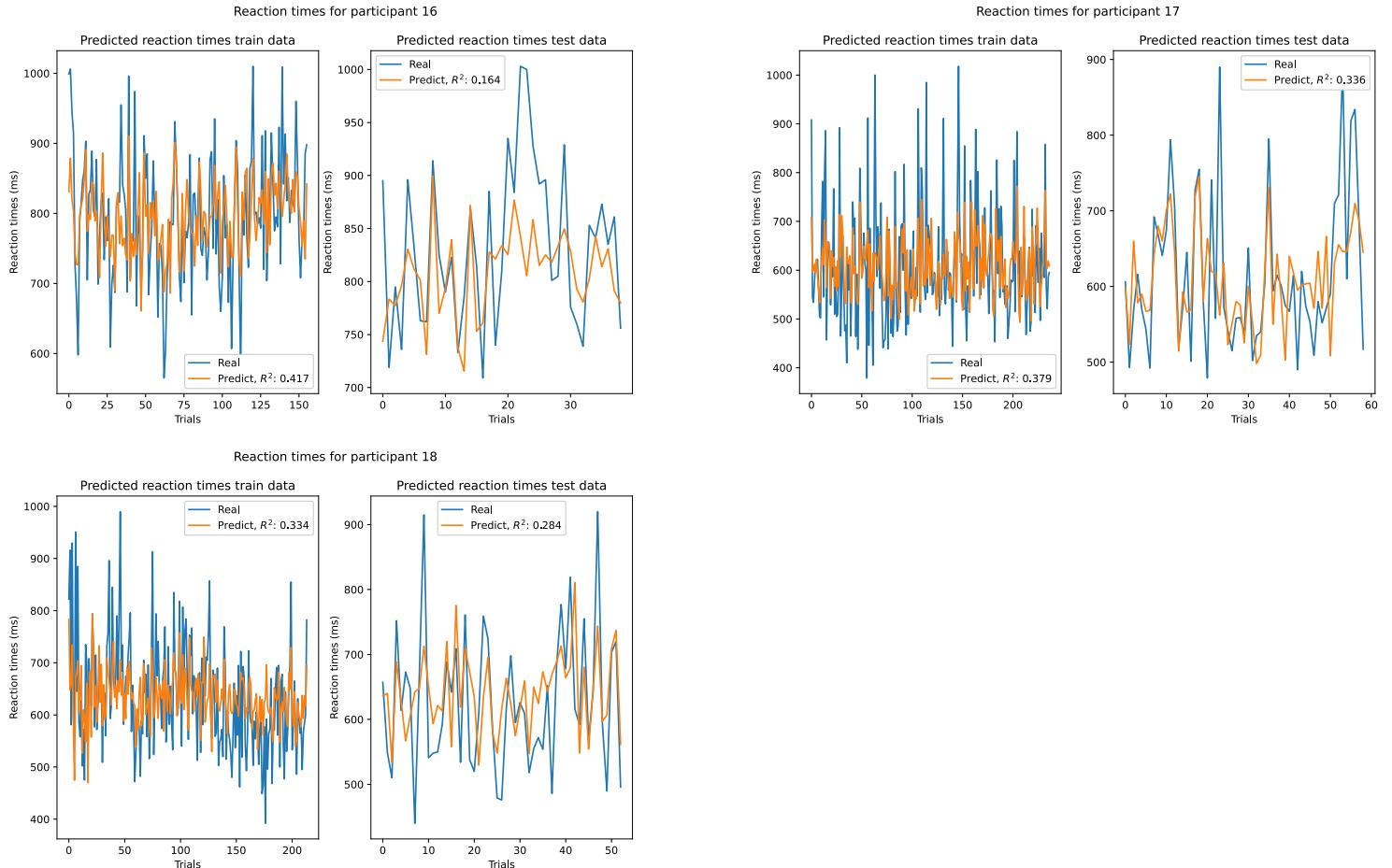
Pre-movement analysis

Regression results - train set



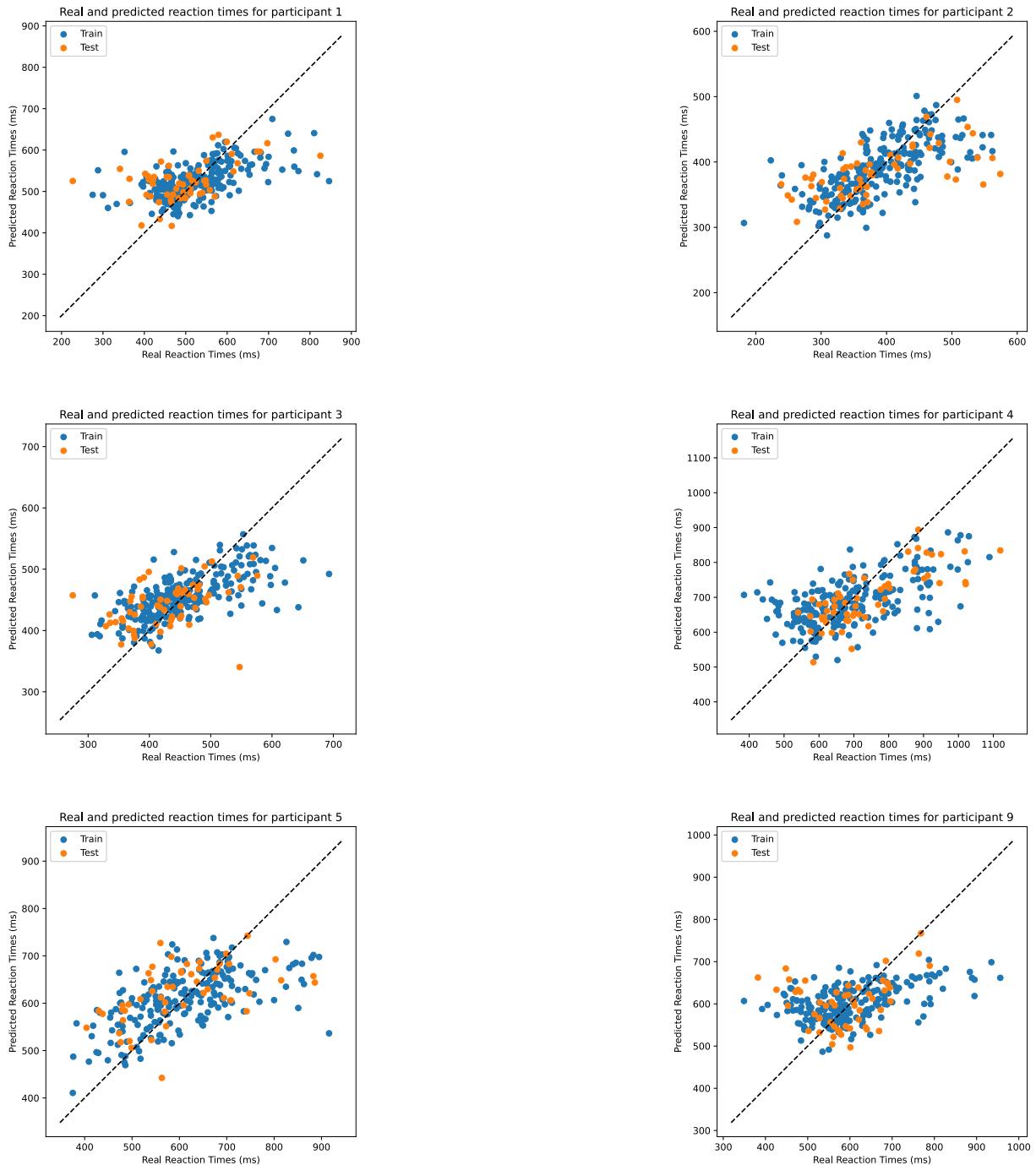
Pre-movement analysis

Regression results - train set



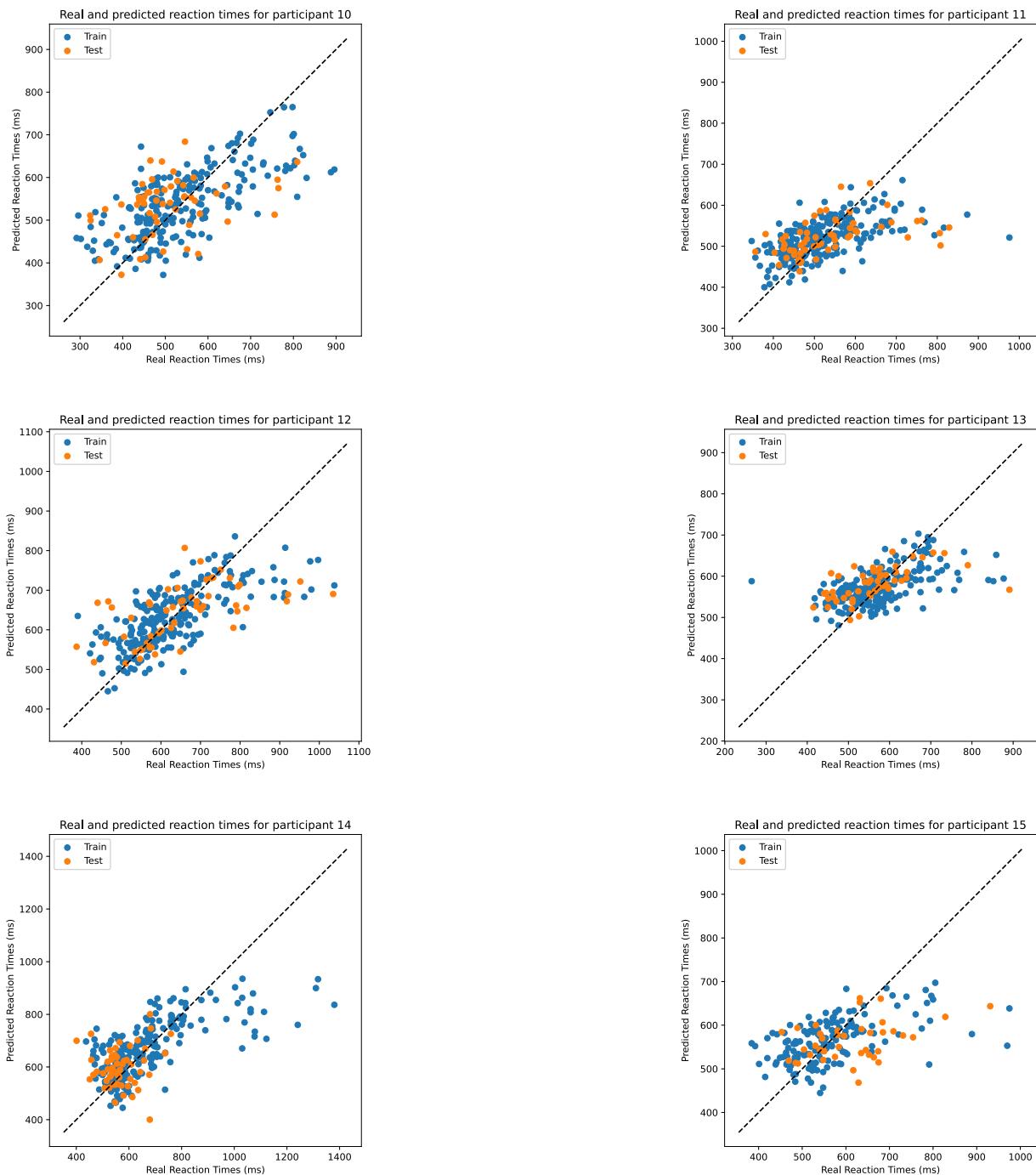
Pre-movement analysis

Regression results scatter plot - train set



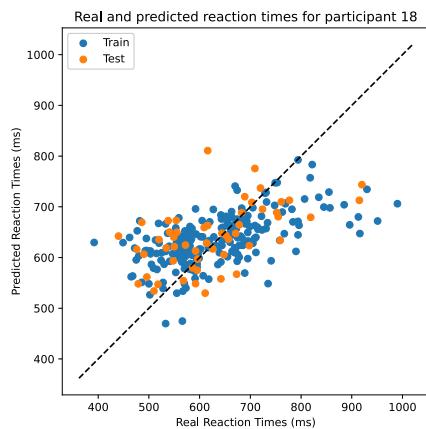
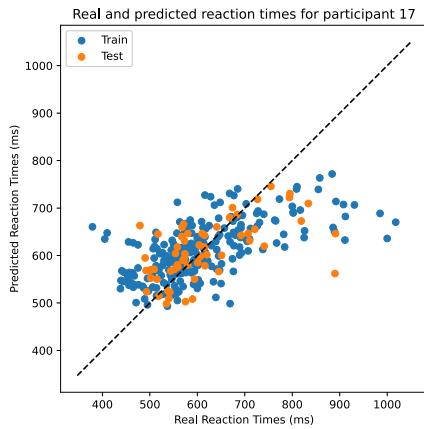
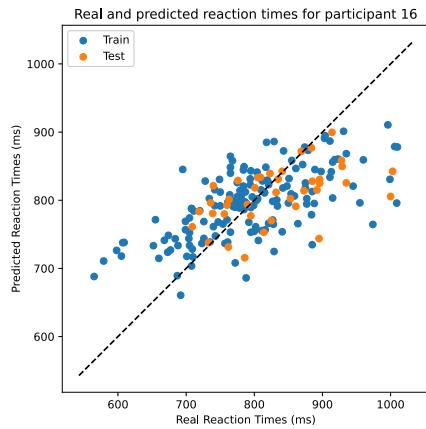
Pre-movement analysis

Regression results scatter plot - train set



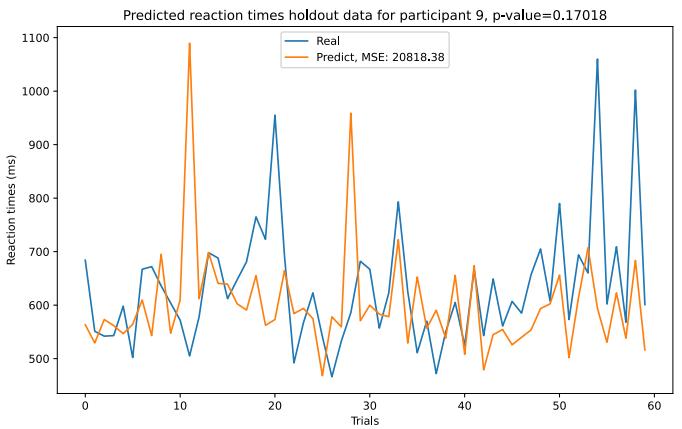
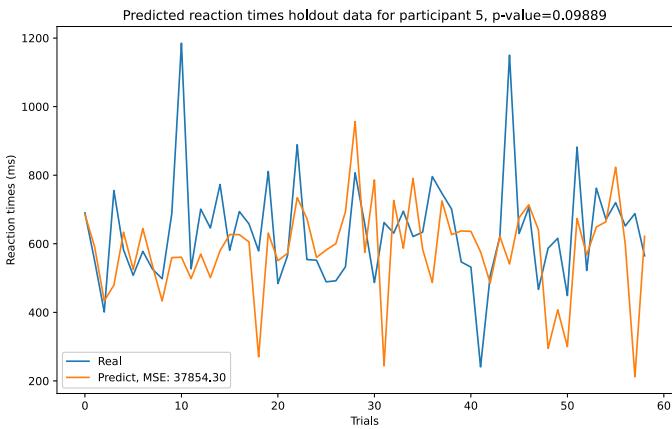
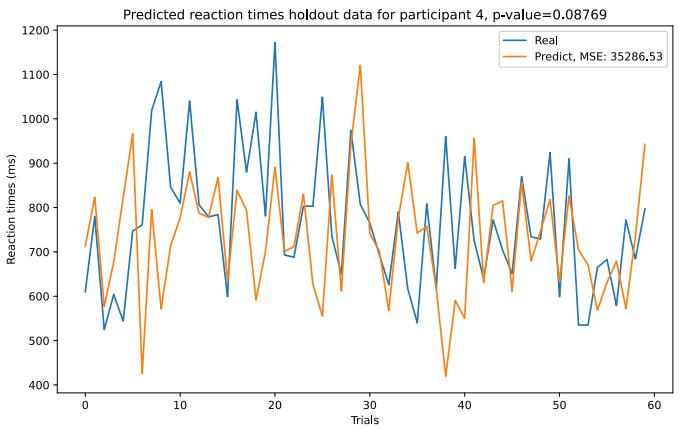
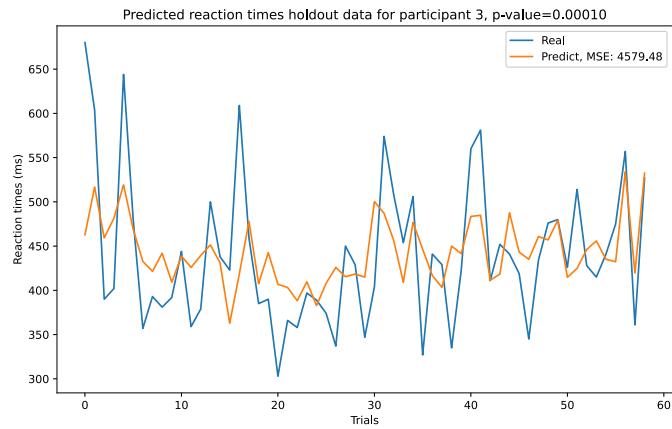
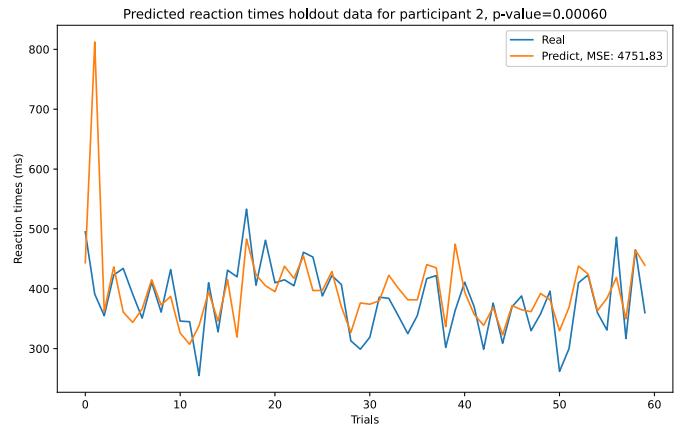
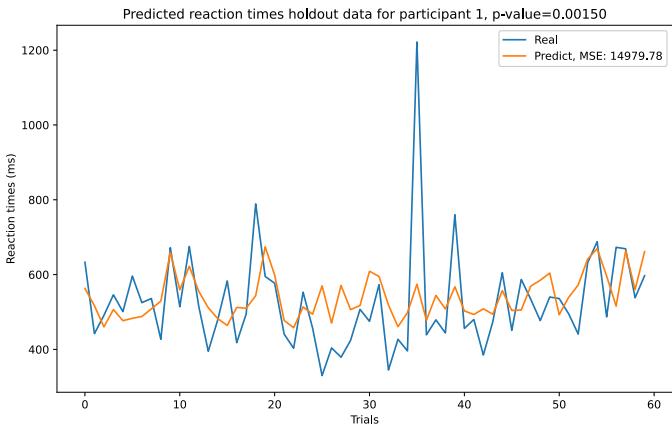
Pre-movement analysis

Regression results scatter plot - train set



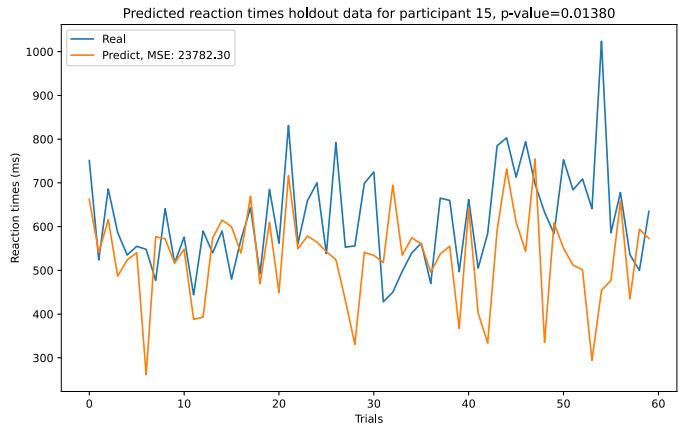
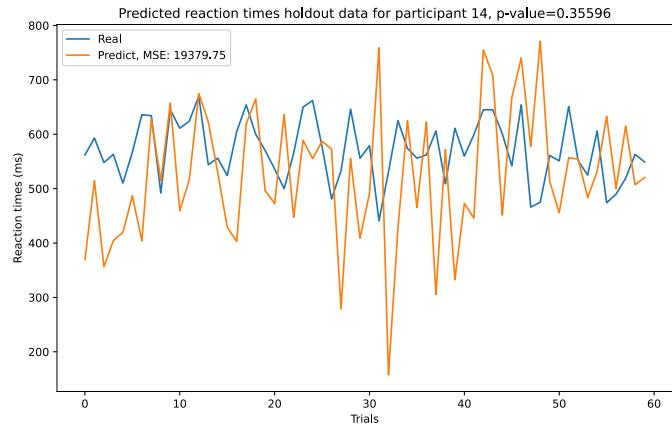
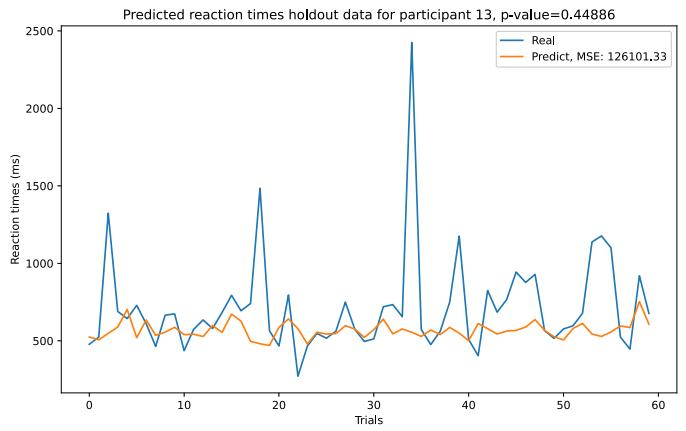
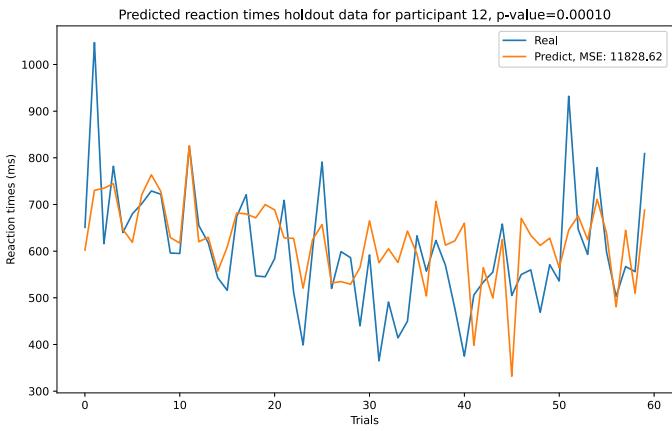
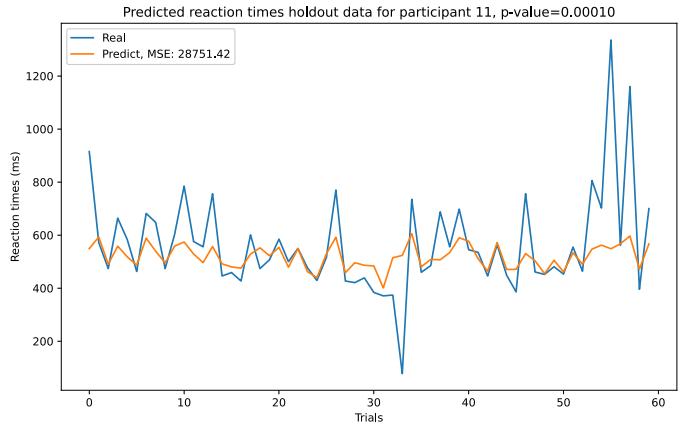
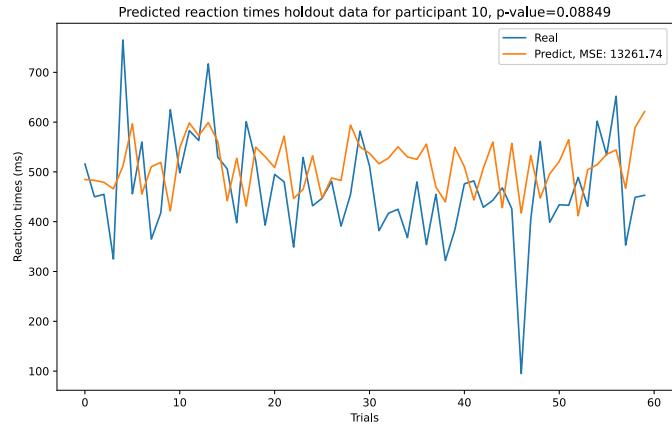
Pre-movement analysis

Regression results - holdout set



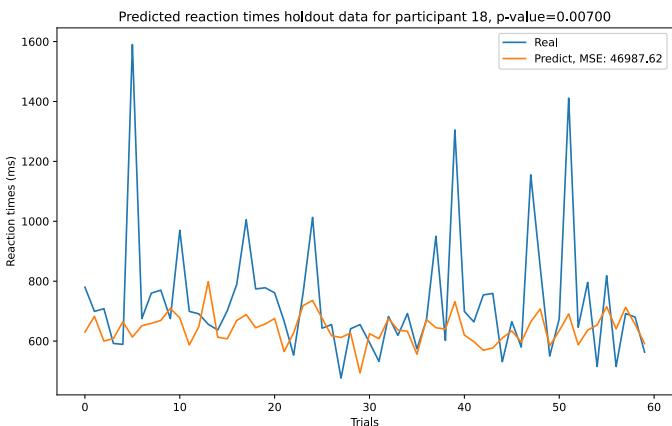
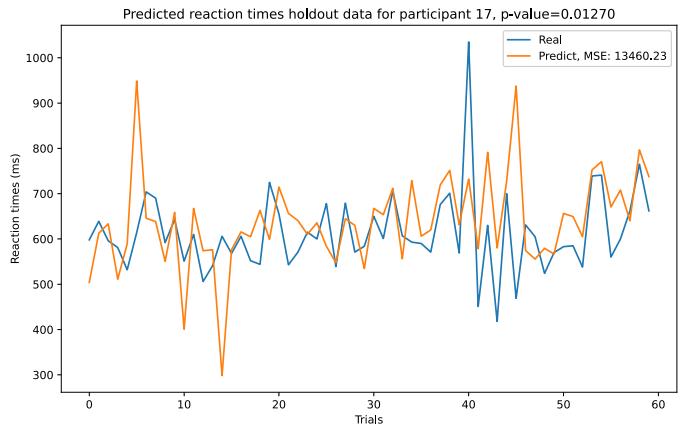
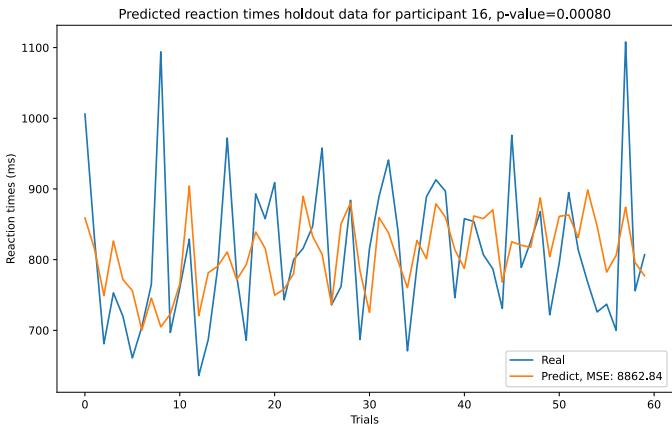
Pre-movement analysis

Regression results - holdout set



Pre-movement analysis

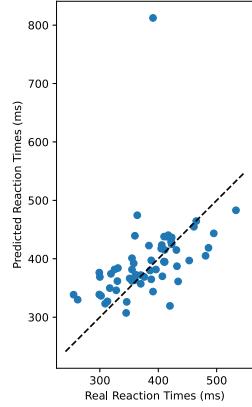
Regression results - holdout set



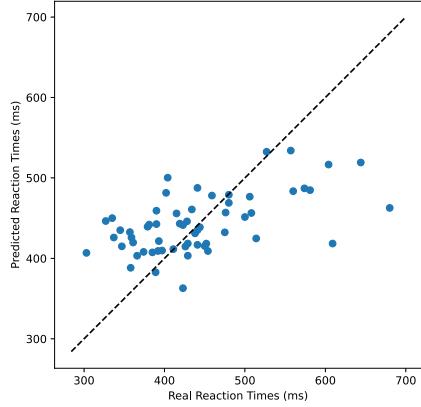
Pre-movement analysis

Regression results scatter plot - holdout set

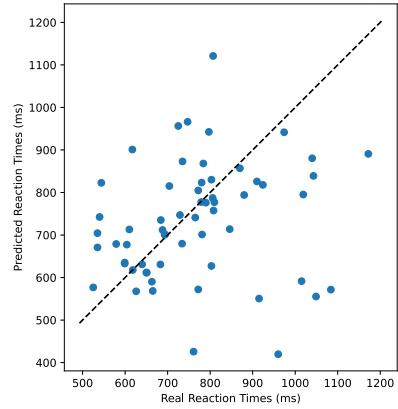
Real and predicted reaction times of holdout data for participant 2



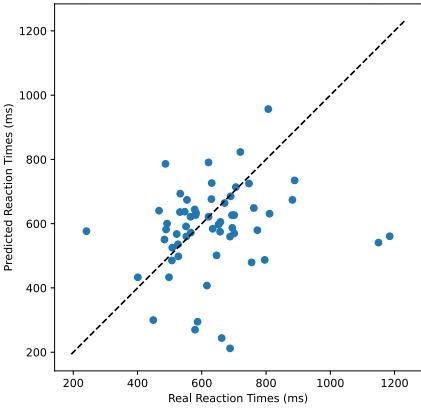
Real and predicted reaction times of holdout data for participant 3



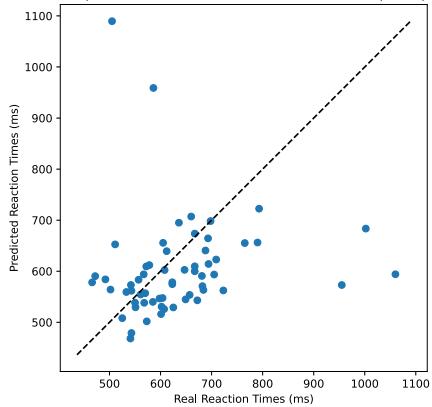
Real and predicted reaction times of holdout data for participant 4



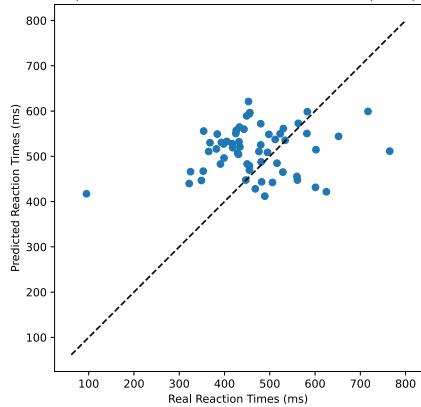
Real and predicted reaction times of holdout data for participant 5



Real and predicted reaction times of holdout data for participant 9

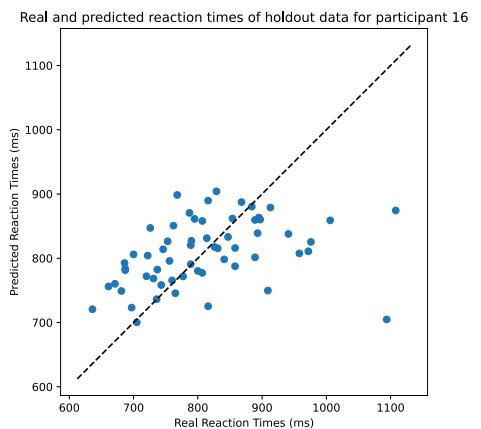
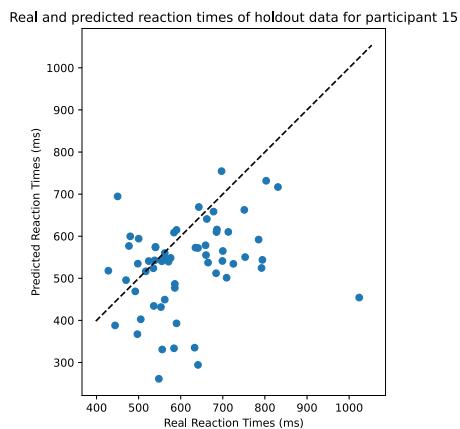
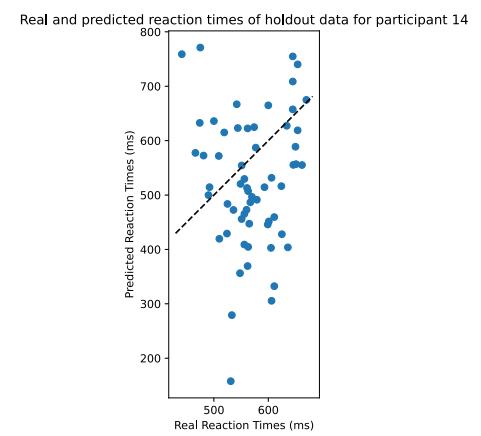
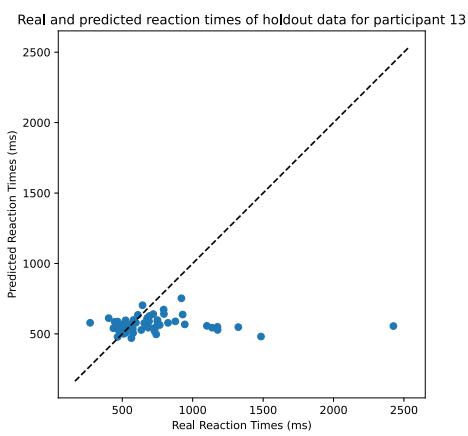
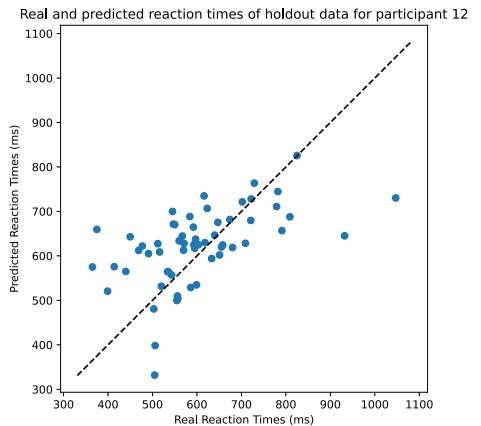
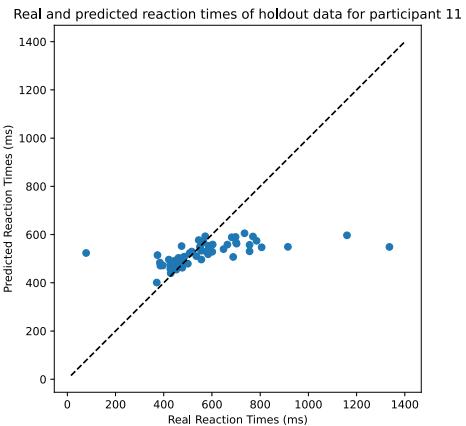


Real and predicted reaction times of holdout data for participant 10



Pre-movement analysis

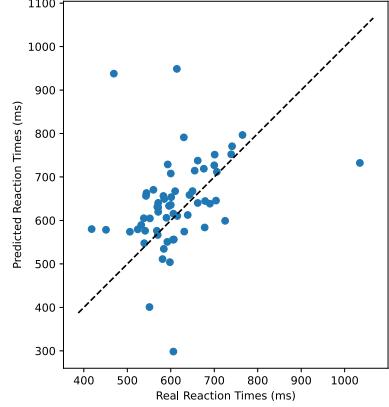
Regression results scatter plot - holdout set



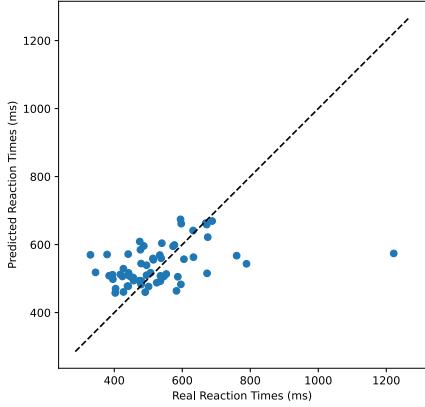
Pre-movement analysis

Regression results scatter plot - holdout set

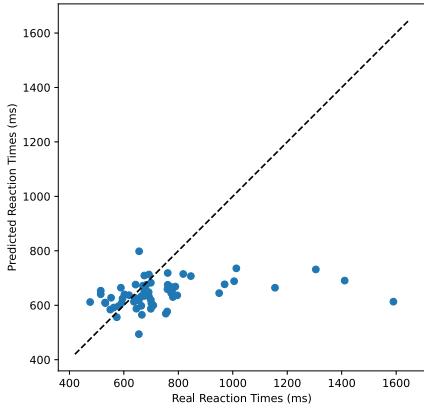
Real and predicted reaction times of holdout data for participant 17



Real and predicted reaction times of holdout data for participant 1

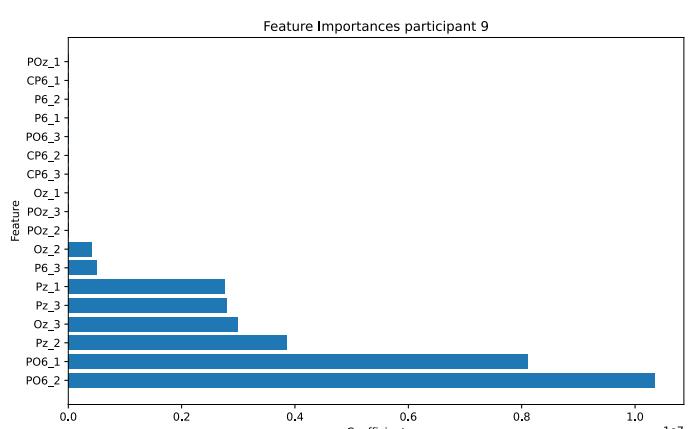
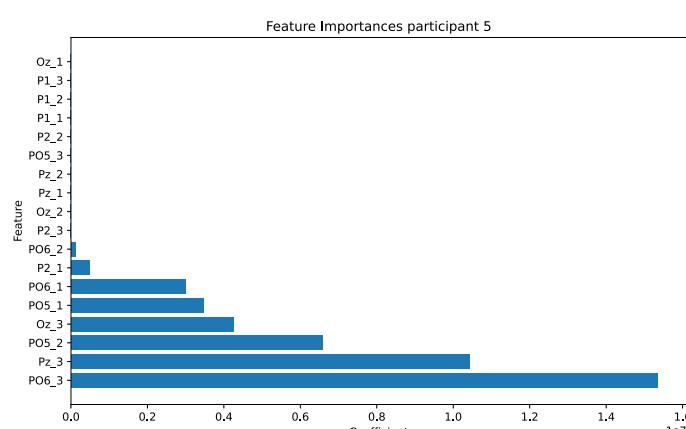
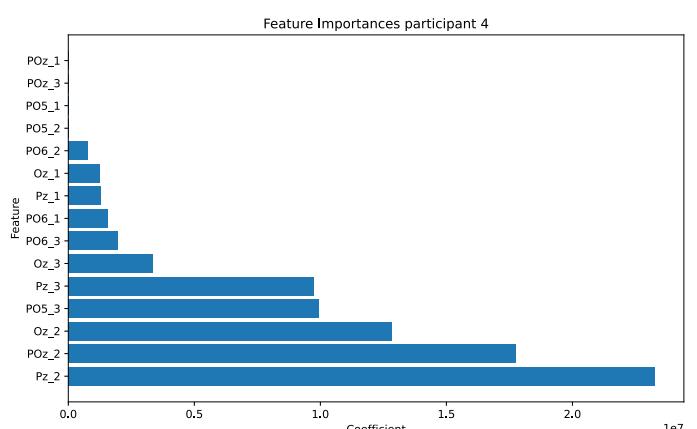
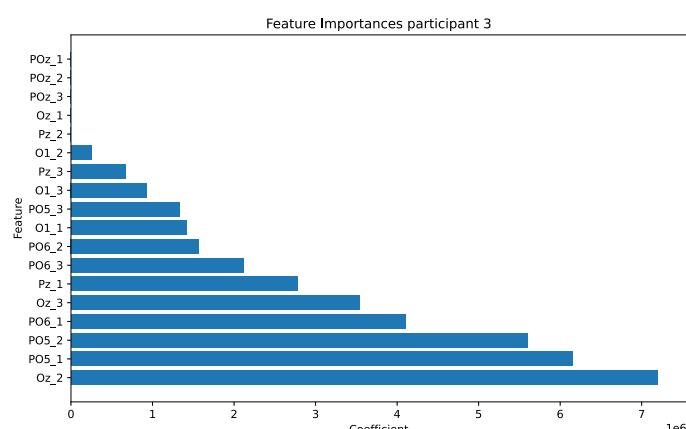
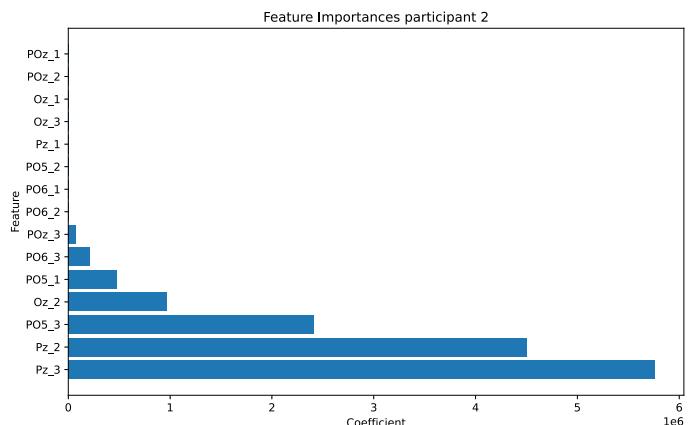
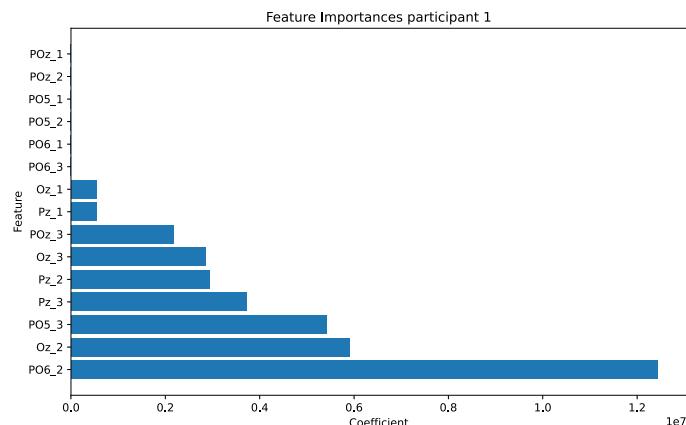


Real and predicted reaction times of holdout data for participant 18



Pre-movement analysis

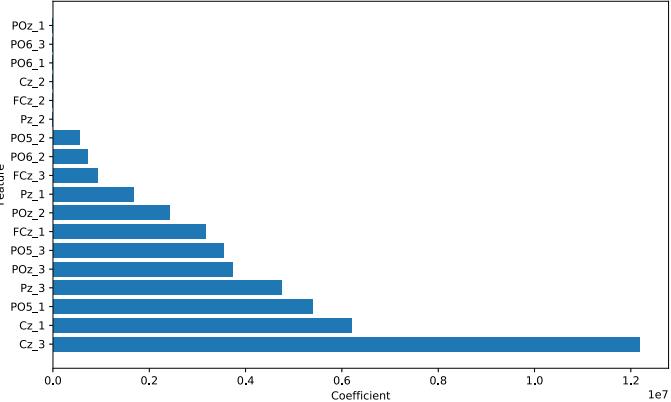
Feature importance - holdout set



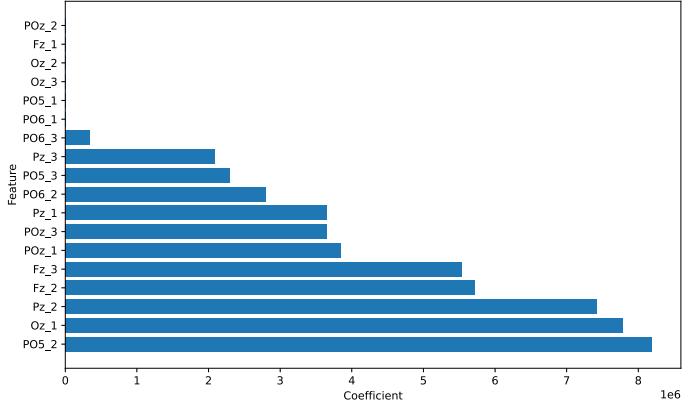
Pre-movement analysis

Feature importance - holdout set

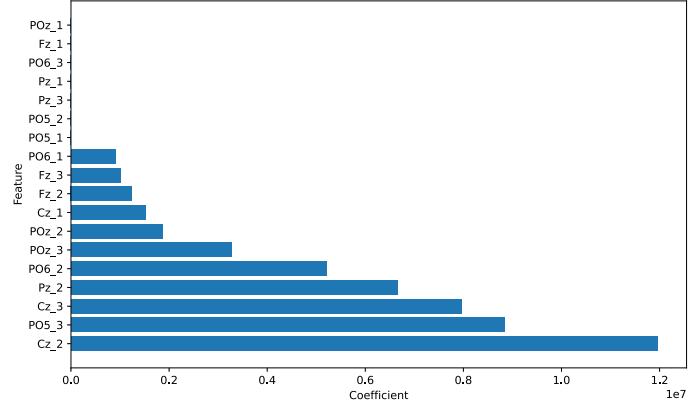
Feature Importances participant 10



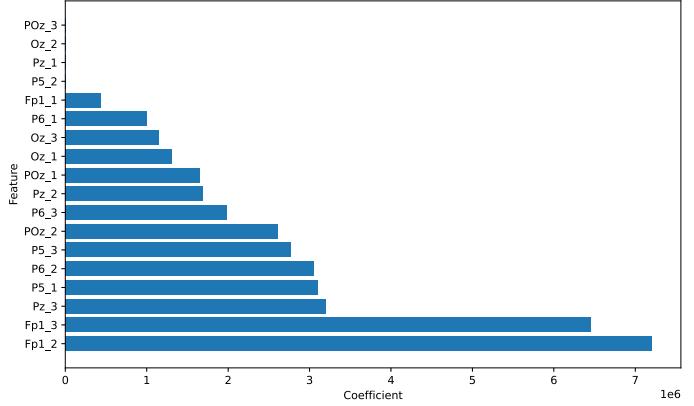
Feature Importances participant 11



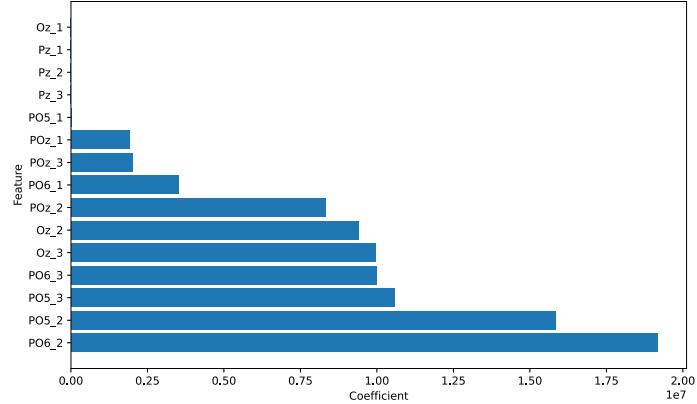
Feature Importances participant 12



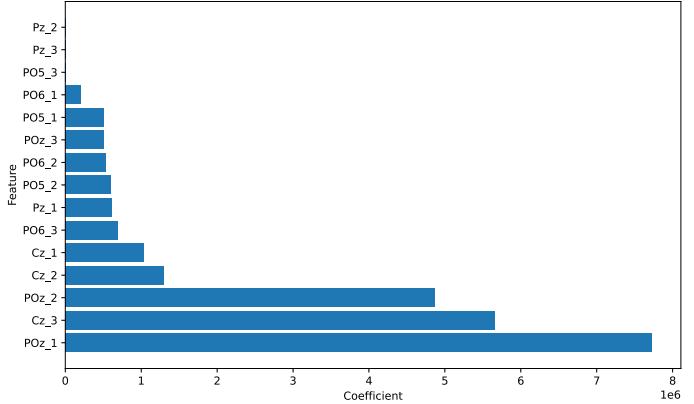
Feature Importances participant 13



Feature Importances participant 14



Feature Importances participant 15



Pre-movement analysis

Feature importance - holdout set

